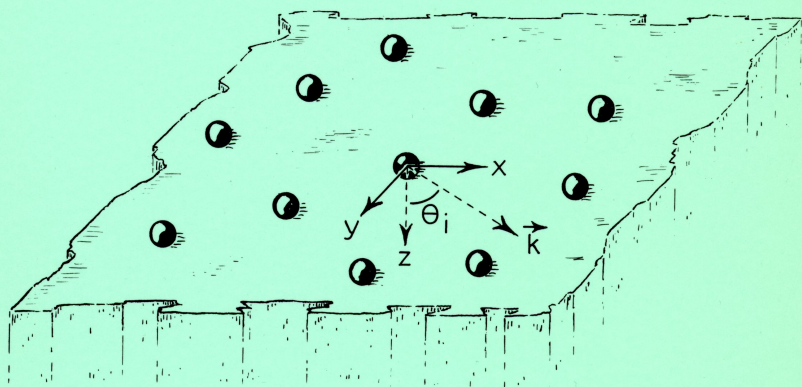


# ON THE OPTICAL PROPERTIES OF SPHERES AND SMALL SPHEROIDS ON A SUBSTRATE



P.A. BOBBERT

**BIBLIOTHEEK  
GORLAEUS LABORATORIUM**

Postbus 9502  
2300 RA LEIDEN

ON THE OPTICAL PROPERTIES OF SPHERES OF  
AND SMALL SPHEROIDS ON A SUBSTRATE

ON A SUBSTRATE

PROLEGOMENA

... VAN HET WETENSCHAPPELIJK INSTITUUT  
... OP HET ZAK VAN DE  
... REFLECTEREN, HOOG-  
... EN NATUUR-  
... VAN HET COLLE-  
... OF DENNEN-  
... NATION

1880

ROBERT

IN 1880

RESEARCH REPORT  
MEDICAL RESEARCH SERVICE

1950

ON THE CRITICAL POINTS OF  
AND SMALL SPHERES OF A  
STATISTICAL ANALYSIS

# ON THE OPTICAL PROPERTIES OF SPHERES AND SMALL SPHEROIDS ON A SUBSTRATE

PROEFSCHRIFT

TER VERKRIJGING VAN DE GRAAD VAN DOCTOR AAN  
DE RIJKSUNIVERSITEIT TE LEIDEN, OP GEZAG VAN DE  
RECTOR MAGNIFICUS DR. J.J.M. BEENAKKER, HOOG-  
LERAAR IN DE FACULTEIT DER WISKUNDE EN NATUUR-  
WETENSCHAPPEN, VOLGENS BESLUIT VAN HET COLLE-  
GE VAN DEKANEN TE VERDEDIGEN OP DONDERDAG  
24 MAART 1988 TE KLOKKE 14.15 UUR

DOOR

PETER ARNOLD BOBBERT

GEBOREN TE LEIDEN IN 1960

ON THE OPTICAL PROPERTIES OF  
SPHERES AND SMALL SPHEROIDS  
ON A SUBSTRATE

Promotie-commissie:

- Promotor: Prof. Dr. D. Bedeaux  
Co-promotor: Dr. J. Vlieger  
Overige leden: Prof. Dr. H.J. Hilhorst  
Prof. Dr. J.M.J. van Leeuwen  
Prof. Dr. W.J.A. Maaskant  
Prof. Dr. W.J. Huiskamp

PETER ARNOOLD BOBBERT

GEBOREN TE LEEUWEN OP 28

# Contents

I. Introduction	1
II. The Phenomena of a Spectrum of the Visible Spectrum	15
1. Introduction	15
2. The spectrum of the visible spectrum	16
3. The spectrum of the visible spectrum	17
4. The spectrum of the visible spectrum	18
5. The spectrum of the visible spectrum	19
6. The spectrum of the visible spectrum	20
7. The spectrum of the visible spectrum	21
8. The spectrum of the visible spectrum	22
III. Light Scattering by a Dielectric Medium	23
1. Introduction	23
2. The dielectric medium	24
3. The dielectric medium	25
4. The dielectric medium	26
5. The dielectric medium	27
6. The dielectric medium	28
7. The dielectric medium	29
8. The dielectric medium	30
9. The dielectric medium	31
10. The dielectric medium	32
11. The dielectric medium	33
12. The dielectric medium	34
Appendix	35
IV. Light Reflection from a Dielectric Medium	36
1. Introduction	36
2. Light reflection from a dielectric medium	37
3. Light reflection from a dielectric medium	38
4. Light reflection from a dielectric medium	39
5. Light reflection from a dielectric medium	40
6. Light reflection from a dielectric medium	41
7. Light reflection from a dielectric medium	42
8. Light reflection from a dielectric medium	43
9. Light reflection from a dielectric medium	44
10. Light reflection from a dielectric medium	45
11. Light reflection from a dielectric medium	46
12. Light reflection from a dielectric medium	47

*aan mijn ouders  
aan Renate*

Administrative

Number: 100-100000000  
Organization: FBI  
Investigation: [illegible]  
Date: [illegible]  
Page: [illegible]

100-100000000  
100-100000000

# Contents

I	Introduction	9
II	The Polarizability of a Spheroidal Particle on a Substrate	13
1	Introduction	13
2	The polarizability of an oblate spheroid on a substrate	14
3	The polarizability of a prolate spheroid on a substrate	21
4	Recurrence relations for the coefficients $a_{j,n}^{\pm}(\xi_0)$ and $b_{j,n}^{\pm}(\xi_0)$	23
5	The disk and the needle	26
6	The dipole approximation	28
7	Application to a square lattice of gold particles on sapphire	31
8	Summary	34
III	Light Scattering by a Sphere on a Substrate	37
1	Introduction	37
2	The Debye potentials	38
3	The Debye potentials of a plane wave	40
4	The Mie solution	42
5	Formal solution of the scattering by a sphere on a substrate	43
6	Weyl's method	44
7	Hertz vectors	46
8	Calculation of the matrix A	50
9	Perfectly conducting substrate	54
10	The static limit	58
11	The far-away scattered field	61
12	Concluding remarks	64
	Appendix	64
IV	Light Reflection from a Substrate Sparsely Seeded with Spheres – Comparison with an Ellipsometric Experiment	69
1	Introduction	69
2	Light reflection by an assembly of non-interacting spheres on a substrate	69
3	Method of computation	73
4	Results of computer calculations – comparison with an ellipsometric experiment	76
5	Summary and discussion	79

<b>Appendix</b>	<b>81</b>
1 Recurrence relations and explicit expressions for Legendre functions of the first and second kind . . . . .	81
2 Recurrence relations and explicit expressions for spherical Bessel functions and Hankel functions of the first kind . . . . .	82
<b>Samenvatting (Summary in Dutch)</b>	<b>83</b>
<b>Curriculum Vitae</b>	<b>86</b>
<b>List of Publications</b>	<b>87</b>

# Chapter I

## Introduction

The last decades a wide interest has arisen in the optical properties of particles on surfaces. Important practical applications are e.g. the manufacturing of optical coatings with special properties, the optical study of growth processes on surfaces and the study of surface enhanced Raman scattering (SERS).

The optical properties of particles *in free space* have been subjected to research for more than a century. In particular the names of Rayleigh, Lorenz and Mie have to be mentioned. Three different situations can be distinguished: (1) the particles are much smaller than the wavelength of the incident light, (2) the size of the particles is comparable to the wavelength or (3) the particles are much larger than the wavelength. In situation 3 geometrical optics can be employed to determine the optical properties. In situation 1 the incident electromagnetic fields can be assumed to be homogeneous in the neighbourhood of the particles and one can use a static theory. Situation 2 is the most difficult one, since no a priori approximations can be made; a general, dynamic approach is required, including both situations 1 and 3 as limiting cases. For all three situations and for various shapes of the particles one has attempted to determine the optical properties.

For particles *on a substrate* the problem is more complicated: the electromagnetic interaction between the particles and the substrate in general plays an important role. Again one can distinguish between the three abovementioned situations and attempt to determine the optical properties for different shapes of the particles.

Berreman<sup>1)</sup> has investigated the optical properties of hemispherical bumps and pits, small compared to the wavelength of the incident light, on or in a substrate. The general case of a small hemispherical particle, of which the material may be different from that of the substrate, was considered by Chauvaux and Meessen<sup>2)</sup>. The optical properties of a small sphere on a substrate were examined by Ruppin<sup>3)</sup>. Recently, a general method was developed to calculate the polarizability of a small truncated sphere on a substrate<sup>4,5)</sup>, which includes both the hemispherical and the spherical shape.

As one often deals with an assembly of particles on a substrate rather than with separate particles, it is in general also important to take into account the *interaction between the particles*. For particles small compared to the wavelength of light Vlioger and Bedeaux have developed a theory in which these interactions are taken into account in dipole approximation<sup>6)</sup>.

In chapter II of this thesis a method is developed to calculate the polarizability of a spheroidal particle on a substrate. The axis of revolution of the spheroid is assumed to be perpendicular to the substrate and its size is supposed to be small compared to the wavelength of the incident light. Then, considering only non-magnetic particles on a non-magnetic substrate, the electric field vector in and around the particle can be obtained from an electric potential. The three different media, the ambient, the substrate and the particle, are characterized by their, possibly frequency dependent and complex, dielectric constants. The electric potential is now expanded into *spheroidal multipole fields*, with spheroidal multipoles located at the centre of the spheroid and spheroidal *image multipoles* at the centre of the mirror image of the spheroid in the substrate. Spheroidal multipole fields rather than the usual spherical multipole fields are used in order to adapt the method to the geometry of the particle. Furthermore, by the introduction of spheroidal image multipoles the boundary conditions for the electric field at the surface of the substrate are easily satisfied. The boundary conditions at the surface of the spheroid now lead to an infinite set of linear inhomogeneous equations for the multipole coefficients. For the matrix elements appearing in these equations a complete set of recurrence relations is derived, by which they can be evaluated explicitly. The polarizability can then be calculated to any desired accuracy by truncating the infinite set of equations to a large enough finite set and solving for a finite number of multipole coefficients. Polarizabilities normal and parallel to the substrate are obtained, corresponding to an external electric field normal or parallel to the substrate.

For the two limiting cases of a disk and a needle on a substrate it is shown that the interaction with the substrate effectively vanishes, so that the polarizabilities become equal to those of a *free* disk and needle.

The *spheroidal* dipole approximation for the interaction between spheroid and substrate is considered in more detail. It is compared to the usual *spherical* dipole approximation for this interaction and found to be a very substantial improvement.

The developed method is applied to a transmission experiment performed by Niklasson and Craighead<sup>7,8</sup>) with a system of small identical gold particles arranged in a square lattice on a sapphire substrate. Apart from a clear flattening and rotational symmetry about an axis normal to the substrate, the precise shape of the particles could not be established experimentally. In ref. 5 the particles were modeled as truncated spheres and a good agreement with the experimental transmittance could be obtained. The value assumed for the axial ratio of the particles (the ratio between diameter and height of the particles), however, was smaller than the experimentally observed value. With an oblate spheroidal model also good agreement with the experimental transmittance can be obtained, but now a much too large axial ratio has to be assumed. This suggests that the actual shape is a hybrid of the two models, though probably closer to the truncated spherical than to the oblate spheroidal model.

In chapter III the problem of light scattering by a sphere on a substrate is studied. *The size of the sphere is now allowed to be of the same order of magnitude as the wavelength of the incident light.* The problem is solved by combining Mie's solution for scattering by a sphere in free space with an extension of Weyl's method

for the calculation of the reflection of dipole radiation by a flat surface to higher order multipole radiation. The result is again an infinite set of linear inhomogeneous equations for the electric and now also magnetic multipole coefficients. The coefficient matrix of these equations is expressed in terms of a matrix representing the scattering by the sphere and a matrix characterizing the reflection of multipole radiation by the substrate. The elements of the first matrix are well-known closed expressions. The elements of the second matrix are expressed as integrals over plane waves travelling into various directions given by a complex angle. These integrals contain Fresnel reflection amplitudes, by which it becomes impossible to evaluate them analytically. In general, therefore, they have to be calculated numerically. Only for the special case of a perfectly conducting substrate the integrals can be performed analytically. Again approximate values for the multipole coefficients can be obtained by truncation of the infinite set of equations.

It is proved that for small spheres the formalism reduces to the static theory for a sphere on a substrate, which can be considered as a special case of the truncated spherical model, treated in refs. 4 and 5, as well as of the spheroidal model, treated in chapter II.

Finally, expressions are given for the far-away scattered electric field above the substrate in terms of the electric and magnetic multipole coefficients.

In chapter IV the light reflection from a substrate sparsely seeded with spheres is calculated in the approximation that the interaction between the spheres can be neglected. One is then essentially left with the one-particle problem of chapter III. The amplitude for reflection is obtained by simply adding the scattered fields of all the spheres. The theory is applied to an ellipsometric experiment by Greef<sup>9</sup>) with a system of growing mercury particles, with sizes of the order of the wavelength of the incident light, on a carbon substrate. Because of the large surface tension of mercury these particles are supposed to be practically spherical. Good agreement between theory and experiment is obtained if a small dispersion in the sizes of the particles is assumed.

In this thesis extensive use will be made of the properties of the associated Legendre functions of the first and second kind as well as of the spherical Bessel functions and Hankel functions of the first kind. In the appendix a compilation is given of the most important recurrence relations for these functions and some explicit expressions for the lowest values of their indices.

## References

- 1) D.W. Berreman, Phys. Rev. **163** (1967) 855.
- 2) R. Chauvaux and A. Meessen, Thin Solid Films **62** (1979) 125.
- 3) R. Ruppin, Surface Science **127** (1983) 108.
- 4) M.M. Wind, J. Vliieger and D. Bedeaux, Physica **141A** (1987) 33.
- 5) M.M. Wind, P.A. Bobbert, J. Vliieger and D. Bedeaux, Physica **143A** (1987) 164.

- 6) J. Vlieger and D. Bedeaux, *Thin Solid Films* **69** (1980) 107.
- 7) H.G. Craighead and G.A. Niklasson, *Appl. Phys. Lett.* **44** (1984) 1134.
- 8) G.A. Niklasson and H.G. Craighead, *Thin Solid Films* **125** (1985) 165.
- 9) R. Greef, *Ber. Bunsenges. Phys. Chem.* **88** (1984) 150.

## Chapter II

# The Polarizability of a Spheroidal Particle on a Substrate

### 1. Introduction

In previous work<sup>1)</sup> a method was developed to calculate the polarizability of a truncated spherical particle on a substrate. A multipole method was introduced with multipoles located at the centre of the truncated sphere and 'image multipoles' at the image of this centre with respect to the surface of the substrate. In this way the boundary conditions for the electric field at the surface of the substrate could easily be satisfied. The boundary conditions at the surface of the curved part of the truncated sphere led to an infinite set of linear inhomogeneous equations for the multipole coefficients, which could be solved approximately by considering a large enough finite set of equations for a finite number of multipoles. The matrix elements appearing in these equations contained rather complicated integrals, for which later a complete set of recurrence relations was derived<sup>2)</sup>.

The method was then applied<sup>2)</sup> to a transmission experiment by Niklasson and Craighead<sup>3,4)</sup> with a system of gold particles arranged in a square lattice on a sapphire substrate. A good agreement with the experimental transmittance was found after fitting the axial ratio and the radius of the truncated sphere. The fitted values for the axial ratio and the radius, however, were appreciably smaller than the experimentally observed ones. While the discrepancy between the observed and fitted radius could be explained, the discrepancy in the axial ratio remained unaccounted for. It was therefore suggested in ref. 2 that an oblate spheroidal model would possibly be closer to reality.

In this chapter we shall develop a method, analogous to that of ref. 1, for the calculation of the polarizability of a spheroidal particle on a substrate. We shall assume that the axis of revolution of the spheroid is normal to the substrate and that its linear dimensions are small compared to the wavelength of the incident light. An important aspect of our method is the use of *spheroidal multipoles*. In sections 2 and 3 the cases of an oblate and a prolate spheroid are treated respectively. As in ref. 1 an infinite set of linear inhomogeneous equations for the multipole coefficients is derived. The matrix elements of these equations contain coefficients that can be evaluated by means of a complete set of recurrence relations derived in section 4.

Section 5 deals with the limiting cases of a thin circular disk and a needle. For these cases it is proved that the interaction with the substrate vanishes, so that the polarizabilities become equal to the polarizabilities in free space. In section 6 the spheroidal dipole approximation is examined and compared with the conventional spherical dipole approximation. It is found that there is a considerable difference between the two. In section 7 we apply our theory for the oblate spheroidal model to the experiments of Niklasson and Craighead<sup>3,4</sup>). We summarize all our results in section 8.

In the following we assume that the reader is acquainted with the basic properties of the Legendre functions of the first and second kind, which can be found in standard textbooks such as Morse and Feshbach<sup>5,6</sup>).

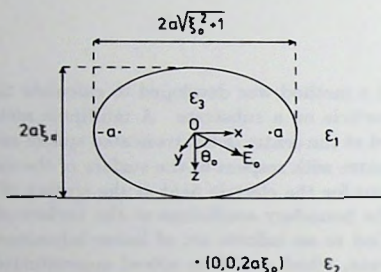


Fig. 1. An oblate spheroid on a substrate. Cross-section through the  $x$ - $z$  plane.

## 2 The polarizability of an oblate spheroid on a substrate

We consider an oblate spheroidal particle with a frequency dependent dielectric constant  $\epsilon_3(\omega)$  on a substrate with dielectric constant  $\epsilon_2(\omega)$  and surrounded by an ambient with dielectric constant  $\epsilon_1(\omega)$ . The surface of the substrate is planar. We choose the origin of our coordinate system at the centre of the spheroid, with the  $z$ -axis, which is supposed to be the axis of revolution, downward. The radius of the ring of foci of the oblate spheroid will be denoted by  $a$ . The two long axes of the spheroid have length  $2a\sqrt{\xi_0^2 + 1}$  and the short axis has length  $2a\xi_0$ , which defines a flattening parameter  $\xi_0$  ( $0 \leq \xi_0 < \infty$ ) (see fig. 1). The limit  $\xi_0 \rightarrow \infty$ ,  $a \rightarrow 0$ ,  $a\xi_0 = R$  corresponds to a sphere with radius  $R$ , whereas the limit  $\xi_0 \rightarrow 0$  corresponds to a thin circular disk with radius  $a$ .

If the linear dimensions of the particle are small compared to the wavelength of the incident light, we may neglect retardation effects in and around the particle and assume that the incident electric and magnetic fields are homogeneous. If we furthermore assume that the particle is non-magnetic, then the magnetic field is

unaffected by its presence, whereas the electric field  $\mathbf{E}(\mathbf{r})$  ( $\mathbf{r} = (x, y, z)$ ) is determined by an electric potential  $V(\mathbf{r})$  ( $\mathbf{E}(\mathbf{r}) = -\partial V/\partial \mathbf{r}$ ), which satisfies the Laplace equation in the three media:

$$\Delta V(\mathbf{r}) = 0, \quad (2.1)$$

with  $\Delta$  the Laplace operator. In addition the potential and its normal derivative times the dielectric constant should be continuous across each interface between the three media. We choose our coordinate system such that the incident electric field  $\mathbf{E}_0$  in the ambient lies in the  $x$ - $z$  plane and has a positive  $x$ -component  $E_{0x}$ . The angle between  $\mathbf{E}_0$  and the positive  $z$ -axis is denoted by  $\theta_0$  (see fig. 1).

In ref. 1 the polarizability of a truncated sphere on a substrate was calculated by means of a multipole expansion of the potential, with multipoles located at the centre of the truncated sphere and 'image multipoles' at the centre of the image of the truncated sphere with respect to the surface of the substrate. The introduction of these image multipoles made it very easy to satisfy the boundary conditions at the surface of the substrate. An analogous method will be employed here, but in order to adapt the method to the different geometry of the particle it is more convenient to introduce (oblate) *spheroidal multipoles*. For that purpose we first introduce oblate spheroidal coordinates  $\xi$ ,  $\eta$  and  $\phi$  ( $0 \leq \xi < \infty$ ,  $-1 \leq \eta \leq 1$ ,  $0 \leq \phi \leq 2\pi$ ), defined as follows<sup>6</sup>:

$$\xi \equiv \sqrt{\left(\frac{\rho_1 + \rho_2}{2a}\right)^2 - 1}, \quad \eta \equiv \pm \sqrt{1 - \left(\frac{\rho_1 - \rho_2}{2a}\right)^2}, \quad \phi \equiv \arctan\left(\frac{y}{x}\right), \quad (2.2)$$

with

$$\begin{aligned} \rho_1 &\equiv \sqrt{z^2 + (x + a \cos \phi)^2 + (y + a \sin \phi)^2}, \\ \rho_2 &\equiv \sqrt{z^2 + (x - a \cos \phi)^2 + (y - a \sin \phi)^2}. \end{aligned} \quad (2.3)$$

Here  $\rho_1$  and  $\rho_2$  are the distances of the point  $(x, y, z)$  to the points of intersection of the ring of foci with the plane through  $(x, y, z)$  and the  $z$ -axis, whereas  $\phi$  is the angle of orientation of this plane with respect to the  $x$ - $z$  plane. The positive sign in eq. (2.2) should be used if  $z > 0$  and the negative sign if  $z < 0$ . The inverse of the transformation eqs. (2.2) and (2.3) is

$$x = a\sqrt{(\xi^2 + 1)(1 - \eta^2)} \cos \phi, \quad y = a\sqrt{(\xi^2 + 1)(1 - \eta^2)} \sin \phi, \quad z = a\xi\eta. \quad (2.4)$$

In terms of these spheroidal coordinates the surface of the spheroid is given by  $\xi = \xi_0$ . The Laplace equation (2.1) is separable in these coordinates and the solutions split up into two types: solutions that satisfy the Laplace equation everywhere but are unequal to zero if  $\xi \rightarrow \infty$  and solutions that are zero if  $\xi \rightarrow \infty$  but satisfy the Laplace equation only for  $\xi > 0$ . The first type of solutions can be expressed in terms of the functions<sup>6</sup>

$$P_l^m(i\xi)P_l^m(\eta) \begin{pmatrix} \cos m\phi \\ \sin m\phi \end{pmatrix} \quad (l = 0, 1, 2, \dots; m = 0, 1, \dots, l), \quad (2.5)$$

where  $P_l^m(\eta)$  and  $P_l^m(i\xi)$  are associated Legendre functions of the first kind of degree  $l$  and order  $m$ , defined by

$$P_l^m(\eta) \equiv \frac{(1-\eta^2)^{m/2}}{2^l l!} \frac{d^{l+m}}{d\eta^{l+m}} (\eta^2 - 1)^l \quad (-1 \leq \eta \leq 1), \quad (2.6a)$$

$$P_l^m(i\xi) \equiv (-1)^m i^{l+m} \frac{(1+\xi^2)^{m/2}}{2^l l!} \frac{d^{l+m}}{d\xi^{l+m}} (1+\xi^2)^l \quad (0 \leq \xi < \infty). \quad (2.6b)$$

The second type of solutions can be expressed in terms of the functions<sup>6)</sup>

$$Q_l^m(i\xi) P_l^m(\eta) \begin{pmatrix} \cos m\phi \\ \sin m\phi \end{pmatrix} \quad (l = 0, 1, 2, \dots; m = 0, 1, \dots, l), \quad (2.7)$$

where  $Q_l^m(i\xi)$  is an associated Legendre function of the second kind:

$$Q_l^m(i\xi) \equiv (-1)^{m+1} i^{l+1} \frac{(1+\xi^2)^{m/2}}{2^l l!} \frac{d^m}{d\xi^m} \left\{ 2 \frac{d^l}{d\xi^l} \left[ \arctan \left( \frac{1}{\xi} \right) (1+\xi^2)^l \right] - \arctan \left( \frac{1}{\xi} \right) \frac{d^l}{d\xi^l} (1+\xi^2)^l \right\} \quad (0 \leq \xi < \infty). \quad (2.8)$$

We note that either the functions (2.7) themselves or their derivatives with respect to  $z$  are discontinuous across the disk  $\xi = 0$ . Charge distributions giving rise to potentials of the form eq. (2.7) we shall call (oblate) *spheroidal multipoles*.

We shall now express the potential  $V$  in the regions 1, 2 and 3 in terms of the functions (2.5) and (2.7). Instead of using  $V$  itself, however, it is more convenient to introduce a reduced potential  $\psi$ , by

$$\psi(\mathbf{r}) \equiv -\frac{V(\mathbf{r})}{E_0 a \xi_0}, \quad (2.9)$$

with  $E_0 = |\mathbf{E}_0|$ . Furthermore it is convenient to introduce functions  $X_l^m(\xi, \xi_0)$  and  $Y_l^m(\xi, \xi_0)$  by

$$X_l^m(\xi, \xi_0) \equiv \frac{2^l l! (l-m)!}{(2l)!} i^m \frac{1}{(i\xi_0)^l} P_l^m(i\xi), \quad (2.10)$$

$$Y_l^m(\xi, \xi_0) \equiv \frac{(2l+1)!}{2^l l! (l+m)!} (i\xi_0)^{l+1} Q_l^m(i\xi). \quad (2.11)$$

In view of the asymptotic behaviour of the functions  $P_l^m(i\xi)$  and  $Q_l^m(i\xi)$ :

$$P_l^m(i\xi) \simeq \frac{(2l)!}{2^l l! (l-m)!} i^{-m} (i\rho)^l \quad (\xi \rightarrow \infty), \quad (2.12)$$

$$Q_l^m(i\xi) \simeq \frac{2^l l! (l+m)!}{(2l+1)!} \frac{1}{(i\rho)^{l+1}} \quad (\xi \rightarrow \infty), \quad (2.13)$$

with  $\rho \equiv \sqrt{x^2 + y^2 + z^2}$ , the functions  $X_l^m(\xi, \xi_0)$  and  $Y_l^m(\xi, \xi_0)$  have the following property:

$$X_l^m(\xi, \xi_0) \simeq r^l \quad (\xi, \xi_0 \rightarrow \infty, a \rightarrow 0, a\xi_0 = R), \quad (2.14)$$

$$Y_l^m(\xi, \xi_0) \simeq \frac{1}{r^{l+1}} \quad (\xi, \xi_0 \rightarrow \infty, a \rightarrow 0, a\xi_0 = R), \quad (2.15)$$

with  $r \equiv \rho/R$ . Analogously to ref. 1 we introduce image multipoles at the point  $(0, 0, 2a\xi_0)$  (see fig. 1) and express the potentials in the regions 1, 2 and 3 as follows:

$$\begin{aligned} \psi_1(\xi, \eta, \phi) = & X_1^0(\xi, \xi_0)P_1^0(\eta) \cos \theta_0 + X_1^1(\xi, \xi_0)P_1^1(\eta) \cos \phi \sin \theta_0 \\ & + \sum_{j=1}^{\infty} \{A_{1,j}Y_j^0(\xi, \xi_0)P_j^0(\eta) + B_{1,j}Y_j^1(\xi, \xi_0)P_j^1(\eta) \cos \phi\} \\ & + \sum_{j=1}^{\infty} \{A'_{1,j}V_j^0(\xi, \xi_0, \eta) + B'_{1,j}V_j^1(\xi, \xi_0, \eta) \cos \phi\}, \quad (2.16) \end{aligned}$$

$$\begin{aligned} \psi_2(\xi, \eta, \phi) = & \psi_2' + \alpha X_1^0(\xi, \xi_0)P_1^0(\eta) \cos \theta_0 + \beta X_1^1(\xi, \xi_0)P_1^1(\eta) \cos \phi \sin \theta_0 \\ & + \sum_{j=1}^{\infty} \{A_{2,j}Y_j^0(\xi, \xi_0)P_j^0(\eta) + B_{2,j}Y_j^1(\xi, \xi_0)P_j^1(\eta) \cos \phi\}, \quad (2.17) \end{aligned}$$

$$\begin{aligned} \psi_3(\xi, \eta, \phi) = & \psi_3' \\ & + \sum_{j=1}^{\infty} \{A_{3,j}X_j^0(\xi, \xi_0)P_j^0(\eta) + B_{3,j}X_j^1(\xi, \xi_0)P_j^1(\eta) \cos \phi\}. \quad (2.18) \end{aligned}$$

The functions  $V_j^m(\xi, \xi_0, \eta)$  ( $m = 0, 1$ ) appearing in eq. (2.16) are defined as

$$V_j^m(\xi, \xi_0, \eta) \equiv Y_j^m(\xi'(\xi, \eta), \xi_0)P_j^m(\eta'(\xi, \eta)), \quad (2.19)$$

in which  $\xi'$  and  $\eta'$  are the first two spheroidal coordinates of the point  $(x, y, z)$  in the shifted coordinate system with origin at  $(0, 0, 2a\xi_0)$ . The first two terms in eq. (2.16) correspond to the potential due to the incident electric field  $E_0$ , as one easily verifies. A possible constant contribution to this potential has been chosen equal to zero. Since this potential only contains terms with  $m = 0, 1$  and no coupling can occur between different  $m$ -values, because of the rotational symmetry of the system about the  $z$ -axis, all potentials will only have terms with  $m = 0, 1$ , and for  $m = 1$  only terms with  $\cos \phi$  can appear. The coefficients  $\psi_2', \psi_3', \alpha, \beta$  and  $A_{1,j}, B_{1,j}, A'_{1,j}, B'_{1,j}, A_{2,j}, B_{2,j}, A_{3,j}, B_{3,j}$  ( $j = 1, 2, \dots$ ) have to be determined in such a way that the boundary conditions at the interfaces between the three media are satisfied. We note that because of eqs. (2.14) and (2.15) the expressions for the potentials eqs. (2.16)–(2.18) exactly reduce to eqs. (2.2), (2.6) and (2.7) of ref. 1 for the case of a sphere with radius  $R$  if  $\xi, \xi_0 \rightarrow \infty, a \rightarrow 0, a\xi_0 = R$ .

Thanks to the introduction of image multipoles the boundary conditions at the surface of the substrate ( $z = a\xi_0, \eta = \xi_0/\xi$ ) are easily satisfied. The continuity of  $\psi$  across this boundary implies

$$\begin{aligned} -\psi_2' + (1 - \alpha) \cos \theta_0 + (1 - \beta) \frac{1}{\xi_0} \sqrt{(1 + \xi^2)(1 - [\xi_0/\xi]^2)} \cos \phi \sin \theta_0 \\ + \sum_{j=1}^{\infty} \{A_{1,j} + (-1)^j A'_{1,j} - A_{2,j}\} (-1)^j V_j^0(\xi, \xi_0, \xi_0/\xi) \\ + \sum_{j=1}^{\infty} \{B_{1,j} + (-1)^{j+1} B'_{1,j} - B_{2,j}\} (-1)^{j+1} V_j^1(\xi, \xi_0, \xi_0/\xi) \cos \phi \\ = 0 \quad (\xi_0 \leq \xi < \infty, 0 \leq \phi \leq 2\pi). \quad (2.20) \end{aligned}$$

The continuity of the normal derivative of the potential times the dielectric constant leads to the condition

$$\begin{aligned} & \frac{1}{a\xi_0}(\epsilon_1 - \alpha\epsilon_2) \cos \theta_0 \\ & + \sum_{j=1}^{\infty} \left\{ \epsilon_1 A_{1,j} - \epsilon_1 (-1)^j A'_{1,j} - \epsilon_2 A_{2,j} \right\} (-1)^{j+1} \frac{d}{dz} \left[ V_j^0(\xi, \xi_0, \eta) \right]_{\eta=\xi_0/\xi} \\ & + \sum_{j=1}^{\infty} \left\{ \epsilon_1 B_{1,j} - \epsilon_1 (-1)^{j+1} B'_{1,j} - \epsilon_2 B_{2,j} \right\} (-1)^j \frac{d}{dz} \left[ V_j^1(\xi, \xi_0, \eta) \right]_{\eta=\xi_0/\xi} \cos \phi \\ & = 0 \quad (\xi_0 \leq \xi < \infty, 0 \leq \phi \leq 2\pi). \end{aligned} \quad (2.21)$$

Both equations (2.20) and (2.21) can be satisfied by putting

$$\begin{aligned} \psi'_2 &= \left( 1 - \frac{\epsilon_1}{\epsilon_2} \right) \cos \theta_0, \quad \alpha = \frac{\epsilon_1}{\epsilon_2}, \quad \beta = 1, \\ A_{2,j} &= \frac{2\epsilon_1}{\epsilon_1 + \epsilon_2} A_{1,j}, \quad A'_{1,j} = \frac{\epsilon_1 - \epsilon_2}{\epsilon_1 + \epsilon_2} (-1)^j A_{1,j}, \\ B_{2,j} &= \frac{2\epsilon_1}{\epsilon_1 + \epsilon_2} B_{1,j}, \quad B'_{1,j} = \frac{\epsilon_1 - \epsilon_2}{\epsilon_1 + \epsilon_2} (-1)^{j+1} B_{1,j}, \end{aligned} \quad (2.22)$$

which is almost exactly equal to eqs. (2.12) of ref. 1.

To solve the boundary conditions at the surface of the spheroid we make use of the fact that the functions  $P_l^m(\eta) \cos m\phi$ ,  $P_l^m(\eta) \sin m\phi$  ( $l = 0, 1, 2, \dots$ ;  $m = 0, 1, \dots, l$ ) constitute a complete orthogonal set on this surface. Multiplying the boundary conditions with  $P_k^m(\eta) \cos m\phi$  ( $m = 0, 1$ ) (the only choices for which we get a non-trivial result) and integrating over the surface of the spheroid yields:

$$\int_{-1}^1 d\eta \int_0^{2\pi} d\phi [\psi_1 - \psi_3]_{\xi=\xi_0} P_k^m(\eta) \cos m\phi = 0, \quad (2.23)$$

$$\int_{-1}^1 d\eta \int_0^{2\pi} d\phi \left[ \epsilon_1 \frac{\partial}{\partial \xi} \psi_1 - \epsilon_3 \frac{\partial}{\partial \xi} \psi_3 \right]_{\xi=\xi_0} P_k^m(\eta) \cos m\phi = 0. \quad (2.24)$$

Before continuing we note that as the functions  $V_j^m(\xi, \xi_0, \eta) \cos m\phi$  satisfy the Laplace equation in the region  $\xi < 2\xi_0$  (see eq. (2.19) and the remark below eq. (2.8)) it must be possible to express them in terms of the functions  $X_l^m(\xi, \xi_0) P_l^m(\eta) \cos m\phi$  in this region:

$$V_j^m(\xi, \xi_0, \eta) \cos m\phi = \sum_{l=m}^{\infty} c_{j,l}^m(\xi_0) X_l^m(\xi, \xi_0) P_l^m(\eta) \cos m\phi \quad (\xi < 2\xi_0). \quad (2.25)$$

(Because the primed coordinate system was obtained by a shift along the  $z$ -axis the  $\phi$ -dependence is unchanged.) In section 4 we shall derive a complete set of recurrence relations by which the coefficients  $c_{j,l}^m(\xi_0)$  appearing in this equation can be determined explicitly.

Using eq. (2.25) and the orthogonality relations of the associated Legendre functions:

$$\int_{-1}^1 d\eta P_j^m(\eta) P_k^m(\eta) = \frac{2(k+m)!}{(2k+1)(k-m)!} \delta_{j,k}, \quad (2.26)$$

the integrations in eqs. (2.23), (2.24) can be performed, and after eliminating the coefficients  $A'_{1,j}$  and  $B'_{1,j}$  by means of eqs. (2.22) we obtain the following set of equations for  $m=0$ :

$$\begin{aligned} & Y_k^0(\xi_0, \xi_0) A_{1,k} - X_k^0(\xi_0, \xi_0) A_{3,k} \\ & + \frac{\epsilon_1 - \epsilon_2}{\epsilon_1 + \epsilon_2} X_k^0(\xi_0, \xi_0) \sum_{j=1}^{\infty} c_{j,k}^0(\xi_0) (-1)^j A_{1,j} \\ & = -\delta_{k,1} X_1^0(\xi_0, \xi_0) \cos \theta_0 \quad (k=1, 2, \dots), \\ & \epsilon_1 \left[ \frac{\partial}{\partial \xi} Y_k^0(\xi, \xi_0) \right]_{\xi=\xi_0} A_{1,k} - \epsilon_3 \left[ \frac{\partial}{\partial \xi} X_k^0(\xi, \xi_0) \right]_{\xi=\xi_0} A_{3,k} \\ & + \epsilon_1 \frac{\epsilon_1 - \epsilon_2}{\epsilon_1 + \epsilon_2} \left[ \frac{\partial}{\partial \xi} X_k^0(\xi, \xi_0) \right]_{\xi=\xi_0} \sum_{j=1}^{\infty} c_{j,k}^0(\xi_0) (-1)^j A_{1,j} \\ & = -\epsilon_1 \delta_{k,1} \left[ \frac{\partial}{\partial \xi} X_1^0(\xi, \xi_0) \right]_{\xi=\xi_0} \cos \theta_0 \quad (k=1, 2, \dots), \end{aligned} \quad (2.27)$$

and for  $m=1$ :

$$\begin{aligned} & Y_k^1(\xi_0, \xi_0) B_{1,k} - X_k^1(\xi_0, \xi_0) B_{3,k} \\ & + \frac{\epsilon_1 - \epsilon_2}{\epsilon_1 + \epsilon_2} X_k^1(\xi_0, \xi_0) \sum_{j=1}^{\infty} c_{j,k}^1(\xi_0) (-1)^{j+1} B_{1,j} \\ & = -\delta_{k,1} X_1^1(\xi_0, \xi_0) \sin \theta_0 \quad (k=1, 2, \dots), \\ & \epsilon_1 \left[ \frac{\partial}{\partial \xi} Y_k^1(\xi, \xi_0) \right]_{\xi=\xi_0} B_{1,k} - \epsilon_3 \left[ \frac{\partial}{\partial \xi} X_k^1(\xi, \xi_0) \right]_{\xi=\xi_0} B_{3,k} \\ & + \epsilon_1 \frac{\epsilon_1 - \epsilon_2}{\epsilon_1 + \epsilon_2} \left[ \frac{\partial}{\partial \xi} X_k^1(\xi, \xi_0) \right]_{\xi=\xi_0} \sum_{j=1}^{\infty} c_{j,k}^1(\xi_0) (-1)^{j+1} B_{1,j} \\ & = -\epsilon_1 \delta_{k,1} \left[ \frac{\partial}{\partial \xi} X_1^1(\xi, \xi_0) \right]_{\xi=\xi_0} \sin \theta_0 \quad (k=1, 2, \dots). \end{aligned} \quad (2.28)$$

We further note that eq. (2.23) for  $m=0$  and  $k=0$  gives  $\psi'_3 = 0$  whereas eq. (2.24) for  $m=0$  and  $k=0$  is trivially satisfied. The coefficients  $A_{3,k}$  and  $B_{3,k}$  can be eliminated from eqs. (2.27) resp. (2.28) by dividing the first equation by  $X_k^m(\xi_0, \xi_0)/\epsilon_3$ , the second equation by  $\left[ \frac{\partial}{\partial \xi} X_k^m(\xi, \xi_0) \right]_{\xi=\xi_0}$  and subtracting the two, after which we obtain for  $m=0$ :

$$\begin{aligned} & \left\{ \epsilon_3 \frac{Y_k^0(\xi_0, \xi_0)}{X_k^0(\xi_0, \xi_0)} - \epsilon_1 \left[ \frac{\frac{\partial}{\partial \xi} Y_k^0(\xi, \xi_0)}{\frac{\partial}{\partial \xi} X_k^0(\xi, \xi_0)} \right]_{\xi=\xi_0} \right\} A_{1,k} \\ & + \frac{\epsilon_1 - \epsilon_2}{\epsilon_1 + \epsilon_2} (\epsilon_3 - \epsilon_1) \sum_{j=1}^{\infty} c_{j,k}^0(\xi_0) (-1)^j A_{1,j} \\ & = -(\epsilon_3 - \epsilon_1) \delta_{k,1} \cos \theta_0 \quad (k=1, 2, \dots), \end{aligned} \quad (2.29)$$

and for  $m = 1$ :

$$\left\{ \epsilon_3 \frac{Y_k^1(\xi_0, \xi_0)}{X_k^1(\xi_0, \xi_0)} - \epsilon_1 \left[ \frac{\partial Y_k^1(\xi, \xi_0)}{\partial \xi} X_k^1(\xi, \xi_0) \right]_{\xi=\xi_0} \right\} B_{1,k} + \frac{\epsilon_1 - \epsilon_2}{\epsilon_1 + \epsilon_2} (\epsilon_3 - \epsilon_1) \sum_{j=1}^{\infty} c_{j,k}^1(\xi_0) (-1)^{j+1} B_{1,j} = -(\epsilon_3 - \epsilon_1) \delta_{k,1} \sin \theta_0 \quad (k = 1, 2, \dots). \quad (2.30)$$

Approximate values for the dipole coefficients  $A_{1,1}$  or  $B_{1,1}$  are obtained by truncating the set of equations (2.29) or (2.30) at a sufficiently large value  $M$  of  $k$  and  $j$  and solving a now finite number of linear inhomogeneous equations. The quantities  $X_k^m(\xi_0, \xi_0)$ ,  $Y_k^m(\xi_0, \xi_0)$  and  $\left[ \frac{\partial X_k^m(\xi, \xi_0)}{\partial \xi} \right]_{\xi=\xi_0}$ ,  $\left[ \frac{\partial Y_k^m(\xi, \xi_0)}{\partial \xi} \right]_{\xi=\xi_0}$  appearing in these equations—which are essentially Legendre functions and their derivatives, see eqs. (2.10) and (2.11)—can be calculated by means of existing recurrence relations. The coefficients  $c_{j,k}^1(\xi_0)$  can be calculated with the help of recurrence relations that will be derived, as announced, in section 4. The coefficients  $A_{1,1}$  and  $B_{1,1}$  are of course spheroidal dipole coefficients, but they are also dipole coefficients in the usual sense since far from the particle ( $\xi \gg 1$ ) the spheroidal dipole fields are asymptotically equal to the usual (spherical) dipole fields, because of eqs. (2.11) and (2.13).

To define the polarizabilities normal and parallel to the substrate we proceed in a similar way as in ref. 1. We replace the particle by a point dipole just above the substrate with such a strength that the fields of this point dipole in the ambient and the substrate are asymptotically equal to the fields eqs. (2.16) and (2.17). The polarizability is then defined as the quotient of this dipole strength and the external electric field in the ambient. Defining a polarizability  $\alpha_{\perp}^e$  normal to the substrate and a polarizability  $\alpha_{\parallel}^e$  parallel to the substrate in this way, we obtain:

$$\alpha_{\perp}^e = -4\pi\epsilon_1(a\xi_0)^3(\cos \theta_0)^{-1} A_{1,1}, \quad (2.31)$$

$$\alpha_{\parallel}^e = -4\pi\epsilon_1(a\xi_0)^3(\sin \theta_0)^{-1} B_{1,1}. \quad (2.32)$$

Often it is more convenient to define the polarizability with respect to the so-called  $N$ -field<sup>7</sup>:

$$N \equiv (E_x, E_y, D_z), \quad (2.33)$$

with  $D_z$  the displacement field in the  $z$ -direction ( $D_z = \epsilon_1 E_z$  in the ambient). Denoting the thus defined polarizabilities by  $\alpha_{\perp}^n$  and  $\alpha_{\parallel}^n$  respectively, one obtains (confer ref. 1):

$$\alpha_{\perp}^n = \epsilon_1^{-2} \alpha_{\perp}^e = -4\pi\epsilon_1^{-1}(a\xi_0)^3(\cos \theta_0)^{-1} A_{1,1}, \quad (2.34)$$

$$\alpha_{\parallel}^n = \alpha_{\parallel}^e = -4\pi\epsilon_1(a\xi_0)^3(\sin \theta_0)^{-1} B_{1,1}. \quad (2.35)$$

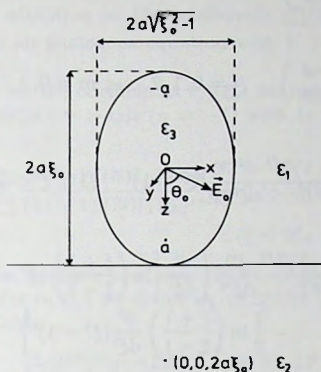


Fig. 2. A prolate spheroid on a substrate. Cross-section through the  $x$ - $z$  plane.

### 3 The polarizability of a prolate spheroid on a substrate

We now consider a prolate spheroidal particle on a substrate with axis of revolution normal to the surface of the substrate. The two foci lie at the axis of revolution at a distance  $a$  from the centre of the spheroid. The long axis has length  $2a\xi_0$  and the two short axes have length  $2a\sqrt{\xi_0^2 - 1}$  ( $1 \leq \xi_0 < \infty$ ), defining an elongation parameter  $\xi_0$  (see fig. 2). The limit  $\xi_0 \rightarrow \infty$ ,  $a \rightarrow 0$ ,  $a\xi_0 = R$  again corresponds to a sphere with radius  $R$  and the limit  $\xi_0 \rightarrow 1$  to a 'needle' with length  $2a$ .

The calculation of the polarizability of the prolate spheroid on a substrate is almost completely analogous to that of the oblate spheroid. We shall only briefly indicate the differences.

The spheroidal coordinates  $\xi$ ,  $\eta$  and  $\phi$  ( $1 \leq \xi < \infty$ ,  $-1 \leq \eta \leq 1$ ,  $0 \leq \phi \leq 2\pi$ ) should now be defined as<sup>6</sup>)

$$\xi \equiv \frac{\rho_1 + \rho_2}{2a}, \quad \eta \equiv \frac{\rho_1 - \rho_2}{2a}, \quad \phi \equiv \arctan\left(\frac{y}{x}\right), \quad (3.1)$$

with

$$\rho_1 \equiv \sqrt{(z+a)^2 + x^2 + y^2}, \quad \rho_2 \equiv \sqrt{(z-a)^2 + x^2 + y^2}. \quad (3.2)$$

Here  $\rho_1$  and  $\rho_2$  are the distances of the point  $(x, y, z)$  to the two foci and  $\phi$  is again the orientation of the plane through  $(x, y, z)$  and the  $z$ -axis with respect to the  $x$ - $z$  plane. The inverse of the transformation eqs. (3.1) and (3.2) now is

$$x = a\sqrt{(\xi^2 - 1)(1 - \eta^2)} \cos \phi, \quad y = a\sqrt{(\xi^2 - 1)(1 - \eta^2)} \sin \phi, \quad z = a\xi\eta. \quad (3.3)$$

Instead of the functions (2.5) and (2.7) we should use<sup>6</sup>)

$$P_l^m(\xi)P_l^m(\eta) \begin{pmatrix} \cos m\phi \\ \sin m\phi \end{pmatrix} \quad (l = 0, 1, 2, \dots; m = 0, 1, \dots, l) \quad (3.4)$$

and

$$Q_l^m(\xi)P_l^m(\eta) \begin{pmatrix} \cos m\phi \\ \sin m\phi \end{pmatrix} \quad (l = 0, 1, 2, \dots; m = 0, 1, \dots, l), \quad (3.5)$$

with

$$P_l^m(\xi) \equiv (-i)^m \frac{(\xi^2 - 1)^{m/2}}{2^l l!} \frac{d^{l+m}}{d\xi^{l+m}} (\xi^2 - 1)^l \quad (1 \leq \xi < \infty), \quad (3.6)$$

$$Q_l^m(\xi) \equiv (-1)^m \frac{(\xi^2 - 1)^{m/2}}{2^l l!} \frac{d^m}{d\xi^m} \left\{ \frac{d^l}{d\xi^l} \left[ \ln \left( \frac{\xi + 1}{\xi - 1} \right) (\xi^2 - 1)^l \right] - \frac{1}{2} \ln \left( \frac{\xi + 1}{\xi - 1} \right) \frac{d^l}{d\xi^l} (\xi^2 - 1)^l \right\} \quad (1 < \xi < \infty). \quad (3.7)$$

Note that the functions  $Q_l^m(\xi)$  are singular in  $\xi = 1$ .

We leave the definition eq. (2.9) of the reduced potential unchanged, but instead of the functions  $X_l^m(\xi, \xi_0)$  and  $Y_l^m(\xi, \xi_0)$  we introduce functions  $\bar{X}_l^m(\xi, \xi_0)$  and  $\bar{Y}_l^m(\xi, \xi_0)$  by

$$\bar{X}_l^m(\xi, \xi_0) \equiv \frac{2^l l! (l - m)!}{(2l)!} i^m \frac{1}{\xi_0^l} P_l^m(\xi), \quad (3.8)$$

$$\bar{Y}_l^m(\xi, \xi_0) \equiv \frac{(2l + 1)!}{2^l l! (l + m)!} \xi_0^{l+1} Q_l^m(\xi). \quad (3.9)$$

These definitions are such that the functions  $\bar{X}_l^m$  and  $\bar{Y}_l^m$  again have the property eqs. (2.14) and (2.15) respectively, with  $\bar{X}$  and  $\bar{Y}$  instead of  $X$  and  $Y$ . In the expressions eqs. (2.16)–(2.18) for the reduced potential one should replace all  $X$ 's by  $\bar{X}$ 's,  $Y$ 's by  $\bar{Y}$ 's and  $V$ 's by  $\bar{V}$ 's. The functions  $\bar{V}_j^m(\xi, \xi_0, \eta)$  are defined analogously to eq. (2.19). Now, however, we have to restrict  $\xi$  to the region  $1 \leq \xi < 2\xi_0 - 1$  since the functions  $\bar{V}_j^m(\xi, \xi_0, \eta)$  are singular on the line segment  $2\xi_0 - 1 \leq \xi \leq 2\xi_0 + 1$ ,  $\eta = 1$ . (This follows from eq. (2.19) with  $\bar{V}$ ,  $\bar{Y}$  and the fact that  $\bar{Y}_j^m(\xi', \xi_0)$  is singular for  $\xi' = 1$ .)

The boundary conditions at the surface of the substrate are again easily seen to be fulfilled if eqs. (2.22) are satisfied.

The boundary conditions at the surface of the spheroid lead to sets of equations similar to eqs. (2.29) and (2.30); one just has to replace  $X \rightarrow \bar{X}$ ,  $Y \rightarrow \bar{Y}$  and  $c \rightarrow \bar{c}$ . The coefficients  $\bar{c}_{j,l}^m(\xi_0)$  are defined by an equation analogous to eq. (2.25) with  $V \rightarrow \bar{V}$ ,  $c \rightarrow \bar{c}$ ,  $X \rightarrow \bar{X}$  and now  $1 \leq \xi < 2\xi_0 - 1$ . These coefficients satisfy recurrence relations similar to those for  $c_{j,l}^m(\xi_0)$ . This issue will be discussed in the next section.

The definitions eqs. (2.31), (2.32) and (2.34), (2.35) for the polarizabilities remain unchanged.

#### 4 Recurrence relations for the coefficients $c_{j,l}^m(\xi_0)$ and $\bar{c}_{j,l}^m(\xi_0)$

We now focus our attention on the coefficients  $c_{j,l}^m(\xi_0)$ , defined by eq. (2.25), and  $\bar{c}_{j,l}^m(\xi_0)$ , defined by an analogous equation with  $V \rightarrow \bar{V}$ ,  $c \rightarrow \bar{c}$ ,  $X \rightarrow \bar{X}$  and  $1 \leq \xi < 2\xi_0 - 1$ .

Concentrating first on the coefficients  $c_{j,l}^m(\xi_0)$  we remark that in particular eq. (2.25) is valid on the negative  $z$ -axis ( $\eta = -1$ ) with  $|z| < 2a\xi_0$ . Here we obtain, taking  $m = 0$ :

$$Q_j^0(i\xi + 2i\xi_0) = \sum_{l=0}^{\infty} \frac{2^{j+l}(j!)^2(l!)^2}{(2j+1)!(2l)!} \frac{(-1)^{j+l}}{(i\xi_0)^{j+l+1}} c_{j,l}^0(\xi_0) P_l^0(i\xi) \quad (\xi < 2\xi_0, j = 0, 1, 2, \dots). \quad (4.1)$$

To obtain this equation we have used eqs. (2.19), (2.10) and (2.11) and the fact that  $P_l^0(-1) = (-1)^l$ . For  $m = 1$  we divide eq. (2.25) by  $\sqrt{1 - \eta^2} \cos \phi$  and take the limit  $\eta \rightarrow -1$ , which yields:

$$\frac{Q_j^1(i\xi + 2i\xi_0)}{\sqrt{1 + (\xi + 2\xi_0)^2}} = \sum_{l=1}^{\infty} \frac{2^{j+l} j!(j-1)! l!(l+1)!}{(2j+1)!(2l)!} \frac{i(-1)^{j+l}}{(i\xi_0)^{j+l+1}} c_{j,l}^1(\xi_0) \frac{P_l^1(i\xi)}{\sqrt{1 + \xi^2}} \quad (\xi < 2\xi_0, j = 1, 2, \dots). \quad (4.2)$$

Here we have also used eqs. (2.19), (2.10) and (2.11) and furthermore the properties

$$\lim_{\eta \rightarrow -1} \frac{P_l^1(\eta)}{\sqrt{1 - \eta^2}} = \frac{1}{2} l(l+1) (-1)^{l+1} \quad (4.3)$$

and ( $\eta'$  defined as in section 2)

$$\lim_{\eta \rightarrow -1} \frac{\sqrt{1 - \eta'^2}}{\sqrt{1 - \eta^2}} = \frac{\sqrt{1 + \xi^2}}{\sqrt{1 + (\xi + 2\xi_0)^2}}. \quad (4.4)$$

Now from eqs. (2.6b) and (2.8) we observe that

$$P_l^1(i\xi) = -i\sqrt{1 + \xi^2} \frac{d}{d\xi} P_l^0(i\xi) \quad (l = 1, 2, \dots), \quad (4.5)$$

$$Q_l^1(i\xi) = -\sqrt{1 + \xi^2} \frac{d}{d\xi} Q_l^0(i\xi) \quad (l = 1, 2, \dots). \quad (4.6)$$

So differentiating eq. (4.1) with respect to  $\xi$  and comparing the result with eq. (4.2) we can make the following identification:

$$c_{j,l}^1(\xi_0) = -\frac{j}{l+1} c_{j,l}^0(\xi_0) \quad (j, l = 1, 2, \dots). \quad (4.7)$$

We can thus restrict our attention to the coefficients  $c_{j,l}^0$ .

The functions  $P_l^0(i\xi)$  and  $Q_j^0(i\xi + 2i\xi_0)$  in eq. (4.1) can be analytically continued to complex  $z = i\xi$  in a region around the origin. For  $P_l^0(i\xi)$  we can do this by means of eq. (2.6a), taking  $\eta$  complex, and for  $Q_j^0(i\xi + 2i\xi_0)$  by eq. (3.7), taking  $\xi$  complex. One can then verify that the function  $Q_j^0(z + 2i\xi_0)$  is analytic within and

on a suitably chosen ellipse  $C$  in the complex  $z$ -plane with foci at  $z = \pm 1$ . We can thus express the coefficients  $c_{j,l}^0$  in eq. (4.1) as follows<sup>5)</sup> (see also the orthogonality relations eq. (2.26) for  $m = 0$ ):

$$c_{j,l}^0(\xi_0) = \frac{(2j+1)!(2l+1)!}{2^{j+l+1}(j!)^2(l!)^2} (-1)^{j+l} \frac{(i\xi_0)^{j+l+1}}{\pi i} \oint_C dz Q_j^0(z + 2i\xi_0) Q_l^0(z) \quad (4.8a)$$

$$= \frac{(2j+1)!(2l+1)!}{2^{j+l+1}(j!)^2(l!)^2} (-1)^{j+l} (i\xi_0)^{j+l+1} \int_{-1}^1 dx Q_j^0(x + 2i\xi_0) P_l^0(x). \quad (4.8b)$$

The integration along the ellipse  $C$  in eq. (4.8a) should be performed counter-clockwise. We now make use of the following recurrence relations for  $P_l^0(z)$  and  $Q_l^0(z)$ :

$$(2l+1)zP_l^0(z) = (l+1)P_{l+1}^0(z) + lP_{l-1}^0(z), \quad (4.9)$$

$$(2l+1)zQ_l^0(z) = (l+1)Q_{l+1}^0(z) + lQ_{l-1}^0(z) + \delta_{l,0}, \quad (4.10)$$

where it is assumed that  $P_l^0$  and  $Q_l^0$  vanish for negative index  $l$ . A recurrence relation for the coefficients  $c_{j,l}^0$  is obtained by applying eqs. (4.9) and (4.10) after one another to eq. (4.8b):

$$\begin{aligned} & \frac{(j+1)^2}{(2j+3)(2j+1)} c_{j+1,l}^0(\xi_0) - \frac{(l+1)^2}{(2l+3)(2l+1)} c_{j,l+1}^0(\xi_0) - 2\xi_0^2 c_{j,l}^0(\xi_0) \\ & + \xi_0^2 (c_{j,l-1}^0(\xi_0) - c_{j-1,l}^0(\xi_0)) = -\xi_0^2 \delta_{j,0} \delta_{l,0}. \end{aligned} \quad (4.11)$$

This equation alone is not sufficient to determine the coefficients  $c_{j,l}^0$ . In order to obtain a second relation we use two other recurrence relations for  $P_l^0(z)$  and  $Q_l^0(z)$ :

$$(2l+1)P_l^0(z) = \frac{d}{dz} P_{l+1}^0(z) - \frac{d}{dz} P_{l-1}^0(z), \quad (4.12)$$

$$(2l+1)Q_l^0(z) = \frac{d}{dz} Q_{l+1}^0(z) - \frac{d}{dz} Q_{l-1}^0(z) + \delta_{l,0} \frac{z}{z^2-1}. \quad (4.13)$$

Applying eqs. (4.12) and (4.13) again one after another to eq. (4.8b) and using partial integration, we find the following relations:

$$\begin{aligned} & \frac{(j+1)}{(2j+3)(2j+1)} c_{j+1,l}^0(\xi_0) + \frac{1}{j} \xi_0^2 c_{j-1,l}^0(\xi_0) \\ & + \frac{(l+1)}{(2l+3)(2l+1)} c_{j,l+1}^0(\xi_0) + \frac{1}{l} \xi_0^2 c_{j,l-1}^0(\xi_0) = 0 \quad (j > 0, l > 0), \end{aligned} \quad (4.14a)$$

$$\begin{aligned} & \frac{(j+1)}{(2j+3)(2j+1)} c_{j+1,0}^0(\xi_0) + \frac{1}{j} \xi_0^2 c_{j-1,0}^0(\xi_0) + \frac{1}{3} c_{j,1}^0(\xi_0) \\ & = \frac{(-1)^j (2j)!}{2^j (j!)^2} \xi_0^{j+2} \text{Im} \{ i^{j+1} Q_{j+1}^0(1 + 2i\xi_0) + i^{j-1} Q_{j-1}^0(1 + 2i\xi_0) \} \\ & \quad (j > 0), \end{aligned} \quad (4.14b)$$

$$c_{j,0}^0(\xi_0) = \frac{(-1)^j (2j)!}{2^j (j!)^2} \xi_0^{j+1} \operatorname{Re} \left\{ i^{j+1} Q_{j+1}^0(1+2i\xi_0) + i^{j-1} Q_{j-1}^0(1+2i\xi_0) \right\} \quad (j > 0), \quad (4.14c)$$

$$c_{0,0}^0(\xi_0) = \xi_0 \arctan \left( \frac{1}{\xi_0} \right) - \frac{1}{2} \xi_0^2 \ln \left( 1 + \frac{1}{\xi_0} \right). \quad (4.14d)$$

To derive these equations we have used the fact that  $P_l^0(1) = 1$  and  $P_l^0(-1) = (-1)^l$ . In eqs. (4.14b)–(4.14d) the right-hand sides do not vanish because the boundary terms resulting from the partial integration do not cancel each other, as has happened in eq. (4.14a). To evaluate these boundary terms we have used the property

$$Q_l^0(-z^*) = (-1)^{l+1} [Q_l^0(z)]^*, \quad (4.15)$$

where the asterisk denotes complex conjugation. With eqs. (4.11) and (4.14) the coefficients  $c_{j,l}^0$  can be determined for all  $j$  and  $l$ . One further observes from these equations that there is a symmetry between the indices  $j$  and  $l$ :

$$c_{l,j}^0(\xi_0) = (-1)^{j+l} c_{j,l}^0(\xi_0). \quad (4.16)$$

(This can also be proved directly from eq. (4.8a).)

Recurrence relations for the coefficients  $\bar{c}_{j,l}^m$  are obtained in a completely analogous way. First of all one may convince oneself that eq. (4.7) is also valid for these coefficients:

$$\bar{c}_{j,l}^1(\xi_0) = -\frac{j}{l+1} \bar{c}_{j,l}^0(\xi_0) \quad (j, l = 1, 2, \dots). \quad (4.17)$$

The derivation of the recurrence relations for  $\bar{c}_{j,l}^0$  essentially amounts to replacing  $\xi_0$  by  $-i\xi_0$  in the above. Instead of eq. (4.11) we then obtain:

$$\begin{aligned} \frac{(j+1)^2}{(2j+3)(2j+1)} \bar{c}_{j+1,l}^0(\xi_0) - \frac{(l+1)^2}{(2l+3)(2l+1)} \bar{c}_{j,l+1}^0(\xi_0) + 2\xi_0^2 \bar{c}_{j,l}^0(\xi_0) \\ - \xi_0^2 (\bar{c}_{j,l-1}^0(\xi_0) - \bar{c}_{j-1,l}^0(\xi_0)) = \xi_0^2 \delta_{j,0} \delta_{l,0}, \end{aligned} \quad (4.18)$$

and instead of eq. (4.14a):

$$\begin{aligned} \frac{(j+1)}{(2j+3)(2j+1)} \bar{c}_{j+1,l}^0(\xi_0) - \frac{1}{j} \xi_0^2 \bar{c}_{j-1,l}^0(\xi_0) \\ + \frac{(l+1)}{(2l+3)(2l+1)} \bar{c}_{j,l+1}^0(\xi_0) - \frac{1}{l} \xi_0^2 \bar{c}_{j,l-1}^0(\xi_0) = 0 \quad (j > 0, l > 0), \end{aligned} \quad (4.19a)$$

In eqs. (4.14b)–(4.14d) we have to re-examine the boundary terms resulting from the partial integration. Doing this, we find:

$$\begin{aligned} \frac{(j+1)}{(2j+3)(2j+1)} \bar{c}_{j+1,0}^0(\xi_0) - \frac{1}{j} \xi_0^2 \bar{c}_{j-1,0}^0(\xi_0) + \frac{1}{3} \bar{c}_{j,1}^0(\xi_0) \\ = -\frac{(-1)^j (2j)!}{2^{j+1} (j!)^2} \xi_0^{j+2} \left\{ Q_{j+1}^0(1+2\xi_0) + Q_{j+1}^0(-1+2\xi_0) \right. \\ \left. - Q_{j-1}^0(1+2\xi_0) - Q_{j-1}^0(-1+2\xi_0) \right\} \quad (j > 0), \end{aligned} \quad (4.19b)$$

$$\bar{c}_{j,0}^0(\xi_0) = \frac{(-1)^j (2j)!}{2^{j+1} (j!)^2} \xi_0^{j+1} \left\{ Q_{j+1}^0(1+2\xi_0) - Q_{j+1}^0(-1+2\xi_0) - Q_{j-1}^0(1+2\xi_0) + Q_{j-1}^0(-1+2\xi_0) \right\} \quad (j > 0), \quad (4.19c)$$

$$\bar{c}_{0,0}^0(\xi_0) = \frac{1}{2} \xi_0 \ln \left( \frac{\xi_0 + 1}{\xi_0 - 1} \right) + \frac{1}{2} \xi_0^2 \ln \left( 1 - \frac{1}{\xi_0^2} \right). \quad (4.19d)$$

The symmetry relation eq. (4.16) is also seen to be valid for the coefficients  $\bar{c}_{j,j}^0$ :

$$\bar{c}_{l,j}^0(\xi_0) = (-1)^{j+l} \bar{c}_{j,l}^0(\xi_0). \quad (4.20)$$

Our problem had been formulated in such a way that the limit  $\xi_0 \rightarrow \infty$ ,  $a \rightarrow 0$ ,  $a\xi_0 = R$  corresponds to a sphere with radius  $R$ , both for the oblate and the prolate spheroid (see sections 2 and 3). If we take the limit  $\xi_0 \rightarrow \infty$  in the recurrence relations above, we obtain:

$$\lim_{\xi_0 \rightarrow \infty} c_{j,j}^m(\xi_0) = \lim_{\xi_0 \rightarrow \infty} \bar{c}_{j,j}^m(\xi_0) = \frac{(j+l)!}{(j-m)!(l+m)!} \frac{(-1)^{j+m}}{2^{j+l+1}}, \quad (4.21)$$

which is in agreement with eq. (3.1) of ref. 1. To derive eq. (4.21) one has to make use of the asymptotic behaviour of the functions  $Q_l^0(z)$ :

$$Q_l^0(z) = \frac{2^l (l!)^2}{(2l+1)!} \frac{1}{z^{l+1}} \left[ 1 + O\left(\frac{1}{z^2}\right) \right] \quad (|z| \rightarrow \infty). \quad (4.22)$$

## 5 The disk and the needle

Two interesting special cases are the limit  $\xi_0 \rightarrow 0$  for the oblate spheroid, which corresponds to a thin circular disk with radius  $a$ , and the limit  $\xi_0 \rightarrow 1$  for the prolate spheroid, corresponding to a needle with length  $2a$ . For both cases we shall show that the interaction with the substrate vanishes, i.e. the second term on the left-hand sides of eqs. (2.29) and (2.30) may be neglected (for the prolate spheroid we should replace  $X$  by  $\bar{X}$ ,  $Y$  by  $\bar{Y}$  and  $c$  by  $\bar{c}$ ). The polarizabilities thus become equal to those for the *free* disk and needle.

To prove this for the disk we need to know the behaviour of the various quantities occurring in eqs. (2.29) and (2.30) if  $\xi_0 \rightarrow 0$ . Inspection of eqs. (2.10), (2.11) and (2.6b), (2.8) teaches us that

$$X_l^m(\xi_0, \xi_0) = \begin{cases} O(1/\xi_0^l) & \text{if } l+m \text{ even,} \\ O(1/\xi_0^{l-1}) & \text{if } l+m \text{ odd,} \end{cases} \quad (5.1a)$$

$$\left[ \frac{\partial}{\partial \xi} X_l^m(\xi, \xi_0) \right]_{\xi=\xi_0} = \begin{cases} O(1/\xi_0^{l-1}) & \text{if } l+m \text{ even,} \\ O(1/\xi_0^l) & \text{if } l+m \text{ odd,} \end{cases} \quad (5.1b)$$

$$Y_l^m(\xi_0, \xi_0) = O(\xi_0^{l+1}), \quad (5.2a)$$

$$\left[ \frac{\partial}{\partial \xi} Y_l^m(\xi, \xi_0) \right]_{\xi=\xi_0} = O(\xi_0^{l+1}). \quad (5.2b)$$

Furthermore eqs. (4.7) and (4.8b) for the coefficients  $c_{j,l}^m$  show us that

$$c_{j,l}^m(\xi_0) = \mathcal{O}(\xi_0^{j+l+1}). \quad (5.3)$$

This is true because the integral appearing in eq. (4.8b) is finite if  $\xi_0 \rightarrow 0$  (for  $\xi_0 = 0$  it is in fact a known integral<sup>8</sup>). To clarify the proof we introduce new multipole coefficients  $A''_{1,j}$  and  $B''_{1,j}$  by

$$A''_{1,j} = \xi_0^{j+1} A_{1,j} \quad (j = 1, 2, \dots), \quad (5.4)$$

$$B''_{1,j} = \xi_0^{j+1} B_{1,j} \quad (j = 1, 2, \dots). \quad (5.5)$$

If we now look at eqs. (2.29) and (2.30), expressed in terms of the new multipole coefficients  $A''_{1,j}$  and  $B''_{1,j}$ , we see that the off-diagonal matrix elements of these equations ( $k \neq j$ ) are always an order  $\xi_0$  smaller than the diagonal matrix elements ( $k = j$ ). So in the limit  $\xi_0 \rightarrow 0$  the coupling between the multipole coefficients by the interaction with the substrate disappears and the dipole coefficients become equal to those for the free disk. These dipole coefficients are easily evaluated (by solving eqs. (2.29) and (2.30) for  $k = 1$  and omitting the second term on the l.h.s.). In terms of the polarizabilities  $\alpha_{\perp}^e$  and  $\alpha_{\parallel}^e$  (eqs. (2.31) and (2.32)) we then find:

$$\lim_{\xi_0 \rightarrow 0} \alpha_{\perp}^e = \epsilon_1 \frac{\epsilon_3 - \epsilon_1}{\epsilon_3} V, \quad (5.6)$$

$$\lim_{\xi_0 \rightarrow 0} \alpha_{\parallel}^e = (\epsilon_3 - \epsilon_1) V, \quad (5.7)$$

with  $V$  the volume of the disk:  $V = \frac{4}{3} \pi a^3 \xi_0 (\xi_0^2 + 1)$ . The results eqs. (5.6) and (5.7) are in agreement with the results eqs. (5.16) and (5.17) found in ref. 1 for the case of a thin spherical cap on a substrate.

For the needle the proof is based on the singular behaviour of the functions  $\tilde{Y}_l^m(\xi, \xi_0)$  and their derivatives in  $\xi = 1$  (see eqs. (3.9) and (3.7)), whereas the functions  $\tilde{X}_l^m(\xi, \xi_0)$  and their derivatives (eqs. (3.8) and (3.6)) and the coefficients  $\tilde{c}_{j,l}^m(\xi_0)$  remain finite if  $\xi \rightarrow 1$  resp.  $\xi_0 \rightarrow 1$ . The finiteness of the coefficients  $\tilde{c}_{j,l}^m(\xi_0)$  is not obvious at first sight, since both  $Q_{j+1}^0(-1 + 2\xi_0)$  and  $Q_{j-1}^0(-1 + 2\xi_0)$  in eqs. (4.19b) and (4.19c) are singular in  $\xi_0 = 1$ . From the recurrence relation eq. (4.10), however, it follows that the singular parts of all functions  $Q_j^0(z)$  in  $z = 1$  are equal. The singularities in eqs. (4.19b) and (4.19c) thus cancel. As a consequence the off-diagonal matrix elements of the equations for the multipole coefficients  $A_{1,j}$  and  $B_{1,j}$  again become negligible with respect to the diagonal matrix elements if  $\xi_0 \rightarrow 1$  (see eqs. (2.29) and (2.30) with  $X \rightarrow \tilde{X}$ ,  $Y \rightarrow \tilde{Y}$ ,  $c \rightarrow \tilde{c}$ ). The polarizabilities  $\alpha_{\perp}^e$  and  $\alpha_{\parallel}^e$  thus become equal to those for the free needle:

$$\lim_{\xi_0 \rightarrow 1} \alpha_{\perp}^e = (\epsilon_3 - \epsilon_1) V, \quad (5.8)$$

$$\lim_{\xi_0 \rightarrow 1} \alpha_{\parallel}^e = 2\epsilon_1 \frac{\epsilon_3 - \epsilon_1}{\epsilon_3 + \epsilon_1} V, \quad (5.9)$$

$V$  being the volume of the needle:  $V = \frac{4}{3} \pi a^3 \xi_0 (\xi_0^2 - 1)$ .

		AR		
		2.0	1.0	0.5
FS		2.54647+0.333484i	4.86589+1.27995i	8.98965+14.0098i
CDA		4.42485+1.045178i	6.01181+2.03719i	7.16624+16.7037i
M	1	3.01631+0.471236i	6.01181+2.03719i	4.33705+18.7764i
	2	3.09676+0.519677i	6.15479+2.21669i	3.20593+18.7597i
	4	3.15785+0.568521i	6.27881+2.42216i	2.14637+18.5674i
	8	3.16913+0.587193i	6.31121+2.53494i	1.55110+18.2659i
	16	3.16897+0.588837i	6.30744+2.55788i	1.38879+18.0829i

Table 1. Values of  $\alpha_{\perp}^0/V$  for different values of the axial ratio (AR) of the spheroid and different values of the number  $M$  of multipoles taken into account ( $\epsilon_1 = 1$ ,  $\epsilon_2 = 3.1329$ ,  $\epsilon_3 = -5.28 + 2.25i$ ). Also included are the values for the free spheroid (FS) and the conventional dipole approximation (CDA).

		AR		
		2.0	1.0	0.5
FS		8.18936+4.34576i	4.86589+1.27995i	3.55249+0.660120i
CDA		3.50688+19.1355i	5.38548+1.59507i	3.61918+0.686066i
M	1	9.61868+7.59232i	5.38548+1.59507i	3.68348+0.711612i
	2	9.63714+8.06880i	5.42439+1.63468i	3.68857+0.714989i
	4	9.58045+8.51897i	5.46024+1.67581i	3.69462+0.719318i
	8	9.53902+8.60783i	5.47159+1.69429i	3.69794+0.722126i
	16	9.53422+8.61056i	5.47219+1.69735i	3.69868+0.723054i

Table 2. Values of  $\alpha_{\parallel}^0/V$ . Details the same as in table 1.

## 6 The dipole approximation

In tables 1 and 2 we have given the results of some calculations for the polarizabilities per unit of volume  $\alpha_{\perp}^0/V$  and  $\alpha_{\parallel}^0/V$  for three different values of the axial ratio (AR) of the spheroid ( $V$  is the volume of the spheroid). We define the axial ratio as the diameter of the particle, as observed from above, divided by its height. An axial ratio of 1 thus corresponds to a sphere, axial ratios larger than 1 correspond to oblate spheroids and axial ratios smaller than 1 to prolate spheroids. The relation between the axial ratio and the parameter  $\xi_0$  is clear from figs. 1 and 2. For the value of  $\epsilon_3$  of the particle we have chosen  $-5.28 + 2.25i$ , which is the dielectric constant of gold at a wavelength  $\lambda$  of 540 nm (in vacuum), interpolated from the values given by Johnson and Christy<sup>9</sup>). The dielectric constant of the substrate is chosen equal to that of sapphire in the region of visible light:  $\epsilon_2 = 3.1329$ . The ambient is assumed to be vacuum:  $\epsilon_1 = 1$ . The calculations were done for different values  $M$  of the number of multipoles taken into account. The value chosen for  $\epsilon_3$  lies in the plasmon resonance region of gold, where the polarizabilities can be expected to be large (see also section 7). Nevertheless the convergence with increasing

$M$  is good for all three values of the axial ratio. Even the dipole approximation ( $M = 1$ ) already gives a quite good result. This approximation can be written in the following form (see eqs. (2.29) and (2.30) for the oblate spheroid, or the same equation with  $\bar{X}$ ,  $\bar{Y}$  and  $\bar{c}$  for the prolate spheroid, and also eqs. (2.31) and (2.32)):

$$\alpha_{\perp}^{e(d)} = \frac{\epsilon_1(\epsilon_3 - \epsilon_1)V}{\epsilon_1 + L_{\perp}(\epsilon_3 - \epsilon_1)}, \quad (6.1)$$

$$\alpha_{\parallel}^{e(d)} = \frac{\epsilon_1(\epsilon_3 - \epsilon_1)V}{\epsilon_1 + L_{\parallel}(\epsilon_3 - \epsilon_1)}, \quad (6.2)$$

with so-called depolarization factors  $L_{\perp}$  and  $L_{\parallel}$ , which can easily be calculated from eqs. (2.10), (2.11) and (4.14b)–(4.14d) for the oblate spheroid and eqs. (3.8), (3.9) and (4.19b)–(4.19d) for the prolate spheroid:

$$L_{\perp} = (1 + \xi_0^2) \left\{ 1 - \xi_0 \arctan \left( \frac{1}{\xi_0} \right) - \frac{\epsilon_1 - \epsilon_2}{\epsilon_1 + \epsilon_2} \left[ \left( \frac{3}{2} + \xi_0^2 \right) \xi_0^2 \ln \left( 1 + \frac{1}{\xi_0^2} \right) - \xi_0 \arctan \left( \frac{1}{\xi_0} \right) - \xi_0^2 \right] \right\}, \quad (6.3)$$

$$L_{\parallel} = (1 + \xi_0^2) \left\{ -\frac{1}{2} \frac{\xi_0^2}{1 + \xi_0^2} + \frac{1}{2} \xi_0 \arctan \left( \frac{1}{\xi_0} \right) - \frac{1}{2} \frac{\epsilon_1 - \epsilon_2}{\epsilon_1 + \epsilon_2} \left[ \left( \frac{3}{2} + \xi_0^2 \right) \xi_0^2 \ln \left( 1 + \frac{1}{\xi_0^2} \right) - \xi_0 \arctan \left( \frac{1}{\xi_0} \right) - \xi_0^2 \right] \right\}, \quad (6.4)$$

for the oblate spheroid, and

$$L_{\perp} = (1 - \xi_0^2) \left\{ 1 - \frac{1}{2} \xi_0 \ln \left( \frac{\xi_0 + 1}{\xi_0 - 1} \right) + \frac{\epsilon_1 - \epsilon_2}{\epsilon_1 + \epsilon_2} \left[ \left( \frac{3}{2} - \xi_0^2 \right) \xi_0^2 \ln \left( 1 - \frac{1}{\xi_0^2} \right) + \frac{1}{2} \xi_0 \ln \left( \frac{\xi_0 + 1}{\xi_0 - 1} \right) - \xi_0^2 \right] \right\}, \quad (6.5)$$

$$L_{\parallel} = (1 - \xi_0^2) \left\{ \frac{1}{2} \frac{\xi_0^2}{1 - \xi_0^2} + \frac{1}{4} \xi_0 \ln \left( \frac{\xi_0 + 1}{\xi_0 - 1} \right) + \frac{1}{2} \frac{\epsilon_1 - \epsilon_2}{\epsilon_1 + \epsilon_2} \left[ \left( \frac{3}{2} - \xi_0^2 \right) \xi_0^2 \ln \left( 1 - \frac{1}{\xi_0^2} \right) + \frac{1}{2} \xi_0 \ln \left( \frac{\xi_0 + 1}{\xi_0 - 1} \right) - \xi_0^2 \right] \right\}, \quad (6.6)$$

for the prolate spheroid. In tables 1 and 2 we have also included the polarizabilities per unit of volume for the free spheroid (FS), which can be obtained from the above formulae by omitting the terms representing the interaction with the substrate (the terms with  $(\epsilon_1 - \epsilon_2)/(\epsilon_1 + \epsilon_2)$ ).

Furthermore we have included in tables 1 and 2 the results found when applying the usual—conventional—dipole approximation (CDA). In this approximation the spheroid is replaced by a point particle at its centre with the same free polarizability. The interaction with the substrate is then calculated in *spherical* dipole approximation<sup>10</sup>). The results found for the polarizabilities  $\alpha_{\perp}^f$  and  $\alpha_{\parallel}^f$  can then also be written in the form eqs. (6.1) and (6.2), but with different depolarization factors, namely:

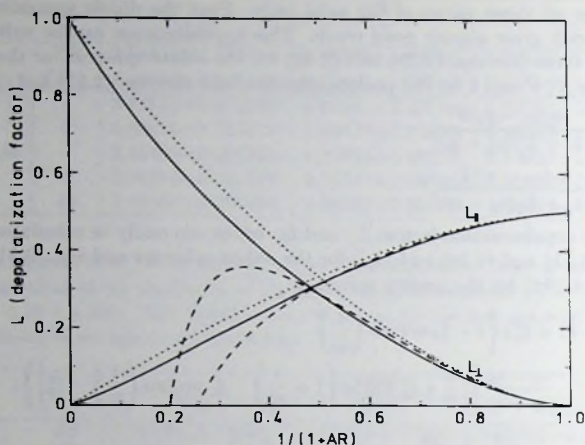


Fig. 3. The depolarization factors  $L_{\perp}$  and  $L_{\parallel}$  as a function of  $1/(1+AR)$  ( $\epsilon_1 = 1$ ,  $\epsilon_2 = 3.1329$ ). The dotted line corresponds to the free depolarization factors, the dashed to the depolarization factors for the spherical dipole approximation and the solid to those for the spheroidal dipole approximation.

$$L_{\perp}^{(cd)} = (1 + \xi_0^2) \left\{ 1 - \xi_0 \arctan \left( \frac{1}{\xi_0} \right) + \frac{1}{12} \frac{1}{\xi_0^2} \frac{\epsilon_1 - \epsilon_2}{\epsilon_1 + \epsilon_2} \right\}, \quad (6.7)$$

$$L_{\parallel}^{(cd)} = (1 + \xi_0^2) \left\{ -\frac{1}{2} \frac{\xi_0^2}{1 + \xi_0^2} + \frac{1}{2} \xi_0 \arctan \left( \frac{1}{\xi_0} \right) + \frac{1}{24} \frac{1}{\xi_0^2} \frac{\epsilon_1 - \epsilon_2}{\epsilon_1 + \epsilon_2} \right\}, \quad (6.8)$$

for the oblate spheroid, and

$$L_{\perp}^{(cd)} = (1 - \xi_0^2) \left\{ 1 - \frac{1}{2} \xi_0 \ln \left( \frac{\xi_0 + 1}{\xi_0 - 1} \right) - \frac{1}{12} \frac{1}{\xi_0^2} \frac{\epsilon_1 - \epsilon_2}{\epsilon_1 + \epsilon_2} \right\}, \quad (6.9)$$

$$L_{\parallel}^{(cd)} = (1 - \xi_0^2) \left\{ \frac{1}{2} \frac{\xi_0^2}{1 - \xi_0^2} + \frac{1}{4} \xi_0 \ln \left( \frac{\xi_0 + 1}{\xi_0 - 1} \right) - \frac{1}{24} \frac{1}{\xi_0^2} \frac{\epsilon_1 - \epsilon_2}{\epsilon_1 + \epsilon_2} \right\}, \quad (6.10)$$

for the prolate spheroid.

In fig. 3 we have plotted the various depolarization factors as a function of  $1/(1+AR)$ . For a disk this quantity is 0 ( $AR = \infty$ ), for a needle it is 1 ( $AR = 0$ ) and it is 0.5 for a sphere ( $AR = 1$ ). Again we have taken  $\epsilon_1 = 1$  (vacuum) and  $\epsilon_2 = 3.1329$  (sapphire). The behaviour of the depolarization factors for the spheroidal dipole approximation if  $AR \rightarrow \infty$  or  $AR \rightarrow 0$  is in agreement with the results of the previous section and in particular with eqs. (5.6)–(5.9). For the sphere

the conventional, spherical dipole approximation and the spheroidal dipole approximation are of course equal and so are their corresponding depolarization factors. For the oblate spheroid the spherical dipole approximation heavily overestimates the interaction with the substrate; the depolarization factors even go to  $-\infty$  for the disk. For the prolate spheroid the spherical dipole approximation underestimates this interaction. Concluding, we may say that as a simple approximation the spheroidal dipole approximation is to be preferred to the spherical dipole approximation.

## 7 Application to a square lattice of gold particles on sapphire

We shall now apply our theory to a transmission experiment performed by Niklasson and Craighead<sup>3,4</sup>) with a square lattice of gold particles on a sapphire substrate. In ref. 2 the particles were modeled as truncated spheres and a good agreement with the experiment was found if the particles were assumed to have a diameter of 26.8 nm and an axial ratio of 1.21. Examining their system by electron microscopy Niklasson and Craighead estimated the diameter of the particles to be 32 nm, with an uncertainty of 2.5 nm, and the axial ratio to be between 1.3 and 1.7. They themselves modeled the particles as oblate spheroids and used the conventional, spherical dipole approximation (see section 6) to incorporate the interaction with the substrate. With the theory developed in this chapter we now have the ability to incorporate this interaction rigorously.

Once the polarizability  $\alpha_{\parallel}^{\text{st}}$  of one oblate spheroidal particle is known, the calculation of the transmittance is analogous to that in ref. 2. One introduces an effective surface susceptibility  $\gamma^{11}$ ), which is given by

$$\gamma = \frac{\alpha_{\parallel}^{\text{st}}/L^2}{1 - (\alpha_{\parallel}^{\text{st}}/8\pi L^3) \left\{ F(0) + [(1 - \epsilon_2)/(1 + \epsilon_2)] F(\xi_0 d / \sqrt{\xi_0^2 + 1} L) \right\}}, \quad (7.1)$$

with  $L$  the lattice constant and  $d$  the diameter of the oblate spheroid, as observed from above. The dielectric constant  $\epsilon_1$  of the ambient is assumed to be 1. The flattening parameter  $\xi_0$  was defined in section 2. The second term in the denominator of eq. (7.1) accounts for local field effects due to the interaction between the particles. This interaction is calculated in (unretarded) dipole approximation. (In this calculation ordinary spherical dipole fields are used; the distance between the particles is large enough to justify this.) The function  $F(x)$  is the following lattice sum:

$$F(x) = \sum'_{i,j} \{i^2 + j^2 + x^2\}^{-3/2} - 3x^2 \sum'_{i,j} \{i^2 + j^2 + x^2\}^{-5/2}, \quad (7.2)$$

where the sums extend over all pairs of integers  $(i, j)$  except  $(0, 0)$ . This function can be approximated numerically without difficulty. At  $x = 0$   $F(x)$  is maximal and has

<sup>1</sup>Since in the transmission experiment the incident light was perpendicular to the sample, and thus the electric field parallel to the substrate, only the polarizability parallel to the substrate plays a role.

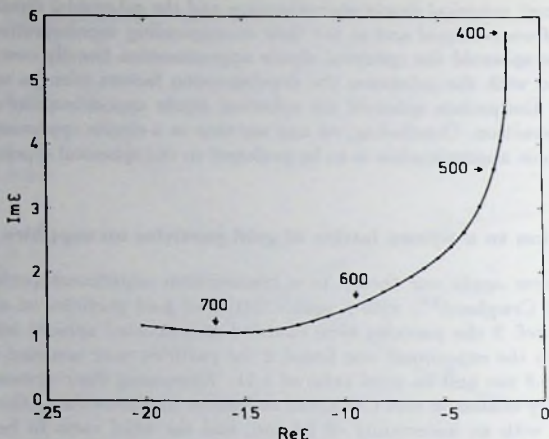


Fig. 4. Interpolated results for the dielectric constant  $\epsilon$  of gold according to Johnson and Christy<sup>9</sup>). The wavelength  $\lambda$  is indicated in nm. The dots indicate intervals of 10 nm.

the value 9.0336. The term with  $F(0)$  in the denominator of eq. (7.1) represents the interaction of a particle with the *direct* dipole fields of the other particles, whereas the second term represents the interaction with the *image* dipole fields of the other particles. From the surface susceptibility  $\gamma$  the transmittance of the sample can be calculated<sup>11</sup>). In the experiment of Niklasson and Craighead the transmittance was measured relative to the bare substrate. This relative transmittance, in percents, is related to the susceptibility  $\gamma$  by<sup>2</sup>)

$$T = \frac{100\%}{|1 - i(\omega/c)\gamma/(1 + n_2)|^2}, \quad (7.3)$$

$\omega$  being the angular frequency of the incident light,  $c$  the speed of light and  $n_2$  the refractive index of the sapphire ( $n_2 = \sqrt{\epsilon_2} = 1.77$ ).

We have calculated the transmittance for our oblate spheroidal model with the help of eqs. (7.1)-(7.3) for different diameters and axial ratios in the wavelength region  $\lambda = 400-750$  nm. For the lattice constant  $L$  we took 50 nm, the value used by Niklasson and Craighead. The dielectric constant  $\epsilon_2$  of the substrate was supposed to be 3.1329 (sapphire). For the dielectric constant of gold we took the values of Johnson and Christy<sup>9</sup>). In fig. 4 we have plotted an interpolation of these data. To obtain good agreement<sup>2</sup>), however, it is necessary to apply a finite size correction to these values. Due to the very small size of the particles the mean free path of the conduction electrons is shorter than in the bulk, which changes the dielectric constant. This effect can be taken into account qualitatively in the

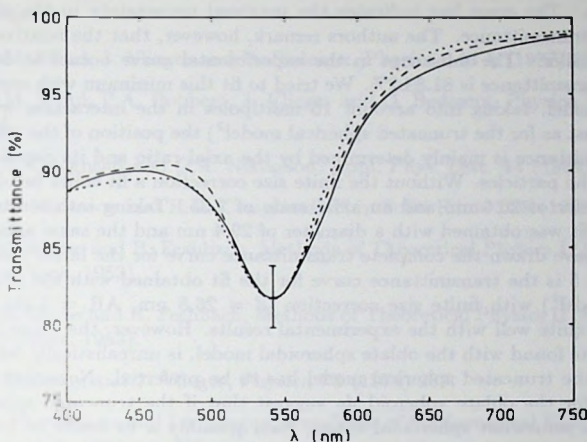


Fig. 5. Relative transmittance as a function of wavelength. The experimental transmittance<sup>3,4</sup>) is indicated by the solid line, the fit for the spheroidal model by the dashed line ( $d = 29.4$  nm,  $AR = 2.35$ ) and the fit for the truncated spherical model<sup>2</sup>) by the dotted line ( $d = 26.8$  nm,  $AR = 1.21$ ).

following way<sup>12</sup>):

$$\epsilon(\omega) = \epsilon_B(\omega) + \frac{\omega_p^2}{\omega^2 + i\omega\tau_B^{-1}} - \frac{\omega_p^2}{\omega^2 + i\omega\tau^{-1}}, \quad (7.4)$$

with  $\epsilon_B(\omega)$  the bulk dielectric constant,  $\omega_p$  the plasma frequency of gold and  $\tau_B$  the relaxation time in the bulk. The time  $\tau$  is the relaxation time corrected for the finite size of the particles:

$$\tau^{-1} = \tau_B^{-1} + v_F R'^{-1}, \quad (7.5)$$

$v_F$  being the Fermi velocity and  $R'$  some effective radius of the particle. As suggested in ref. 12 a good choice for this effective radius should be half the short axis of the particles:

$$R' = \frac{1}{2} \frac{\xi_0}{\sqrt{\xi_0^2 + 1}} d. \quad (7.6)$$

Using eqs. (7.4)–(7.6) we obtained corrected values for the dielectric constant of the gold particle. We took  $\hbar\omega_p = 8.99$  eV,  $\hbar\tau_B^{-1} = 0.027$  eV<sup>13</sup>) and  $\hbar v_F = 0.915$  eV nm<sup>14</sup>).

In fig. 5 we have plotted the transmittance measured by Niklasson and Craighed<sup>3,4</sup>) as a function of wavelength. Clearly visible is the resonance peak around

$\lambda = 540$  nm. The error bar indicates the maximal uncertainty in the absolute value of the transmittance. The authors remark, however, that the relative errors are much smaller. The minimum in the experimental curve occurs at 540 nm, where the transmittance is  $81.8 \pm 2\%$ . We tried to fit this minimum with our oblate spheroidal model, taking into account 16 multipoles in the interaction with the substrate. Just as for the truncated spherical model<sup>2)</sup> the position of the minimum in the transmittance is mainly determined by the axial ratio and its depth by the diameter of the particles. Without the finite size correction a fit could be obtained with a diameter of 26.6 nm and an axial ratio of 2.35. Taking into account this correction a fit was obtained with a diameter of 29.4 nm and the same axial ratio. In fig. 5 we have drawn the complete transmittance curve for the latter case. Also shown in fig. 5 is the transmittance curve for the fit obtained with the truncated spherical model<sup>2)</sup> with finite size correction ( $d = 26.8$  nm,  $AR = 1.21$ ). Both curves agree quite well with the experimental results. However, the value 2.35 for the axial ratio, found with the oblate spheroidal model, is unrealistically large. On this ground the truncated spherical model has to be preferred. Nevertheless, our calculations for the oblate spheroid do suggest that if the truncated sphere has in addition a somewhat spheroidal shape, then possibly a fit could be obtained with an axial ratio in the observed range 1.3–1.7. As regards the diameter of the particles, our calculations have not resolved the discrepancy between the fitted and observed values. Niklasson and Craighead themselves, however, remark that the size of the particles may be overestimated as a result of their fuzziness on the electron micrographs<sup>3,4)</sup>.

## 8 Summary

Adjusting a previously developed multipole method by introducing spheroidal multipoles, a method was devised to calculate the polarizability of a spheroidal particle on a substrate, with axis of revolution normal to the substrate. An infinite set of linear inhomogeneous equations for the multipole coefficients was obtained. For the coefficients appearing in the matrix elements of these equations a complete set of recurrence relations was derived. The polarizability could then be evaluated to any desired order in the number of multipoles taken into account in the interaction with the substrate. For the limiting cases of a disk and a needle it was proved that the interaction with the substrate vanishes, so that the polarizabilities become equal to the free polarizabilities. The spheroidal dipole approximation was compared with the usual spherical dipole approximation and was found to be an improvement. The oblate spheroidal model was then applied to a transmission experiment by Niklasson and Craighead<sup>3,4)</sup> with a square lattice of gold particles on a sapphire substrate. To obtain agreement with this experiment, however, an unrealistically large axial ratio of the particles had to be assumed. It was concluded that the particles probably have a truncated spherical shape, with in addition a somewhat spheroidal flattening.

## References

- 1) M.M. Wind, J. Vlieger and D. Bedeaux, *Physica* **141A** (1987) 33.
- 2) M.M. Wind, P.A. Bobbert, J. Vlieger and D. Bedeaux, *Physica* **143A** (1987) 164.
- 3) H.G. Craighead and G.A. Niklasson, *Appl. Phys. Lett.* **44** (1984) 1134.
- 4) G.A. Niklasson and H.G. Craighead, *Thin Solid Films* **125** (1985) 165.
- 5) P.M. Morse and H. Feshbach, *Methods of Theoretical Physics I* (McGraw-Hill, New York, 1953).
- 6) P.M. Morse and H. Feshbach, *Methods of Theoretical Physics II* (McGraw-Hill, New York, 1953).
- 7) D. Bedeaux and J. Vlieger, *Physica* **73** (1974) 287.
- 8) M. Abramowitz and I.A. Stegun, *Handbook of Mathematical Functions* (Dover, New York, 1965), p. 338.
- 9) P.R. Johnson and R.W. Christy, *Phys. Rev. B* **6** (1972) 4370.
- 10) T. Yamaguchi, S. Yoshida and A. Kinbara, *Thin Solid Films* **21** (1974) 173.
- 11) D. Bedeaux and J. Vlieger, *Physica* **67** (1973) 55.
- 12) S. Norrman, T. Andersson, C.G. Granqvist and O. Hunderi, *Phys. Rev. B* **18** (1978) 674.
- 13) M.A. Ordal, L.L. Long, R.J. Bell, S.E. Bell, R.R. Bell, R.W. Alexander Jr. and C.A. Ward, *Appl. Opt.* **22** (1983) 1099.
- 14) G.B. Smith, G.A. Niklasson, J.S.E.M. Svensson and C.G. Granqvist, *J. Appl. Phys.* **59** (1986) 571.



## Chapter III

# Light Scattering by a Sphere on a Substrate\*

### 1 Introduction

In 1908, Mie<sup>2</sup>) obtained a solution for the diffraction of a plane monochromatic wave by a homogeneous sphere in a homogeneous medium. Shortly afterwards, Debye<sup>3</sup>) published an equivalent solution, introducing the concept of Debye potentials.

To solve the light scattering problem of a sphere on a substrate one has to take into account the electromagnetic interaction between the sphere and the substrate. In 1919 Weyl<sup>4</sup>) developed a method to describe the propagation of dipole radiation along a flat surface. In this chapter we shall use an extension of this method to higher order multipole radiation in order to calculate this interaction.

After giving a survey of the theory of Debye potentials in sections 2 and 3, and of the Mie solution in section 4, we present the formal solution of the scattering problem of a sphere on a substrate in section 5. In this section we introduce a matrix  $A$  characterizing the reflection of spherical waves by the substrate. After generalizing in section 6 an integral expression first used by Weyl, we calculate this matrix in section 8, with the help of so-called Hertz vectors, which are reviewed and related to the Debye potentials in section 7. The matrix elements of  $A$  are obtained as integrals over a complex angle. In general, these integrals can only be evaluated numerically. However, for the case of a perfectly conducting substrate they can be performed analytically, which is shown in section 9. In section 10 it is proved that in the static limit (radius of sphere  $\ll$  wavelength of incident light) the theory is equivalent to the static theory for a sphere on a substrate, which is a limiting case of the truncated spherical shape considered by Wind, Vlieger and Bedeaux<sup>5</sup>) and also of the spheroidal shape considered in chapter II. Finally, in section 11 we give expressions for the far-away scattered electric field above the substrate.

---

\*After publication of this work (Physica 137A (1986) 209) a paper by Takemori, Inoue and Ohtaka<sup>1</sup>) about the same subject appeared, presenting a solution equivalent to the one put forward in this chapter.

## 2 The Debye potentials

Throughout this chapter a time dependence  $e^{-i\omega t}$  is assumed but always omitted,  $\omega$  being the angular frequency of the incident light. Physical quantities can be obtained by multiplying the occurring time-independent quantities by this factor and taking real parts. The wavelength  $\lambda$  and the wavenumber  $k$  in the non-absorbing non-magnetic medium above the substrate (ambient) with refractive index  $n_1$  and dielectric constant  $\epsilon_1 = n_1^2$  are related to  $\omega$  by

$$\lambda = \frac{2\pi v}{\omega}, \quad (2.1)$$

$$k = \frac{\omega}{v}, \quad (2.2)$$

$v$  being the speed of light in this medium. We use rationalized Gaussian units.

For a detailed treatment of the theory of Debye potentials we refer to a paper of Bouwkamp and Casimir<sup>6</sup>). In a completely analogous way as in that paper one can prove that the electromagnetic fields in a region  $D$  between two concentric spheres,  $0 < r_1 \leq r \leq r_2 < \infty$ ,  $0 \leq \phi \leq 2\pi$ ,  $0 \leq \theta \leq \pi$  ( $r, \theta, \phi$  spherical coordinates), in which there are no free charges and currents, are completely determined by two scalar functions  ${}^e\Pi(\mathbf{r})$  and  ${}^h\Pi(\mathbf{r})$ , the so-called electric and magnetic *Debye potentials*. The electric and magnetic fields can be derived from these potentials by

$$\mathbf{E}(\mathbf{r}) = \nabla \times \nabla \times [\mathbf{r}^e\Pi(\mathbf{r})] + ik\nabla \times [\mathbf{r}^h\Pi(\mathbf{r})], \quad (2.3a)$$

$$\mathbf{H}(\mathbf{r}) = n_1 \left\{ -ik\nabla \times [\mathbf{r}^e\Pi(\mathbf{r})] + \nabla \times \nabla \times [\mathbf{r}^h\Pi(\mathbf{r})] \right\}. \quad (2.3b)$$

These potentials are called electric and magnetic because the corresponding fields have vanishing magnetic and electric radial components respectively.

Maxwell's equations can be written in the form:

$$\begin{aligned} \nabla \times \mathbf{E}(\mathbf{r}) - ik\mathbf{H}(\mathbf{r})/n_1 &= 0, & \nabla \cdot \mathbf{E}(\mathbf{r}) &= \bar{\rho}(\mathbf{r}), \\ \nabla \times \mathbf{H}(\mathbf{r})/n_1 + ik\mathbf{E}(\mathbf{r}) &= \bar{\mathbf{i}}(\mathbf{r})/v, & \nabla \cdot \mathbf{H}(\mathbf{r}) &= 0, \end{aligned} \quad (2.4)$$

with  $\bar{\rho}(\mathbf{r})$  the total charge density and  $\bar{\mathbf{i}}(\mathbf{r})$  the total current density, both relative to the ambient:

$$\begin{aligned} \bar{\rho}(\mathbf{r}) &= [\rho(\mathbf{r}) - \nabla \cdot \mathbf{P}_{\text{ex}}(\mathbf{r})]/\epsilon_1, \\ \bar{\mathbf{i}}(\mathbf{r}) &= [\mathbf{i}(\mathbf{r}) - i\omega\mathbf{P}_{\text{ex}}(\mathbf{r})]/\epsilon_1, \end{aligned} \quad (2.5)$$

$\rho(\mathbf{r})$  and  $\mathbf{i}(\mathbf{r})$  being the free charge and current density respectively, and  $\mathbf{P}_{\text{ex}}(\mathbf{r})$  the excess polarization density, which is related to the total polarization density  $\mathbf{P}(\mathbf{r})$  by

$$\mathbf{P}_{\text{ex}}(\mathbf{r}) = \mathbf{P}(\mathbf{r}) - (\epsilon_1 - 1)\mathbf{E}(\mathbf{r}). \quad (2.6)$$

The densities  $\bar{\rho}(\mathbf{r})$  and  $\bar{\mathbf{i}}(\mathbf{r})$  satisfy the continuity equation

$$\nabla \cdot \bar{\mathbf{i}}(\mathbf{r})/v = ik\bar{\rho}(\mathbf{r}). \quad (2.7)$$

In the case that the fields in  $D$  result from currents  $\bar{\mathbf{i}}(\mathbf{r})$  flowing in the region inside  $D$  ( $0 \leq r < r_1$ ) we can derive, in an analogous way as in ref. 6, the following multipole expansions for  ${}^e\Pi(\mathbf{r})$  and  ${}^h\Pi(\mathbf{r})$  in  $D$ :

$${}^e\Pi(\mathbf{r}) = \sum_{l=1}^{\infty} \sum_{m=-l}^l {}^e w_l^m \Pi_l^m(\mathbf{r}), \quad (2.8a)$$

$${}^h\Pi(\mathbf{r}) = \sum_{l=1}^{\infty} \sum_{m=-l}^l {}^h w_l^m \Pi_l^m(\mathbf{r}), \quad (2.8b)$$

in which the electric and magnetic multipole coefficients  ${}^e w_l^m$  and  ${}^h w_l^m$  are given by

$${}^e w_l^m = -\frac{1}{4\pi v} \frac{1}{l(l+1)} (-1)^m \int \bar{\mathbf{i}}(\mathbf{r}) \cdot \nabla \times \nabla \times [\mathbf{r} \Psi_l^{-m}(\mathbf{r})] d\mathbf{r}, \quad (2.9a)$$

$${}^h w_l^m = \frac{ik}{4\pi v} \frac{1}{l(l+1)} (-1)^m \int \bar{\mathbf{i}}(\mathbf{r}) \cdot \nabla \times [\mathbf{r} \Psi_l^{-m}(\mathbf{r})] d\mathbf{r}, \quad (2.9b)$$

with the functions  $\Pi_l^m(\mathbf{r})$  and  $\Psi_l^m(\mathbf{r})$  defined by

$$\Pi_l^m(\mathbf{r}) \equiv h_l^{(1)}(kr) Y_l^m(\theta, \phi), \quad (2.10a)$$

$$\Psi_l^m(\mathbf{r}) \equiv j_l(kr) Y_l^m(\theta, \phi). \quad (2.10b)$$

Here  $h_l^{(1)}(\rho)$  and  $j_l(\rho)$  are spherical Hankel and Bessel functions of order  $l$  respectively:

$$h_l^{(1)}(\rho) \equiv \sqrt{\frac{\pi}{2\rho}} H_{l+\frac{1}{2}}^{(1)}(\rho), \quad (2.11a)$$

$$j_l(\rho) \equiv \sqrt{\frac{\pi}{2\rho}} J_{l+\frac{1}{2}}(\rho), \quad (2.11b)$$

in the notation of Watson<sup>7</sup>), and  $Y_l^m(\theta, \phi)$  is the surface harmonic of degree  $l$  and order  $m$ :

$$Y_l^m(\theta, \phi) \equiv \left[ (2l+1) \frac{(l-m)!}{(l+m)!} \right]^{1/2} P_l^m(\cos \theta) e^{im\phi}, \quad (2.12)$$

with the associated Legendre function  $P_l^m(\cos \theta)$  in the notation of Stratton<sup>8</sup>):

$$P_l^m(\eta) \equiv \frac{(1-\eta^2)^{m/2}}{2^l l!} \frac{d^{l+m}}{d\eta^{l+m}} (\eta^2 - 1)^l \quad (m \geq 0),$$

$$P_l^m(\eta) \equiv (-1)^{-m} \frac{(l+m)!}{(l-m)!} P_l^{-m}(\eta) \quad (m < 0). \quad (2.13)$$

It can be shown<sup>6</sup>), using relations (2.8)–(2.13), that the electromagnetic fields as given by eqs. (2.3a) and (2.3b) indeed satisfy Maxwell's equations (2.4).

Similar expressions can be derived for the case that the fields in  $D$  result from currents flowing in the region *outside*  $D$  ( $r > r_2$ ). Denoting the Debye potentials now by  ${}^e\Psi(\mathbf{r})$  and  ${}^h\Psi(\mathbf{r})$  to emphasize the difference, one obtains:

$${}^e\Psi(\mathbf{r}) = \sum_{l=1}^{\infty} \sum_{m=-l}^l {}^e v_l^m \Psi_l^m(\mathbf{r}), \quad (2.14a)$$

$${}^h\Psi(\mathbf{r}) = \sum_{l=1}^{\infty} \sum_{m=-l}^l {}^h v_l^m \Psi_l^m(\mathbf{r}), \quad (2.14b)$$

with

$${}^e v_l^m = -\frac{1}{4\pi v} \frac{1}{l(l+1)} (-1)^m \int \mathbf{i}(\mathbf{r}) \cdot \nabla \times \nabla \times [\mathbf{r} \Pi_l^{-m}(\mathbf{r})] d\mathbf{r}, \quad (2.15a)$$

$${}^h v_l^m = \frac{ik}{4\pi v} \frac{1}{l(l+1)} (-1)^m \int \mathbf{i}(\mathbf{r}) \cdot \nabla \times [\mathbf{r} \Pi_l^{-m}(\mathbf{r})] d\mathbf{r}. \quad (2.15b)$$

Because the functions  $\Pi_l^m(\mathbf{r})$  and  $\Psi_l^m(\mathbf{r})$  are solutions of Helmholtz's equation:

$$(\nabla \cdot \nabla + k^2) \Pi_l^m(\mathbf{r}) = 0, \quad (\nabla \cdot \nabla + k^2) \Psi_l^m(\mathbf{r}) = 0, \quad (2.16)$$

it follows from eqs. (2.8) and (2.14) that the Debye potentials also satisfy this equation in the region  $D$ .

The Debye potentials are, except for the addition of terms proportional to  $\Pi_0^0$  or  $\Psi_0^0$ , uniquely determined by the electromagnetic fields  $\mathbf{E}$  and  $\mathbf{H}$ . Insertion of  $\Pi_0^0$  or  $\Psi_0^0$  in eq. (2.3) yields  $\mathbf{E} = 0$ ,  $\mathbf{H} = 0$ . We shall always take the coefficients of  $\Pi_0^0$  and  $\Psi_0^0$  equal to zero.

As a concluding remark we would like to emphasize the fact that any electromagnetic field in  $D$  is completely determined by the coefficients  ${}^e v_l^m$ ,  ${}^h v_l^m$  and  ${}^e w_l^m$ ,  ${}^h w_l^m$  given by eqs. (2.15) and (2.9). These coefficients can formally be interpreted as components of two infinite vectors  $\mathbf{V}$  and  $\mathbf{W}$ . With this interpretation an electromagnetic field in  $D$  caused by currents flowing in the region *outside*  $D$  is described by a vector  $\mathbf{V}$ , and by a vector  $\mathbf{W}$  if it is caused by currents flowing in the region *inside*  $D$ . This interpretation will be understood below.

### 3 The Debye potentials of a plane wave

In the case of a plane wave propagating in the  $z$ -direction of our coordinate system, with the electric vector in the  $x$ -direction and with amplitude  $|\mathbf{E}| = |E_x| = |e^{ikz}| = 1$ , the Debye potentials are\*

\*See e.g. Born and Wolf<sup>9</sup>).

$${}^e\Psi(\mathbf{r}) = \frac{1}{k} \sum_{l=1}^{\infty} i^{l-1} \left[ \frac{2l+1}{l(l+1)} \right]^{1/2} \left( \frac{1}{2}\Psi_l^1(\mathbf{r}) - \frac{1}{2}\Psi_l^{-1}(\mathbf{r}) \right), \quad (3.1a)$$

$${}^h\Psi(\mathbf{r}) = -\frac{1}{k} \sum_{l=1}^{\infty} i^l \left[ \frac{2l+1}{l(l+1)} \right]^{1/2} \left( \frac{1}{2}\Psi_l^1(\mathbf{r}) + \frac{1}{2}\Psi_l^{-1}(\mathbf{r}) \right), \quad (3.1b)$$

and with the electric vector in the  $y$ -direction:

$${}^e\Psi(\mathbf{r}) = -\frac{1}{k} \sum_{l=1}^{\infty} i^l \left[ \frac{2l+1}{l(l+1)} \right]^{1/2} \left( \frac{1}{2}\Psi_l^1(\mathbf{r}) + \frac{1}{2}\Psi_l^{-1}(\mathbf{r}) \right), \quad (3.2a)$$

$${}^h\Psi(\mathbf{r}) = -\frac{1}{k} \sum_{l=1}^{\infty} i^{l-1} \left[ \frac{2l+1}{l(l+1)} \right]^{1/2} \left( \frac{1}{2}\Psi_l^1(\mathbf{r}) - \frac{1}{2}\Psi_l^{-1}(\mathbf{r}) \right). \quad (3.2b)$$

In these formulae the functions  $\Psi_l^m(\mathbf{r})$  appear because the electromagnetic fields of a plane wave result from currents flowing at infinity, i.e. outside the region  $D$  of section 2.

To calculate the Debye potentials of a plane wave propagating in another direction than the  $x$ -direction we need to express the surface harmonics in a rotated coordinate system  $(r, \theta', \phi')$  in terms of those in the coordinate system  $(r, \theta, \phi)$ . This can be done by a formula given e.g. by Rose<sup>10)</sup>:

$$Y_l^{m'}(\theta', \phi') = \sum_{m=-l}^l (-1)^{m-m'} D_{m,m'}^l(\beta, \alpha, \gamma) Y_l^m(\theta, \phi). \quad (3.3)$$

Here  $\beta$ ,  $\alpha$  and  $\gamma$  are the so-called *Euler angles*, through which we must rotate the coordinate system  $(r, \theta, \phi)$  to obtain the coordinate system  $(r, \theta', \phi')$ . These angles are defined by performing this rotation in three steps, starting with the coordinate system  $(x, y, z)$ . First a rotation about the  $z$ -axis through an angle  $\beta$ , then a rotation about the new  $y$ -axis through an angle  $\alpha$  and finally a rotation about the new  $z$ -axis through an angle  $\gamma$ , eventually giving the coordinate system  $(x', y', z')$ . The rotation matrix  $D_{m,m'}^l(\beta, \alpha, \gamma)$  can be written as

$$D_{m,m'}^l(\beta, \alpha, \gamma) = e^{-im\beta} d_{m,m'}^l(\alpha) e^{-im'\gamma}, \quad (3.4)$$

with

$$d_{m,m'}^l(\alpha) \equiv \frac{[(l+m')!(l-m')!(l+m)!(l-m)]^{1/2}}{\sum_k (-1)^k \frac{(\cos \frac{1}{2}\alpha)^{2l+m'-m-2k} (-\sin \frac{1}{2}\alpha)^{m-m'+2k}}{(l-m-k)!(l+m'-k)!(k+m-m')!k!}}, \quad (3.5)$$

where the sum extends over all values of the integer  $k$  for which the factorial arguments are non-negative.

Some useful properties of  $d_{m,m'}^l(\alpha)$  are:

\*Our definition eq. (2.13) of the Legendre function of order  $m$  differs from that of Rose by a factor  $(-1)^m$ .

$$d_{m',m}^l(\alpha) = (-1)^{m'-m} d_{m,m'}^l(\alpha), \quad (3.6)$$

$$d_{m',m}^l(\alpha) = d_{-m,-m'}^l(\alpha), \quad (3.7)$$

$$d_{m,1}^l(\pi - \alpha) = (-1)^{l-m} d_{m,-1}^l(\alpha), \quad (3.8a)$$

$$d_{m,-1}^l(\pi - \alpha) = (-1)^{l-m} d_{m,1}^l(\alpha). \quad (3.8b)$$

Now for a plane wave propagating in the  $z'$ -direction of some rotated coordinate system, with electric vector in the  $x'$ -direction and with unit amplitude, the Debye potentials become

$$\begin{aligned} {}^e\Psi(\mathbf{r}) &= \frac{1}{k} \sum_{l=1}^{\infty} \sum_{m=-l}^l i^{l-1} \left[ \frac{2l+1}{l(l+1)} \right]^{1/2} (-1)^{m-1} \\ &\quad \times \left( \frac{1}{2} D_{m,1}^l(\beta, \alpha, \gamma) - \frac{1}{2} D_{m,-1}^l(\beta, \alpha, \gamma) \right) \Psi_l^m(\mathbf{r}), \end{aligned} \quad (3.9a)$$

$$\begin{aligned} {}^h\Psi(\mathbf{r}) &= -\frac{1}{k} \sum_{l=1}^{\infty} \sum_{m=-l}^l i^l \left[ \frac{2l+1}{l(l+1)} \right]^{1/2} (-1)^{m-1} \\ &\quad \times \left( \frac{1}{2} D_{m,1}^l(\beta, \alpha, \gamma) + \frac{1}{2} D_{m,-1}^l(\beta, \alpha, \gamma) \right) \Psi_l^m(\mathbf{r}), \end{aligned} \quad (3.9b)$$

where eqs. (3.1), (2.10b) and (3.3) have been used. For a plane wave propagating in the same direction but with the electric vector in the  $y'$ -direction, we obtain with eqs. (3.2), (2.10b) and (3.3):

$$\begin{aligned} {}^e\Psi(\mathbf{r}) &= -\frac{1}{k} \sum_{l=1}^{\infty} \sum_{m=-l}^l i^l \left[ \frac{2l+1}{l(l+1)} \right]^{1/2} (-1)^{m-1} \\ &\quad \times \left( \frac{1}{2} D_{m,1}^l(\beta, \alpha, \gamma) + \frac{1}{2} D_{m,-1}^l(\beta, \alpha, \gamma) \right) \Psi_l^m(\mathbf{r}), \end{aligned} \quad (3.10a)$$

$$\begin{aligned} {}^h\Psi(\mathbf{r}) &= -\frac{1}{k} \sum_{l=1}^{\infty} \sum_{m=-l}^l i^{l-1} \left[ \frac{2l+1}{l(l+1)} \right]^{1/2} (-1)^{m-1} \\ &\quad \times \left( \frac{1}{2} D_{m,1}^l(\beta, \alpha, \gamma) - \frac{1}{2} D_{m,-1}^l(\beta, \alpha, \gamma) \right) \Psi_l^m(\mathbf{r}). \end{aligned} \quad (3.10b)$$

#### 4 The Mie solution

Let us again consider the region  $D$  of section 2. If there is an object in the region inside  $D$  and a wave  $V$ , according to the interpretation of section 2, incident on it (e.g. a plane wave), then the electromagnetic fields of this wave will induce currents flowing in this object, giving rise to a scattered wave  $W$ . The vectors  $W$  and  $V$  will be linearly related by a matrix  $B$ :

$$W = B \cdot V. \quad (4.1)$$

The matrix B will depend on the geometry and the constitutive electromagnetic properties of the object.

For the case that the object is a homogeneous non-magnetic sphere with refractive index  $n_3$ , centred at the origin of our coordinate system,  $Mie^2$ ) in fact has calculated this matrix. The result is, in our notation (cf. ref. 9):

$$B_{l',m',e,l,m,e} = -\delta_{l,l'}\delta_{m,m'} \frac{\tilde{n}\psi_l'(q)\psi_l(\tilde{n}q) - \psi_l(q)\psi_l'(\tilde{n}q)}{\tilde{n}\zeta_l'(q)\psi_l(\tilde{n}q) - \zeta_l(q)\psi_l'(\tilde{n}q)},$$

$$B_{l',m',h,l,m,h} = -\delta_{l,l'}\delta_{m,m'} \frac{\tilde{n}\psi_l(q)\psi_l'(\tilde{n}q) - \psi_l'(q)\psi_l(\tilde{n}q)}{\tilde{n}\zeta_l(q)\psi_l'(\tilde{n}q) - \zeta_l'(q)\psi_l(\tilde{n}q)}, \quad (4.2)$$

$$B_{l',m',e,l,m,h} = B_{l',m',h,l,m,e} = 0,$$

with  $\tilde{n}$  the relative refractive index of the sphere:

$$\tilde{n} \equiv \frac{n_3}{n_1}, \quad (4.3)$$

and the size parameter  $q$  defined by

$$q \equiv \frac{2\pi a}{\lambda}, \quad (4.4)$$

where  $a$  is the radius of the sphere. The functions  $\psi_l(\rho)$  and  $\zeta_l(\rho)$  are defined as

$$\psi_l(\rho) \equiv \rho j_l(\rho), \quad \zeta_l(\rho) \equiv \rho h_l^{(1)}(\rho). \quad (4.5)$$

The addition of a prime to these functions denotes differentiation with respect to their argument.

The practical importance of this solution is that one can show<sup>3)</sup> that when  $q \gg 1$  the matrix elements in eq. (4.2) fall off rapidly to zero as soon as  $l$  exceeds  $q$ . This is intuitively clear if one observes that the function  $\psi_l(\rho)$  falls off rapidly to zero as soon as its argument is smaller than  $l$ , which means that the electromagnetic fields of an incident partial electric wave ( ${}^e\Psi = \Psi_l^m$ ,  ${}^h\Psi = 0$ ) or a partial magnetic wave ( ${}^e\Psi = 0$ ,  ${}^h\Psi = \Psi_l^m$ ) of order  $l > q$  will vanish in the neighbourhood of the sphere and consequently the scattered wave will vanish as well. This is also clear from eqs. (2.9):  $\Psi_l^{-m}(\mathbf{r})$  will be approximately zero in the region where  $\mathbf{i}(\mathbf{r})$  is different from zero, so the coefficients  ${}^e w_l^m$  and  ${}^h w_l^m$  will be small.

## 5 Formal solution of the scattering by a sphere on a substrate

Let us now consider a sphere on a substrate. For clarity we assume the sphere to be at a distance  $\delta$  above the substrate so that we can introduce a region  $D$  as in section 2 (see fig. 1). At the end of the argument we can take the limit  $\delta \rightarrow 0$ .

Let a wave  $V^1$  (e.g. a plane wave) be incident on this system. If the sphere were absent we could satisfy the boundary conditions at the surface of the substrate by adding a wave  $V^{IR}$  (just Fresnel reflection for the case of an incident plane

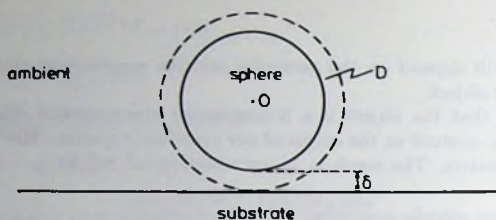


Fig. 1. Sphere on a substrate. The sphere is drawn at a distance  $\delta$  above the substrate. The region  $D$  is indicated. The origin is located at the centre of the sphere.

wave). In the presence of the sphere there will be an additional wave  $W^S$  as a result of currents flowing inside the sphere. But this wave will also be reflected by the substrate, i.e. induce currents flowing in the substrate, which gives rise to another incident wave  $V^{SR}$ . The vectors  $V^{SR}$  and  $W^S$  will be linearly related by some matrix  $A$  characterizing the reflection of multipole radiation by the substrate:

$$V^{SR} = A \cdot W^S. \quad (5.1)$$

We therefore have the following set of equations:

$$\begin{aligned} W^S &= B \cdot (V^I + V^{IR} + V^{SR}), \\ V^{SR} &= A \cdot W^S, \end{aligned} \quad (5.2)$$

with the matrix  $B$  given by eq. (4.2). From the above equations  $W^S$  can be solved in terms of  $V^I$  and  $V^{IR}$ , giving

$$W^S = (1 - B \cdot A)^{-1} \cdot B \cdot (V^I + V^{IR}), \quad (5.3)$$

and this is the formal solution of our scattering problem.

The following sections will be concerned with the calculation of the matrix  $A$ , resulting in an integral expression with integration over a complex angle.

## 6 Weyl's method

In his paper about the propagation of dipole radiation along a flat surface<sup>4)</sup> Weyl derives a formula expressing the spherical wave  $e^{ikr}/ikr$  as an integral over plane waves travelling into various directions\*:

$$\frac{e^{ikr}}{ikr} = h_0^{(1)}(kr) = \Pi_0^0(\mathbf{r}) = \frac{1}{2\pi} \int_0^{2\pi} d\beta \int_0^{\pi/2-i\infty} \sin \alpha d\alpha e^{ikr \cos \gamma}, \quad (6.1)$$

in which  $\cos \gamma$  is the angle between  $\mathbf{r} = (r \sin \theta \cos \phi, r \sin \theta \sin \phi, r \cos \theta)$  and  $\mathbf{k} = (k \sin \alpha \cos \beta, k \sin \alpha \sin \beta, k \cos \alpha)$ :

\*Weyl works with the wave  $e^{-ikr}/-ikr$  rather than  $e^{ikr}/ikr$ .

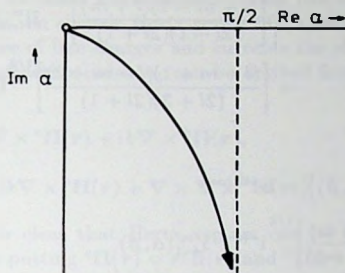


Fig. 2. Path in the complex plane along which the integration over the angle  $\alpha$  should be performed.

$$\cos \gamma = \frac{lz \cdot r}{kr} = \sin \theta \sin \alpha \cos(\phi - \beta) + \cos \theta \cos \alpha. \quad (6.2)$$

The integral  $\int_0^{\pi/2 - i\infty} d\alpha$  is an integral along a path in the complex plane as indicated in fig. 2. The integral expression (6.1) is only valid in the halfspace  $z > 0$ , since only there it converges. A similar expression is valid in the halfspace  $z < 0$ . With the help of eq. (6.1) Weyl now derives an expression for the reflected wave by applying the Fresnel reflection formulae to each plane wave.

Because we want to calculate the reflection of higher order multipole radiation we need a generalization of eq. (6.1). This generalization is

$$\begin{aligned} h_l^{(1)}(kr) Y_l^m(\theta, \phi) &= \Pi_l^m(\mathbf{r}) \\ &= \frac{i^{-l}}{2\pi} \int_0^{2\pi} d\beta \int_0^{\pi/2 - i\infty} \sin \alpha d\alpha e^{ikr \cos \gamma} Y_l^m(\alpha, \beta). \end{aligned} \quad (6.3)$$

The above equation can be proved with the help of the relations

$$\begin{aligned} \frac{\partial}{\partial z} \Pi_l^m(\mathbf{r}) &= k \left\{ \left[ \frac{(l-m)(l+m)}{(2l-1)(2l+1)} \right]^{1/2} \Pi_{l-1}^m(\mathbf{r}) \right. \\ &\quad \left. - \left[ \frac{(l+m+1)(l-m+1)}{(2l+3)(2l+1)} \right]^{1/2} \Pi_{l+1}^m(\mathbf{r}) \right\}, \\ \left( \frac{\partial}{\partial x} + i \frac{\partial}{\partial y} \right) \Pi_l^m(\mathbf{r}) &= -k \left\{ \left[ \frac{(l-m-1)(l-m)}{(2l-1)(2l+1)} \right]^{1/2} \Pi_{l-1}^{m+1}(\mathbf{r}) \right. \\ &\quad \left. + \left[ \frac{(l+m+1)(l+m+2)}{(2l+3)(2l+1)} \right]^{1/2} \Pi_{l+1}^{m+1}(\mathbf{r}) \right\}, \end{aligned} \quad (6.4)$$

$$\left(\frac{\partial}{\partial x} - i\frac{\partial}{\partial y}\right)\Pi_l^m(\mathbf{r}) = k\left\{\left[\frac{(l+m-1)(l+m)}{(2l-1)(2l+1)}\right]^{1/2}\Pi_{l-1}^{m-1}(\mathbf{r}) + \left[\frac{(l-m+1)(l-m+2)}{(2l+3)(2l+1)}\right]^{1/2}\Pi_{l+1}^{m-1}(\mathbf{r})\right\},$$

and

$$\begin{aligned} \frac{\partial}{\partial z}\left\{i^{-l}e^{ikr\cos\gamma}Y_l^m(\alpha,\beta)\right\} &= ke^{ikr\cos\gamma} \\ &\times\left\{\left[\frac{(l-m)(l+m)}{(2l-1)(2l+1)}\right]^{1/2}i^{-(l-1)}Y_{l-1}^m(\alpha,\beta) - \left[\frac{(l+m+1)(l-m+1)}{(2l+3)(2l+1)}\right]^{1/2}i^{-(l+1)}Y_{l+1}^m(\alpha,\beta)\right\}, \\ \left(\frac{\partial}{\partial x} + i\frac{\partial}{\partial y}\right)\left\{i^{-l}e^{ikr\cos\gamma}Y_l^m(\alpha,\beta)\right\} &= -ke^{ikr\cos\gamma} \\ &\times\left\{\left[\frac{(l-m-1)(l-m)}{(2l-1)(2l+1)}\right]^{1/2}i^{-(l-1)}Y_{l-1}^{m+1}(\alpha,\beta) + \left[\frac{(l+m+1)(l+m+2)}{(2l+3)(2l+1)}\right]^{1/2}i^{-(l+1)}Y_{l+1}^{m+1}(\alpha,\beta)\right\}, \end{aligned} \quad (6.5)$$

$$\begin{aligned} \left(\frac{\partial}{\partial x} - i\frac{\partial}{\partial y}\right)\left\{i^{-l}e^{ikr\cos\gamma}Y_l^m(\alpha,\beta)\right\} &= ke^{ikr\cos\gamma} \\ &\times\left\{\left[\frac{(l+m-1)(l+m)}{(2l-1)(2l+1)}\right]^{1/2}i^{-(l-1)}Y_{l-1}^{m-1}(\alpha,\beta) + \left[\frac{(l-m+1)(l-m+2)}{(2l+3)(2l+1)}\right]^{1/2}i^{-(l+1)}Y_{l+1}^{m-1}(\alpha,\beta)\right\}. \end{aligned}$$

These relations can be proved using recurrence relations for Legendre and spherical Hankel functions. Eqs. (6.4) and (6.5) are consistent with eq. (6.3). Since for  $l = m = 0$  eq. (6.3) reduces to Weyl's integral eq. (6.1), it follows that eq. (6.3) is true for any values of  $l$  and  $m$ .

## 7 Hertz vectors

We cannot apply Weyl's method, by means of eq. (6.3), directly to the Debye potentials themselves, written in the form eqs. (2.8), since the integrand would not correspond to a plane electromagnetic wave for which we could use the Fresnel reflection formulae. This is because of the multiplication by  $\mathbf{r}$  in eqs. (2.3). Beside the Debye potentials it is therefore convenient to introduce potentials that are more appropriate to Cartesian symmetry, as we have in the case of reflection by a flat

surface, namely the so-called *Hertz vectors*<sup>9</sup>. Just like the Debye potentials there are two Hertz vectors, an electric Hertz vector  ${}^e\Pi(\mathbf{r})$  and a magnetic Hertz vector  ${}^h\Pi(\mathbf{r})$ . In the absence of free charges and currents the electric and magnetic fields in a medium with refractive index  $n_1$  can be derived from these vectors by means of

$$\mathbf{E}(\mathbf{r}) = \nabla \times \nabla \times {}^e\Pi(\mathbf{r}) + ik\nabla \times {}^h\Pi(\mathbf{r}), \quad (7.1a)$$

$$\mathbf{H}(\mathbf{r}) = n_1 \left\{ -ik\nabla \times {}^e\Pi(\mathbf{r}) + \nabla \times \nabla \times {}^h\Pi(\mathbf{r}) \right\}. \quad (7.1b)$$

From eqs. (2.3) it is clear that Hertz vectors can be obtained from the Debye potentials simply by putting  ${}^e\Pi(\mathbf{r}) = \mathbf{r}^e\Pi(\mathbf{r})$  and  ${}^h\Pi(\mathbf{r}) = \mathbf{r}^h\Pi(\mathbf{r})$ . Unfortunately, these Hertz vectors do not satisfy Helmholtz's equation but the equation

$$(\nabla \cdot \nabla + k^2)r^f\Pi(\mathbf{r}) = 2\nabla^f\Pi(\mathbf{r}), \quad (7.2)$$

where the index  $f$  may be either  $e$  or  $h$ . Consequently, unlike the Debye potentials the Cartesian components of these vectors are not expressible as sums over the functions  $\Pi_l^m(\mathbf{r})$ , so we cannot apply eq. (6.3) to these vectors. However, from eqs. (7.1) it is clear that we can add the gradient of an arbitrary function to the Hertz vectors without changing the electromagnetic fields. This freedom can be exploited to construct Hertz vectors that do satisfy Helmholtz's equation. If we put

$${}^f\Pi(\mathbf{r}) = r^f\Pi(\mathbf{r}) + \frac{1}{k^2}\nabla \left\{ \nabla \cdot [r^f\Pi(\mathbf{r})] - 4{}^f\Pi(\mathbf{r}) \right\}, \quad (7.3)$$

it can easily be checked that this condition is now satisfied. Equation (7.3) can be rewritten as follows:

$${}^f\Pi(\mathbf{r}) = r^f\Pi(\mathbf{r}) + \frac{1}{k^2}r\frac{\partial}{\partial r}\nabla^f\Pi(\mathbf{r}). \quad (7.4)$$

The cartesian components of these vectors should be expressible in terms of the functions  $\Pi_l^m(\mathbf{r})$ . Indeed, taking  ${}^f\Pi = \Pi_l^m$  ( $f = e, h$ ), we find after a lengthy calculation involving recurrence relations for Legendre and spherical Hankel functions:

$$\begin{aligned} {}^f\Pi_x = & \frac{(l-1)}{2k} \left\{ \left[ \frac{(l+m-1)(l+m)}{(2l-1)(2l+1)} \right]^{1/2} \Pi_{l-1}^{m-1} \right. \\ & \left. - \left[ \frac{(l-m-1)(l-m)}{(2l-1)(2l+1)} \right]^{1/2} \Pi_{l-1}^{m+1} \right\} \\ & - \frac{(l+2)}{2k} \left\{ \left[ \frac{(l-m+1)(l-m+2)}{(2l+3)(2l+1)} \right]^{1/2} \Pi_{l+1}^{m-1} \right. \\ & \left. - \left[ \frac{(l+m+1)(l+m+2)}{(2l+3)(2l+1)} \right]^{1/2} \Pi_{l+1}^{m+1} \right\}, \end{aligned}$$

<sup>9</sup>See e.g. Born and Wolf<sup>9</sup>.

$$\begin{aligned}
 {}^j\Pi_v = & i \frac{(l-1)}{2k} \left\{ \left[ \frac{(l+m-1)(l+m)}{(2l-1)(2l+1)} \right]^{1/2} \Pi_{l-1}^{m-1} \right. \\
 & \left. + \left[ \frac{(l-m-1)(l-m)}{(2l-1)(2l+1)} \right]^{1/2} \Pi_{l-1}^{m+1} \right\} \\
 & - i \frac{(l+2)}{2k} \left\{ \left[ \frac{(l-m+1)(l-m+2)}{(2l+3)(2l+1)} \right]^{1/2} \Pi_{l+1}^{m-1} \right. \\
 & \left. + \left[ \frac{(l+m+1)(l+m+2)}{(2l+3)(2l+1)} \right]^{1/2} \Pi_{l+1}^{m+1} \right\}, \quad (7.5)
 \end{aligned}$$

$$\begin{aligned}
 {}^j\Pi_z = & \frac{(l-1)}{k} \left[ \frac{(l-m)(l+m)}{(2l-1)(2l+1)} \right]^{1/2} \Pi_{l-1}^m \\
 & + \frac{(l+2)}{k} \left[ \frac{(l+m+1)(l-m+1)}{(2l+3)(2l+1)} \right]^{1/2} \Pi_{l+1}^m.
 \end{aligned}$$

We have omitted the argument  $\mathbf{r}$  in all the functions occurring in this equation.

Conversely, given a Hertz vector expressed in terms of the functions  $\Pi_l^m$ , one can ask for the corresponding Debye potentials. The way to find these is also described in the paper of Bouwkamp and Casimir<sup>6</sup>). First, one should calculate the electromagnetic fields  $\mathbf{E}$  and  $\mathbf{H}$ , in this case by means of eqs. (7.1), then evaluate the dot products  $\mathbf{r} \cdot \mathbf{E}$  and  $\mathbf{r} \cdot \mathbf{H}$ , which are solutions of Helmholtz's equation, and express these dot products in terms of the functions  $\Pi_l^m$ :

$$\mathbf{r} \cdot \mathbf{E}(\mathbf{r}) = \sum_{l=1}^{\infty} \sum_{m=-l}^l a_{l,m} \Pi_l^m(\mathbf{r}), \quad (7.6a)$$

$$\mathbf{r} \cdot \mathbf{H}(\mathbf{r}) = \sum_{l=1}^{\infty} \sum_{m=-l}^l b_{l,m} \Pi_l^m(\mathbf{r}). \quad (7.6b)$$

Knowing the coefficients  $a_{l,m}$  and  $b_{l,m}$ , the Debye potentials are

$${}^e\Pi(\mathbf{r}) = \sum_{l=1}^{\infty} \sum_{m=-l}^l \frac{a_{l,m}}{l(l+1)} \Pi_l^m(\mathbf{r}), \quad (7.7a)$$

$${}^h\Pi(\mathbf{r}) = \sum_{l=1}^{\infty} \sum_{m=-l}^l \frac{b_{l,m}}{l(l+1)} \Pi_l^m(\mathbf{r}). \quad (7.7b)$$

Carrying out this programme we find after a long calculation, again involving recurrence relations for Legendre and spherical Hankel functions, for  ${}^h\Pi = (\Pi_l^m, 0, 0)^*$

\*This is a shorthand notation for two possibilities; the formulae can be read either with the upper or with the lower superscripts and signs.

(and  ${}^h\Pi = (0, 0, 0)$ ):

$$\begin{aligned}
 {}^c\Pi = & \frac{k}{2l} \left\{ \left[ \frac{(l+m-1)(l+m)}{(2l-1)(2l+1)} \right]^{1/2} \Pi_{l-1}^{m-1} \right. \\
 & - \left. \left[ \frac{(l-m-1)(l-m)}{(2l-1)(2l+1)} \right]^{1/2} \Pi_{l-1}^{m+1} \right\} \\
 & - \frac{k}{2(l+1)} \left\{ \left[ \frac{(l-m+1)(l-m+2)}{(2l+3)(2l+1)} \right]^{1/2} \Pi_{l+1}^{m-1} \right. \\
 & - \left. \left[ \frac{(l+m+1)(l+m+2)}{(2l+3)(2l+1)} \right]^{1/2} \Pi_{l+1}^{m+1} \right\}, \quad (7.8a)
 \end{aligned}$$

and

$$\begin{aligned}
 {}^h\Pi = & \mp \frac{k}{2l(l+1)} \left\{ [(l+m)(l-m+1)]^{1/2} \Pi_l^{m-1} \right. \\
 & + \left. [(l+m+1)(l-m)]^{1/2} \Pi_l^{m+1} \right\}, \quad (7.8b)
 \end{aligned}$$

for  ${}^h\Pi = (0, \Pi_l^m, 0)$ :

$$\begin{aligned}
 {}^c\Pi = & i \frac{k}{2l} \left\{ \left[ \frac{(l+m-1)(l+m)}{(2l-1)(2l+1)} \right]^{1/2} \Pi_{l-1}^{m-1} \right. \\
 & + \left. \left[ \frac{(l-m-1)(l-m)}{(2l-1)(2l+1)} \right]^{1/2} \Pi_{l-1}^{m+1} \right\} \\
 & - i \frac{k}{2(l+1)} \left\{ \left[ \frac{(l-m+1)(l-m+2)}{(2l+3)(2l+1)} \right]^{1/2} \Pi_{l+1}^{m-1} \right. \\
 & + \left. \left[ \frac{(l+m+1)(l+m+2)}{(2l+3)(2l+1)} \right]^{1/2} \Pi_{l+1}^{m+1} \right\}, \quad (7.8c)
 \end{aligned}$$

and

$$\begin{aligned}
 {}^h\Pi = & \mp i \frac{k}{2l(l+1)} \left\{ [(l+m)(l-m+1)]^{1/2} \Pi_l^{m-1} \right. \\
 & - \left. [(l+m+1)(l-m)]^{1/2} \Pi_l^{m+1} \right\}, \quad (7.8d)
 \end{aligned}$$

whereas for  ${}^c\Pi = (0, 0, \Pi_l^m)$ :

$$\begin{aligned}
 {}^h\Pi = & \frac{k}{l} \left[ \frac{(l-m)(l+m)}{(2l-1)(2l+1)} \right]^{1/2} \Pi_{l-1}^m \\
 & + \frac{k}{l+1} \left[ \frac{(l+m+1)(l-m+1)}{(2l+3)(2l+1)} \right]^{1/2} \Pi_{l+1}^m, \quad (7.8e)
 \end{aligned}$$

and

$${}^h\Pi = \pm \frac{k}{l(l+1)} m \Pi_l^m. \quad (7.8f)$$

One can finally check, using eqs. (7.8), that the Debye potentials corresponding to the Hertz vector eq. (7.5) are, for  $f = e$ :  ${}^e\Pi = \Pi_l^m$ ,  ${}^h\Pi = 0$  and for  $f = h$ :  ${}^e\Pi = 0$ ,  ${}^h\Pi = \Pi_l^m$ , which means that eqs. (7.8) are indeed the inverse of eq. (7.5).

All formulae in this section are also valid if all  $\Pi$ 's are replaced by  $\Psi$ 's.

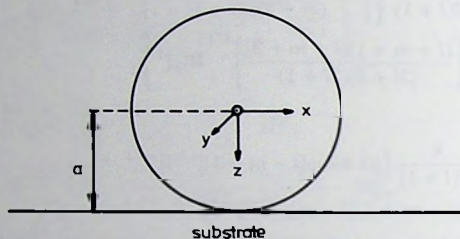


Fig. 3. Choice of the coordinate system.

## 8 Calculation of the matrix A

We choose our coordinate system as indicated in fig. 3. In this section we shall express the electromagnetic wave corresponding to the Debye potential  ${}^f\Pi = \Pi_l^m$  after its reflection by the substrate in terms of the Debye potentials  ${}^f\Psi = \Psi_l^m$  ( $f = e, h$ ). This will then give us the matrix A defined by eq. (5.1).

By means of eqs. (7.5) and (6.3) the Hertz vector corresponding to the Debye potential  ${}^f\Pi = \Pi_l^m$  can be written as an integral over plane waves:

$${}^f\Pi(r, \theta, \phi) = \frac{1}{2\pi} \int_0^{2\pi} d\beta \int_0^{\pi/2-i\infty} \sin \alpha d\alpha \pi(\alpha, \beta) e^{ikr \cos \gamma}, \quad (8.1)$$

in which  $\cos \gamma$  is defined by eq. (6.2), and with

$$\begin{aligned} \pi_x = & \frac{(l-1)_{-l-1}}{2k} \left\{ \left[ \frac{(l+m-1)(l+m)}{(2l-1)(2l+1)} \right]^{1/2} Y_{l-1}^{m-1} \right. \\ & \left. - \left[ \frac{(l-m-1)(l-m)}{(2l-1)(2l+1)} \right]^{1/2} Y_{l-1}^{m+1} \right\} \\ & - \frac{(l+2)_{-l+1}}{2k} \left\{ \left[ \frac{(l-m+1)(l-m+2)}{(2l+3)(2l+1)} \right]^{1/2} Y_{l+1}^{m-1} \right. \\ & \left. - \left[ \frac{(l+m+1)(l+m+2)}{(2l+3)(2l+1)} \right]^{1/2} Y_{l+1}^{m+1} \right\}, \end{aligned}$$

$$\begin{aligned}
\pi_y = & i \frac{(l-1)}{2k} i_{-(l-1)} \left\{ \left[ \frac{(l+m-1)(l+m)}{(2l-1)(2l+1)} \right]^{1/2} Y_{l-1}^{m-1} \right. \\
& + \left. \left[ \frac{(l-m-1)(l-m)}{(2l-1)(2l+1)} \right]^{1/2} Y_{l-1}^{m+1} \right\} \\
& - i \frac{(l+2)}{2k} i_{-(l+1)} \left\{ \left[ \frac{(l-m+1)(l-m+2)}{(2l+3)(2l+1)} \right]^{1/2} Y_{l+1}^{m-1} \right. \\
& + \left. \left[ \frac{(l+m+1)(l+m+2)}{(2l+3)(2l+1)} \right]^{1/2} Y_{l+1}^{m+1} \right\}, \quad (8.2)
\end{aligned}$$

$$\begin{aligned}
\pi_z = & \frac{(l-1)}{k} i_{-(l-1)} \left[ \frac{(l-m)(l+m)}{(2l-1)(2l+1)} \right]^{1/2} Y_{l-1}^m \\
& + \frac{(l+2)}{k} i_{-(l+1)} \left[ \frac{(l+m+1)(l-m+1)}{(2l+3)(2l+1)} \right]^{1/2} Y_{l+1}^m,
\end{aligned}$$

where we have omitted the arguments  $\alpha$  and  $\beta$  in the angular functions.

Let us now first consider one plane wave in the integral eq. (8.1) with wave vector  $\mathbf{k} = (k \sin \alpha \cos \beta, k \sin \alpha \sin \beta, k \cos \alpha)$ . Corresponding to this plane wave we introduce a coordinate system  $(x', y', z')$  with unit vectors  $\hat{\mathbf{x}}'$ ,  $\hat{\mathbf{y}}'$  and  $\hat{\mathbf{z}}'$ :

$$\begin{aligned}
\hat{\mathbf{x}}' &= (\cos \alpha \cos \beta, \cos \alpha \sin \beta, -\sin \alpha), \\
\hat{\mathbf{y}}' &= (-\sin \beta, \cos \beta, 0), \\
\hat{\mathbf{z}}' &= (\sin \alpha \cos \beta, \sin \alpha \sin \beta, \cos \alpha),
\end{aligned} \quad (8.3)$$

which can be obtained from the coordinate system  $(x, y, z)$  by a rotation through the Euler angles  $\beta, \alpha, 0$  (see section 3). We have chosen this coordinate system in such a way that  $\hat{\mathbf{z}}'$  is the direction of propagation of the plane wave,  $\hat{\mathbf{x}}'$  the direction parallel to the plane of incidence (p-direction) and  $\hat{\mathbf{y}}'$  the direction normal to the plane of incidence (s-direction). Using eqs. (7.1a), (8.2) and (8.3) we can calculate the p- and s-components of the electric field of this plane wave. Omitting the phase factor  $e^{ikr \cos \gamma}$ , we obtain, for  $f = e$ :

$$E_p = k \bar{V}_l^m (\cos \alpha) e^{im\beta}, \quad E_s = ik \bar{U}_l^m (\cos \alpha) e^{im\beta}, \quad (8.4a)$$

and for  $f = h$ :

$$E_p = ik \bar{U}_l^m (\cos \alpha) e^{im\beta}, \quad E_s = -k \bar{V}_l^m (\cos \alpha) e^{im\beta}, \quad (8.4b)$$

with the abbreviations

$$\begin{aligned}
\bar{U}_l^m = & \frac{(l-1)}{2} i_{-(l-1)} \left\{ \left[ \frac{(l+m-1)(l+m)}{(2l-1)(2l+1)} \right]^{1/2} \bar{P}_{l-1}^{m-1} \right. \\
& + \left. \left[ \frac{(l-m-1)(l-m)}{(2l-1)(2l+1)} \right]^{1/2} \bar{P}_{l-1}^{m+1} \right\}
\end{aligned}$$

$$\begin{aligned}
& - \frac{(l+2)}{2} i^{-(l+1)} \left\{ \left[ \frac{(l-m+1)(l-m+2)}{(2l+3)(2l+1)} \right]^{1/2} \bar{P}_{l+1}^{m-1} \right. \\
& \left. + \left[ \frac{(l+m+1)(l+m+2)}{(2l+3)(2l+1)} \right]^{1/2} \bar{P}_{l+1}^{m+1} \right\}, \quad (8.5a)
\end{aligned}$$

$$\begin{aligned}
\bar{V}_l^m &= \frac{1}{2} i^{-(l-1)} \left\{ [(l-m+1)(l+m)]^{1/2} \bar{P}_l^{m-1} \right. \\
& \left. - [(l+m+1)(l-m)]^{1/2} \bar{P}_l^{m+1} \right\}, \quad (8.5b)
\end{aligned}$$

and with the normalized Legendre function

$$\bar{P}_l^m(\cos \alpha) \equiv \left[ (2l+1) \frac{(l-m)!}{(l+m)!} \right]^{1/2} P_l^m(\cos \alpha). \quad (8.6)$$

We have omitted the argument  $\cos \alpha$  in eq. (8.5).

The reflected plane wave can be calculated with the help of the Fresnel reflection coefficients

$$r_p(\cos \alpha) = \frac{n_2 \cos \alpha - n_1 \cos \alpha_t}{n_2 \cos \alpha + n_1 \cos \alpha_t}, \quad (8.7a)$$

$$r_s(\cos \alpha) = \frac{n_1 \cos \alpha - n_2 \cos \alpha_t}{n_1 \cos \alpha + n_2 \cos \alpha_t}, \quad (8.7b)$$

with  $n_2$  the refractive index of the substrate and

$$\cos \alpha_t = \sqrt{1 - \frac{n_1^2}{n_2^2} (1 - \cos^2 \alpha)}, \quad (8.8)$$

where the sign of the square root has to be chosen in such a way that  $n_2 \cos \alpha_t$  has a non-negative imaginary part. This excludes the unphysical situation that the transmitted wave would increase exponentially with increasing  $z$ .

We now introduce a coordinate system  $(x'', y'', z'')$ , corresponding to the reflected wave, with unit vectors  $\hat{x}''$ ,  $\hat{y}''$  and  $\hat{z}''$ :

$$\begin{aligned}
\hat{x}'' &= (-\cos \alpha \cos \beta, -\cos \alpha \sin \beta, -\sin \alpha), \\
\hat{y}'' &= (-\sin \beta, \cos \beta, 0), \\
\hat{z}'' &= (\sin \alpha \cos \beta, \sin \alpha \sin \beta, -\cos \alpha),
\end{aligned} \quad (8.9)$$

which can be obtained from  $(x, y, z)$  by a rotation through the Euler angles  $\beta$ ,  $\pi - \alpha$ , 0. We have chosen this coordinate system such that  $\hat{z}''$  is the direction of propagation of the reflected wave,  $\hat{x}''$  its p- and  $\hat{y}''$  its s-direction. In this coordinate system the electric field  $E^r$  of the reflected plane wave has p- and s-components, again omitting the phase factor,

$$E_p^r = r_p(\cos \alpha)E_p, \quad E_s^r = r_s(\cos \alpha)E_s. \quad (8.10)$$

By means of eqs. (3.9) and (3.10) the Debye potentials corresponding to the reflected plane wave can be found:

$$\begin{aligned} e\Psi_{\alpha,\beta} = & e^{2iq \cos \alpha} \frac{1}{k} \sum_{l'=1}^{\infty} \sum_{m'=-l'}^{l'} i^{l'-1} \left[ \frac{2l'+1}{l'(l'+1)} \right]^{1/2} (-1)^{m'-1} \\ & \times \left\{ E_p^r \left( \frac{1}{2} D_{m',1}^{l'}(\beta, \pi - \alpha, 0) - \frac{1}{2} D_{m',-1}^{l'}(\beta, \pi - \alpha, 0) \right) \right. \\ & \left. - i E_s^r \left( \frac{1}{2} D_{m',1}^{l'}(\beta, \pi - \alpha, 0) + \frac{1}{2} D_{m',-1}^{l'}(\beta, \pi - \alpha, 0) \right) \right\} \Psi_{l'}^{m'}, \quad (8.11a) \end{aligned}$$

$$\begin{aligned} h\Psi_{\alpha,\beta} = & -e^{2iq \cos \alpha} \frac{1}{k} \sum_{l'=1}^{\infty} \sum_{m'=-l'}^{l'} i^{l'} \left[ \frac{2l'+1}{l'(l'+1)} \right]^{1/2} (-1)^{m'-1} \\ & \times \left\{ E_p^r \left( \frac{1}{2} D_{m',1}^{l'}(\beta, \pi - \alpha, 0) + \frac{1}{2} D_{m',-1}^{l'}(\beta, \pi - \alpha, 0) \right) \right. \\ & \left. - i E_s^r \left( \frac{1}{2} D_{m',1}^{l'}(\beta, \pi - \alpha, 0) - \frac{1}{2} D_{m',-1}^{l'}(\beta, \pi - \alpha, 0) \right) \right\} \Psi_{l'}^{m'}. \quad (8.11b) \end{aligned}$$

The subscripts  $\alpha$  and  $\beta$  indicate that these Debye potentials correspond to the reflection of the plane wave propagating in the direction given by these angles. The phase factor  $e^{2iq \cos \alpha}$  arises from the phase difference between the plane wave and the reflected plane wave at the origin. From eq. (3.4) we have

$$D_{m',\pm 1}^{l'}(\beta, \pi - \alpha, 0) = e^{-im'\beta} d_{m',\pm 1}^{l'}(\pi - \alpha). \quad (8.12)$$

Equations (8.11) should now be integrated over all angles  $\alpha$  and  $\beta$ . Inserting eqs. (8.10), (8.4) and (8.12), and performing the integration over  $\beta$ :

$$\frac{1}{2\pi} \int_0^{2\pi} d\beta e^{i(m-m')\beta} = \delta_{m,m'}, \quad (8.13)$$

we are left with an integration over  $\alpha$ :

$$\begin{aligned} l'\Psi = & \sum_{l'=1}^{\infty} \sum_{m'=-l'}^{l'} \left\{ i^{l'-1} \left[ \frac{2l'+1}{l'(l'+1)} \right]^{1/2} (-1)^{m'-1} \delta_{m,m'} \right. \\ & \left. \times \int_0^{\pi/2-i\infty} \sin \alpha d\alpha e^{2iq \cos \alpha} a_{l',j',i,j}^m(\alpha) \right\} \Psi_{l'}^{m'}, \quad (8.14) \end{aligned}$$

with the abbreviations

$$\begin{aligned} a_{l',e,i,e}^m(\alpha) = & r_p(\cos \alpha) \bar{V}_l^m(\cos \alpha) d_{m,-}^{l'}(\pi - \alpha) \\ & + r_s(\cos \alpha) \bar{U}_l^m(\cos \alpha) d_{m,+}^{l'}(\pi - \alpha), \end{aligned}$$

$$\begin{aligned} a_{l',h,i,e}^m(\alpha) = & -i \left\{ r_p(\cos \alpha) \bar{V}_l^m(\cos \alpha) d_{m,+}^{l'}(\pi - \alpha) \right. \\ & \left. + r_s(\cos \alpha) \bar{U}_l^m(\cos \alpha) d_{m,-}^{l'}(\pi - \alpha) \right\}, \end{aligned}$$

$$a_{l',e,j,h}^m(\alpha) = i \left\{ r_p(\cos \alpha) \bar{U}_l^m(\cos \alpha) d_{m,-}^{l'}(\pi - \alpha) + r_s(\cos \alpha) \bar{V}_l^m(\cos \alpha) d_{m,+}^{l'}(\pi - \alpha) \right\}, \quad (8.15)$$

$$a_{l',h,j,h}^m(\alpha) = r_p(\cos \alpha) \bar{U}_l^m(\cos \alpha) d_{m,+}^{l'}(\pi - \alpha) + r_s(\cos \alpha) \bar{V}_l^m(\cos \alpha) d_{m,-}^{l'}(\pi - \alpha),$$

and

$$\begin{aligned} d_{m,-}^{l'}(\pi - \alpha) &= \frac{1}{2} d_{m,1}^{l'}(\pi - \alpha) - \frac{1}{2} d_{m,-1}^{l'}(\pi - \alpha), \\ d_{m,+}^{l'}(\pi - \alpha) &= \frac{1}{2} d_{m,1}^{l'}(\pi - \alpha) + \frac{1}{2} d_{m,-1}^{l'}(\pi - \alpha). \end{aligned} \quad (8.16)$$

From eq. (8.14) we see that the matrix A, characterizing the reflection of electric and magnetic multipole radiation by the substrate, is

$$\begin{aligned} A_{l',m',j',j,m,f} &= i^{l'-1} \left[ \frac{2l'+1}{l'(l'+1)} \right]^{1/2} (-1)^{m-1} \delta_{m,m'} \\ &\times \int_0^{\pi/2-i\infty} \sin \alpha \, d\alpha \, e^{2iq \cos \alpha} a_{l',j',j,f}^m(\alpha). \end{aligned} \quad (8.17)$$

It is noteworthy that the matrix A is diagonal with respect to the index  $m$ , just as the matrix B for the case of a sphere (eq. (4.2)). One could call this "conservation of angular momentum along the  $z$ -axis". It is a consequence of the rotational symmetry about the  $z$ -axis. This means that the calculation of the scattered field can be done for each  $m$  separately.

An additional remark should be made at this point about the integration path of the integral over  $\alpha$  (see fig. 2). In principle, the Fresnel reflection coefficients eqs. (8.7), which appear in the integral eq. (8.17) via eq. (8.15), can become singular. It is not very difficult to show that the reflection coefficient  $r_s(\cos \alpha)$  does not have a pole in the complex  $\cos \alpha$  plane. The reflection coefficient  $r_p(\cos \alpha)$ , however, has a pole in  $\cos \alpha = -n_1/\sqrt{n_2^2 + n_1^2}$ , located in the second quadrant of the complex  $\cos \alpha$  plane. This pole is connected with a so-called surface mode, which is an electromagnetic wave that propagates along the substrate and vanishes exponentially for  $z \rightarrow \pm\infty$ . By choosing the integration path as indicated in fig. 2 we exclude this surface mode from our solution, since  $\cos \alpha$  is then always in the first quadrant of the complex plane. This issue was also discussed by Weyl<sup>4</sup>).

In general, it is impossible to perform the integration over  $\alpha$  in eq. (8.17) analytically, because of the Fresnel factors  $r_p$  and  $r_s$  appearing in it. However, if the substrate is a perfect conductor, then  $r_p$  and  $r_s$  are 1 and  $-1$  respectively and eq. (8.17) becomes integrable. We shall discuss this situation in the next section.

## 9 Perfectly conducting substrate

If the substrate is a perfect conductor,  $r_p = 1$  and  $r_s = -1$ , eq. (8.15) becomes

$$\begin{aligned}
a_{l',e;l,e}^m(\alpha) &= \tilde{V}_l^m(\cos \alpha) d_{m,-}^{l'}(\pi - \alpha) - \tilde{U}_l^m(\cos \alpha) d_{m,+}^{l'}(\pi - \alpha), \\
a_{l',h;l,e}^m(\alpha) &= -i \left\{ \tilde{V}_l^m(\cos \alpha) d_{m,+}^{l'}(\pi - \alpha) - \tilde{U}_l^m(\cos \alpha) d_{m,-}^{l'}(\pi - \alpha) \right\}, \\
a_{l',e;l,h}^m(\alpha) &= i \left\{ \tilde{U}_l^m(\cos \alpha) d_{m,-}^{l'}(\pi - \alpha) - \tilde{V}_l^m(\cos \alpha) d_{m,+}^{l'}(\pi - \alpha) \right\}, \\
a_{l',h;l,h}^m(\alpha) &= \tilde{U}_l^m(\cos \alpha) d_{m,+}^{l'}(\pi - \alpha) - \tilde{V}_l^m(\cos \alpha) d_{m,-}^{l'}(\pi - \alpha).
\end{aligned} \tag{9.1}$$

Using eqs. (8.5) and (3.5) one can show that in this case the integral over  $\alpha$  in eq. (8.17) can be written in the form

$$\int_1^{i\infty} d(\cos \alpha) P(\cos \alpha),$$

where  $P(\cos \alpha)$  is a polynomial in  $\cos \alpha$ . This integral could in principle be performed analytically with the help of

$$\begin{aligned}
\int_1^{i\infty} d(\cos \alpha) e^{2iq \cos \alpha} \cos^n \alpha &= \frac{d^n}{d(2iq)^n} \int_1^{i\infty} d(\cos \alpha) e^{2iq \cos \alpha} \\
&= \frac{d^n}{d(2iq)^n} \left\{ -\frac{1}{2iq} e^{2iq} \right\}.
\end{aligned} \tag{9.2}$$

Here, however, we shall employ a quite different method of calculating **A**. Beside  $(x, y, z)$  we introduce a coordinate system  $(x', y', z')$  by shifting the origin a distance  $2a$  along the positive  $z$ -axis:

$$x' = x, \quad y' = y, \quad z' = z - 2a. \tag{9.3}$$

We can express the electromagnetic wave corresponding to the Debye potentials  ${}^f\Pi(\mathbf{r}) = \Pi_l^m(\mathbf{r})$  in terms of the Debye potentials  ${}^f\Psi(\mathbf{r}') = \Psi_l^m(\mathbf{r}')$  in the shifted coordinate system in the region  $r' < 2a$ . In this way a matrix **T** can be introduced. The calculation of **T** can be performed in a completely analogous way as that of **A**. The only difference is that there is now no reflection, so that

$$\begin{aligned}
T_{l',m',f;l,m,f} &= i^{l'-1} \left[ \frac{2l'+1}{l'(l'+1)} \right]^{1/2} (-1)^{m-1} \delta_{m,m'} \\
&\quad \times \int_0^{\pi/2-i\infty} \sin \alpha \, d\alpha \, e^{2iq \cos \alpha} t_{l',f;l,f}^m(\alpha),
\end{aligned} \tag{9.4}$$

with

$$\begin{aligned}
t_{l',e;l,e}^m(\alpha) &= \tilde{V}_l^m(\cos \alpha) d_{m,-}^{l'}(\alpha) + \tilde{U}_l^m(\cos \alpha) d_{m,+}^{l'}(\alpha), \\
t_{l',h;l,e}^m(\alpha) &= -i \left\{ \tilde{V}_l^m(\cos \alpha) d_{m,+}^{l'}(\alpha) + \tilde{U}_l^m(\cos \alpha) d_{m,-}^{l'}(\alpha) \right\}, \\
t_{l',e;l,h}^m(\alpha) &= i \left\{ \tilde{U}_l^m(\cos \alpha) d_{m,-}^{l'}(\alpha) + \tilde{V}_l^m(\cos \alpha) d_{m,+}^{l'}(\alpha) \right\}, \\
t_{l',h;l,h}^m(\alpha) &= \tilde{U}_l^m(\cos \alpha) d_{m,+}^{l'}(\alpha) + \tilde{V}_l^m(\cos \alpha) d_{m,-}^{l'}(\alpha).
\end{aligned} \tag{9.5}$$

Using eqs. (3.8) we see that there is a simple relation between A and T:

$$\begin{aligned} A_{l',m',e;l,m,e} &= (-1)^{l'-m-1} T_{l',m',e;l,m,e}, \\ A_{l',m',h;l,m,e} &= (-1)^{l'-m} T_{l',m',h;l,m,e}, \\ A_{l',m',e;l,m,h} &= (-1)^{l'-m-1} T_{l',m',e;l,m,h}, \\ A_{l',m',h;l,m,h} &= (-1)^{l'-m} T_{l',m',h;l,m,h}. \end{aligned} \quad (9.6)$$

But there is also a direct way of calculating T by application of an addition theorem:

$$\Pi_l^m(\mathbf{r}) = \sum_{l'=|m|}^{\infty} c_{l,l'}^m \Psi_{l'}^m(\mathbf{r}'), \quad (9.7)$$

valid in the region  $r' < 2a$ . In the appendix we prove the following recurrence relations for the coefficients  $c_{l,l'}^m$ :

$$\begin{aligned} \sqrt{(2l'+1)(l-m)(l+m+1)} c_{l,l'}^m &= \sqrt{(2l'+1)(l'-m)(l'+m+1)} c_{l,l'+1}^{m+1} \\ &+ 2q \left\{ \sqrt{\frac{(l'+m+1)(l'+m+2)}{2l'+3}} c_{l,l'+1}^{m+1} \right. \\ &\left. + \sqrt{\frac{l(l'-m)(l'-m-1)}{2l'-1}} c_{l,l'-1}^{m+1} \right\}, \end{aligned} \quad (9.8a)$$

$$\begin{aligned} \sqrt{(2l'+1)(l+m)(l-m+1)} c_{l,l'}^m &= \sqrt{(2l'+1)(l'+m)(l'-m+1)} c_{l,l'}^{m-1} \\ &+ 2q \left\{ \sqrt{\frac{(l'-m+1)(l'-m+2)}{2l'+3}} c_{l,l'+1}^{m-1} \right. \\ &\left. + \sqrt{\frac{(l'+m)(l'+m-1)}{2l'-1}} c_{l,l'-1}^{m-1} \right\}, \end{aligned} \quad (9.8b)$$

$$\begin{aligned} \sqrt{2l'+1} \left\{ \frac{l}{\sqrt{2l-1}} c_{l-1,l'}^0 - \frac{(l+1)}{\sqrt{2l+3}} c_{l+1,l'}^0 \right\} &= \\ = \sqrt{2l+1} \left\{ \frac{(l+1)}{\sqrt{2l'+3}} c_{l,l'+1}^0 - \frac{l'}{\sqrt{2l'-1}} c_{l,l'-1}^0 \right\}. \end{aligned} \quad (9.9)$$

From the addition theorem\*

$$\Pi_0^0(\mathbf{r}) = \sum_{l'=0}^{\infty} \sqrt{2l'+1} (-1)^{l'} h_{l'}^{(1)}(2q) \Psi_{l'}^0(\mathbf{r}'), \quad (9.10)$$

we have

$$c_{0,l'}^0 = \sqrt{2l'+1} (-1)^{l'} h_{l'}^{(1)}(2q). \quad (9.11)$$

\*See e.g. ref. 8.

By means of eqs. (9.8), (9.9) and (9.11) the coefficients  $c_{l',m'}^m$  can be calculated for all  $l, l'$  and  $m$ .

Again, one should not apply the addition theorem eq. (9.7) directly to the Debye potentials but to the corresponding Hertz vectors, given by eq. (7.5). One then finally returns to the Debye potentials by means of eqs. (7.8). In this way the following expressions for the matrix elements of  $T$  are found:

$$\begin{aligned}
 T_{l',m',e;l,m,e} = T_{l',m',h;l,m,h} &= \frac{1}{2} \frac{1}{\sqrt{(2l+1)(2l'+1)}} \delta_{m,m'} \\
 &\times \left[ \frac{1}{l'} (l-1) \left\{ \left[ \frac{(l+m-1)(l+m)(l'+m-1)(l'+m)}{(2l-1)(2l'-1)} \right]^{1/2} c_{l-1,l'-1}^{m-1} \right. \right. \\
 &+ \left[ \frac{(l-m-1)(l-m)(l'-m-1)(l'-m)}{(2l-1)(2l'-1)} \right]^{1/2} c_{l-1,l'-1}^{m+1} \\
 &+ 2 \left[ \frac{(l-m)(l+m)(l'-m)(l'+m)}{(2l-1)(2l'-1)} \right]^{1/2} c_{l-1,l'-1}^m \left. \right\} \\
 &- (l+2) \left\{ \left[ \frac{(l-m+1)(l-m+2)(l'+m-1)(l'+m)}{(2l+3)(2l'-1)} \right]^{1/2} c_{l+1,l'-1}^{m-1} \right. \\
 &+ \left[ \frac{(l+m+1)(l+m+2)(l'-m-1)(l'-m)}{(2l+3)(2l'-1)} \right]^{1/2} c_{l+1,l'-1}^{m+1} \\
 &- 2 \left[ \frac{(l-m+1)(l+m+1)(l'-m)(l'+m)}{(2l+3)(2l'-1)} \right]^{1/2} c_{l+1,l'-1}^m \left. \right\} \\
 &- \frac{1}{l'+1} (l-1) \left\{ \left[ \frac{(l+m-1)(l+m)(l'+m+1)(l'+m+2)}{(2l-1)(2l'+3)} \right]^{1/2} c_{l-1,l'+1}^{m-1} \right. \\
 &+ \left[ \frac{(l-m-1)(l-m)(l'+m+1)(l'+m+2)}{(2l-1)(2l'+3)} \right]^{1/2} c_{l-1,l'+1}^{m+1} \\
 &- 2 \left[ \frac{(l-m)(l+m)(l'-m+1)(l'+m+1)}{(2l-1)(2l'+3)} \right]^{1/2} c_{l-1,l'+1}^m \left. \right\} \\
 &- (l+2) \left\{ \left[ \frac{(l-m+1)(l-m+2)(l'-m+1)(l'-m+2)}{(2l+3)(2l'+3)} \right]^{1/2} c_{l+1,l'+1}^{m-1} \right. \\
 &+ \left[ \frac{(l+m+1)(l+m+2)(l'+m+1)(l'+m+2)}{(2l+3)(2l'+3)} \right]^{1/2} c_{l+1,l'+1}^{m+1} \\
 &+ 2 \left[ \frac{(l-m+1)(l+m+1)(l'-m+1)(l'+m+1)}{(2l+3)(2l'+3)} \right]^{1/2} c_{l+1,l'+1}^m \left. \right\} \left. \right], \tag{9.12a}
 \end{aligned}$$

$$T_{l',m',h;l,m,e} = -T_{l',m',e;l,m,h} = \frac{1}{2} \frac{1}{\sqrt{2l+1}} \delta_{m,m'} \frac{1}{l'(l'+1)}$$

$$\begin{aligned}
& \times \left( -(l-1) \left\{ \left[ \frac{(l+m-1)(l+m)(l'-m+1)(l'+m)}{(2l-1)} \right]^{1/2} c_{l-1,l'}^{m-1} \right. \right. \\
& - \left[ \frac{(l-m-1)(l-m)(l'+m+1)(l'-m)}{(2l-1)} \right]^{1/2} c_{l-1,l'}^{m+1} \\
& \left. \left. - 2m \left[ \frac{(l-m)(l+m)}{(2l-1)} \right]^{1/2} c_{l-1,l'}^m \right\} \right. \\
& + (l+2) \left\{ \left[ \frac{(l-m+1)(l-m+2)(l'-m+1)(l'+m)}{(2l+3)} \right]^{1/2} c_{l+1,l'}^{m-1} \right. \\
& - \left[ \frac{(l+m+1)(l+m+2)(l'+m+1)(l'-m)}{(2l+3)} \right]^{1/2} c_{l+1,l'}^{m+1} \\
& \left. \left. + 2m \left[ \frac{(l-m+1)(l+m+1)}{(2l+3)} \right]^{1/2} c_{l+1,l'}^m \right\} \right). \tag{9.12b}
\end{aligned}$$

The matrix A is then found from eq. (9.6).

## 10 The static limit

In this section we shall consider the static limit, i.e.  $a \ll \lambda/2\pi$  or  $q \ll 1$ , and show that in this limit the solution presented in this chapter is equivalent to the solution given by Wind, Vlioger and Bedeaux<sup>5</sup>) for the polarizability of a small sphere on a substrate, or to the solution presented in chapter II for the polarizability of a small spheroidal particle on a substrate, in the limiting case of a sphere.

Because we assume the sphere and the substrate to be non-magnetic we only have to consider the electric field (the magnetic field will be homogeneous in and around the sphere in the static limit) and the electric Debye potentials, so that we may drop the index  $f$ , assuming it to be  $e$ . In the static limit the matrix B, eq. (4.2), becomes\*

$$B_{l',m',l,m} = i\delta_{l,l'}\delta_{m,m'} \frac{l+1}{2l+1} \frac{q^{2l+1}}{[(2l-1)!!]^2} \frac{n_3^2 - n_1^2}{ln_3^2 + (l+1)n_1^2}, \tag{10.1}$$

with the convention

$$(2l-1)!! \equiv (2l-1)(2l-3)\cdots 3 \cdot 1. \tag{10.2}$$

If a plane wave is incident on the system, then for  $r \ll \lambda/2\pi$  or  $kr \ll 1$  in eqs. (3.9a) and (3.10a) only the term with  $l=1$  is important. This is clear if one expands the function  $j_l(\rho)$  into powers of  $\rho^\dagger$ :

$$j_l(\rho) = 2^l \rho^l \sum_{k=0}^{\infty} \frac{(-1)^k (l+k)!}{k!(2l+2k+1)!} \rho^{2k}. \tag{10.3}$$

\*See e.g. Born and Wolf<sup>3</sup>).

†See e.g. Stratton<sup>8</sup>).

So in the neighbourhood of the sphere only the partial waves with  $l = 1$  and  $m = 0, \pm 1$  are important in eqs. (3.9a) and (3.10a). Because of conservation of  $m$  we only have to consider the cases  $m = 0, \pm 1$  in the whole analysis.

In order to calculate the static limit of  $A$  we develop  $r_p(\cos \alpha)$  and  $r_s(\cos \alpha)$ , given by eqs. (8.7), into powers of  $1/\cos^2 \alpha$ :

$$r_p(\cos \alpha) = \sum_{n=0}^{\infty} r_{p,n} \frac{1}{(\cos^2 \alpha)^n}, \quad (10.4a)$$

$$r_s(\cos \alpha) = \sum_{n=0}^{\infty} r_{s,n} \frac{1}{(\cos^2 \alpha)^n}. \quad (10.4b)$$

From eq. (9.2) we see that the static limit is obtained by integration of the term with the highest power of  $\cos \alpha$ , which yields the lowest power in  $q$ . So in the integrand of eq. (8.17) we only have to know the coefficient of the highest power of  $\cos \alpha$ . Using this fact and the fact that

$$r_{p,0} = \frac{n_2^2 - n_1^2}{n_2^2 + n_1^2}, \quad (10.5a)$$

$$r_{s,0} = 0, \quad (10.5b)$$

which is easily verified, we can write eq. (8.17) in the static limit, for  $m, m' = 0, \pm 1$ , as

$$A_{l',m';l,m} = i^{l'-1} \left[ \frac{2l'+1}{l'(l'+1)} \right]^{1/2} (-1)^{m-1} \delta_{m,m'} \\ \times \frac{n_2^2 - n_1^2}{n_2^2 + n_1^2} \int_0^{\pi/2 - i\infty} \sin \alpha \, d\alpha \, e^{2iq \cos \alpha} \tilde{V}_l^m(\cos \alpha) d_{m,-}^{l'}(\pi - \alpha). \quad (10.6)$$

Furthermore, one can show that the expansion of  $\tilde{U}_l^m(\cos \alpha) d_{m,+}^{l'}(\pi - \alpha)$  into powers of  $\cos \alpha$  has a lower highest power than the expansion of  $\tilde{V}_l^m(\cos \alpha) d_{m,-}^{l'}(\pi - \alpha)$  for the cases  $m = 0, \pm 1$ , so that in the static limit we can identify the static solution eq. (10.6) with the solution for a perfectly conducting substrate, eqs. (8.17) and (9.1), apart from the factor  $(n_2^2 - n_1^2)/(n_2^2 + n_1^2)$ . Using this solution, eqs. (9.6) and (9.12), and the expansion of  $h_l^{(1)}(\rho)$  (see also ref. 8):

$$h_l^{(1)}(\rho) = j_l(\rho) - \frac{i}{2l\rho^{l+1}} \sum_{k=0}^{\infty} \frac{\Gamma(2l-2k+1)}{k!\Gamma(l-k+1)} \rho^{2k}, \quad (10.7)$$

one can show that in the limit  $q \rightarrow 0$   $A$  becomes, for  $m = 0, \pm 1$ ,

$$A_{l',0;l,0} = -i \frac{n_2^2 - n_1^2}{n_2^2 + n_1^2} \sqrt{(2l'+1)(2l+1)} \\ \times \frac{(2l'-1)!!(l'+l)!(2l-1)!!}{(l'+1)!(l-1)!} \frac{1}{(2q)^{l'+l+1}}, \quad (10.8a)$$

$$A_{l', \pm 1; l, \pm 1} = -i \frac{n_2^2 - n_1^2}{n_2^2 + n_1^2} \sqrt{\frac{l'(2l' + 1)l(2l + 1)}{(l' + 1)(l + 1)}} \times \frac{(2l' - 1)!!(l' + l)!(2l - 1)!!}{(l' + 1)!(l - 1)!} \frac{1}{(2q)^{l'+l+1}} \quad (10.8b)$$

In order to compare the results obtained above with those found by Wind, Vlieger and Bedeaux<sup>5</sup>, we first remark that in the static limit the potential  $V$  used by these authors and in chapter II is related to the electric Debye potential  ${}^e\Pi$  by (see also ref. 9)

$$V = -\frac{\partial(r^e\Pi)}{\partial r} \quad (10.9)$$

Comparing the multipole expansion eq. (2.2) of ref. 5 for the electric potential corresponding to the *direct* scattered electric field in the region above the substrate and outside the particle, or the multipole expansion eq. (II.2.16), using eqs. (II.2.14) and (II.2.15) for the spherical case, with multipole coefficients  $A_{1,j}$  and  $B_{1,j}$ , to the expansion eq. (2.8a) of the electric Debye potential in terms of the functions  $\Pi_l^m$ , in which the coefficients  ${}^e w_l^m$  are obtained from eq. (5.3), we conclude, using eqs. (10.7) and (10.9), that in the static limit we have to make the identifications

$$S_{j,0;1,0} = -i \frac{2}{\sqrt{3}} \frac{1}{\sqrt{2j+1}} \frac{1}{j} \frac{1}{(2j-1)!!} q^{j+2} A_{1,j} / \cos \theta_0, \quad (10.10a)$$

$$S_{j,\pm 1;1,\pm 1} = -i \sqrt{\frac{2}{3}} \sqrt{\frac{j(j+1)}{2j+1}} \frac{1}{j} \frac{1}{(2j-1)!!} q^{j+2} B_{1,j} / \sin \theta_0, \quad (10.10b)$$

with the matrix  $S$  defined by

$$S \equiv (1 - B \cdot A)^{-1} \cdot B. \quad (10.11)$$

The angle  $\theta_0$  in eqs. (10.10) is the angle between the incident electric field and the  $z$ -axis. The relation eq. (10.11) can also be written as

$$(1 - B \cdot A) \cdot S = B, \quad (10.12)$$

which means that  $S_{j,0;1,0}$  and  $S_{j,\pm 1;1,\pm 1}$  satisfy the relations

$$\sum_{j=1}^{\infty} \{\delta_{k,j} - B_{k,0;k,0} A_{k,0;j,0}\} S_{j,0;1,0} = \delta_{k,1} B_{1,0;1,0}, \quad (10.13a)$$

$$\sum_{j=1}^{\infty} \{\delta_{k,j} - B_{k,\pm 1;k,\pm 1} A_{k,\pm 1;j,\pm 1}\} S_{j,\pm 1;1,\pm 1} = \delta_{k,1} B_{1,\pm 1;1,\pm 1}, \quad (10.13b)$$

for  $k = 1, 2, \dots$ , where we have used the fact that  $B$  is diagonal in the index  $k$ . Using eqs. (10.1), (10.8) and (10.10) it can easily be shown that in the static limit

eqs. (10.13a) and (10.13b) are equivalent to the relations eqs. (3.6) and (3.7) of ref. 5 for a sphere on a substrate:

$$\sum_{j=1}^{\infty} \left\{ \delta_{k,j} + \frac{(\epsilon_2 - \epsilon_1)k(\epsilon_1 - \epsilon_3)}{(\epsilon_2 + \epsilon_1)[(k+1)\epsilon_1 + k\epsilon_3]} \frac{(k+j)!}{k!j!2^{k+j+1}} \right\} A_{1,j} \\ = \frac{\epsilon_1 - \epsilon_3}{2\epsilon_1 + \epsilon_3} \cos \theta_0 \delta_{k,1}, \quad (10.14a)$$

$$\sum_{j=1}^{\infty} \left\{ \delta_{k,j} + \frac{(\epsilon_2 - \epsilon_1)k(\epsilon_1 - \epsilon_3)}{(\epsilon_2 + \epsilon_1)[(k+1)\epsilon_1 + k\epsilon_3]} \frac{(k+j)!}{(k+1)!(j-1)!2^{k+j+1}} \right\} B_{1,j} \\ = \frac{\epsilon_1 - \epsilon_3}{2\epsilon_1 + \epsilon_3} \sin \theta_0 \delta_{k,1}, \quad (10.14b)$$

with  $\epsilon_i = n_i^2$  ( $i = 1, 2, 3$ ). With the help of eqs. (II.2.10)–(II.2.15) also the equivalence with eqs. (II.2.29) and (II.2.30) for the spherical case is established.

Furthermore it can be shown, making use of eq. (10.6) and the results of the preceding section, that the reflected scattered electric field can be identified with the field of an *image scattering centre* located at the mirror image point  $(0, 0, 2a)$  of the origin. With this image a scattering matrix  $S'$  can be related, having the relevant matrix elements

$$S'_{j,0;1,0} = \frac{n_2^2 - n_1^2}{n_2^2 + n_1^2} (-1)^{j-1} S_{j,0;1,0}, \quad (10.15a)$$

$$S'_{j,\pm 1;1,\pm 1} = \frac{n_2^2 - n_1^2}{n_2^2 + n_1^2} (-1)^j S_{j,\pm 1;1,\pm 1}. \quad (10.15b)$$

This is equivalent to the relations

$$A'_{1,j} = \frac{\epsilon_2 - \epsilon_1}{\epsilon_2 + \epsilon_1} (-1)^{j-1} A_{1,j}, \quad (10.16a)$$

$$B'_{1,j} = \frac{\epsilon_2 - \epsilon_1}{\epsilon_2 + \epsilon_1} (-1)^j B_{1,j}, \quad (10.16b)$$

found in eq. (2.12) of ref. 5 or eq. (II.2.22) for the image multipole coefficients in the expansion eq. (2.2) of ref. 5 or eq. (II.2.16).

## 11 The far-away scattered field

In most practical situations one is interested in the scattered electric field at large distances, i.e.  $r \gg \lambda/2\pi$  and  $r \gg a$ . At such distances we are in the so-called radiation zone, where the electromagnetic fields have negligible radial components. Above the substrate ( $\theta > \pi/2$ ) we have two contributions to the scattered field: the contribution of the *direct* scattered wave  $W^S$  (see section 5) and that of the *reflection* of  $W^S$  by the substrate.

Let us first consider  $W^S$  itself. The electric field can be obtained from eq. (2.3a). Written in spherical coordinates this equation becomes

$$E_r(r, \theta, \phi) = \frac{\partial^2(r^e \Pi)}{\partial r^2} + k^2 r^e \Pi,$$

$$E_\theta(r, \theta, \phi) = \frac{1}{r} \frac{\partial^2(r^e \Pi)}{\partial r \partial \theta} + ik \frac{1}{r \sin \theta} \frac{\partial(r^h \Pi)}{\partial \phi}, \quad (11.1)$$

$$E_\phi(r, \theta, \phi) = \frac{1}{r \sin \theta} \frac{\partial^2(r^e \Pi)}{\partial r \partial \phi} - ik \frac{1}{r} \frac{\partial(r^h \Pi)}{\partial \theta},$$

with the Debye potentials given by eqs. (2.8):

$${}^e \Pi = \sum_{l=1}^{\infty} \sum_{m=-l}^l {}^e w_l^m \Pi_l^m = \sum_{l=1}^{\infty} \sum_{m=-l}^l {}^e w_l^m h_l^{(1)}(kr) \bar{P}_l^m(\cos \theta) e^{im\phi}, \quad (11.2a)$$

$${}^h \Pi = \sum_{l=1}^{\infty} \sum_{m=-l}^l {}^h w_l^m \Pi_l^m = \sum_{l=1}^{\infty} \sum_{m=-l}^l {}^h w_l^m h_l^{(1)}(kr) \bar{P}_l^m(\cos \theta) e^{im\phi}, \quad (11.2b)$$

in which the multipole coefficients  ${}^e w_l^m$  and  ${}^h w_l^m$  are found from eq. (6.3). When  $r \gg \lambda/2\pi$  we have asymptotically\*

$$r h_l^{(1)}(kr) \simeq \frac{1}{k} (-i)^{l+1} e^{ikr} \quad (kr \rightarrow \infty). \quad (11.3)$$

Inserting this relation and eqs. (11.2) into eq. (11.1), we find the asymptotic formulae

$$E_r(r, \theta, \phi) \simeq 0,$$

$$E_\theta(r, \theta, \phi) \simeq \frac{e^{ikr}}{r} \sum_{l=1}^{\infty} \sum_{m=-l}^l \left\{ {}^e w_l^m (-i)^l \frac{d}{d\theta} \bar{P}_l^m(\cos \theta) e^{im\phi} - {}^h w_l^m (-i)^{l+1} \frac{1}{\sin \theta} \bar{P}_l^m(\cos \theta) m e^{im\phi} \right\}, \quad (11.4)$$

$$E_\phi(r, \theta, \phi) \simeq \frac{e^{ikr}}{r} \sum_{l=1}^{\infty} \sum_{m=-l}^l \left\{ -{}^e w_l^m (-i)^{l+1} \frac{1}{\sin \theta} \bar{P}_l^m(\cos \theta) m e^{im\phi} - {}^h w_l^m (-i)^l \frac{d}{d\theta} \bar{P}_l^m(\cos \theta) e^{im\phi} \right\}.$$

In order to calculate the electric field corresponding to the reflection of  $W^S$  by the substrate at a point  $(r, \theta, \phi)$  ( $\theta > \pi/2$ ) we introduce a rotated coordinate system  $(x', y', z')$  with the  $z'$ -axis pointing towards the mirror image point  $(r^r, \theta^r, \phi)$  of  $(r, \theta, \phi)$  (see fig. 4). In an analogous way as in section 8 we can express the electric field corresponding to the wave  $W^S$  as an integral over plane waves in the coordinate system  $(x', y', z')$ . The electric field corresponding to the reflection of  $W^S$

\* See e.g. ref. 8.

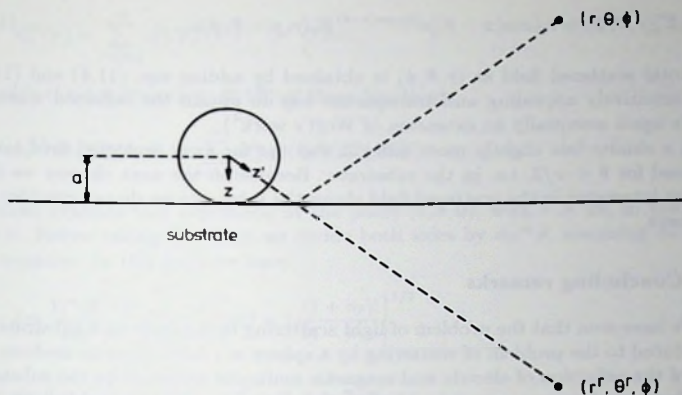


Fig. 4. Choice of the  $z'$ -axis for the calculation of the scattered wave after being reflected by the substrate.

then becomes the sum of an integral over  $p$ - and an integral over  $s$ -polarized plane waves, each wave multiplied by its corresponding Fresnel factor. But, according to eq. (6.3) with the integration path of fig. 2, at the point  $(r, \theta, \phi)$  in these integrals all plane waves except the reflected waves of the plane waves propagating in the  $z'$ -direction are attenuated. So at large distances ( $r \gg \lambda/2\pi$ ) only the reflected waves of the plane waves propagating in directions within a small solid angle about the  $z'$ -direction will contribute to the integrals. Because the Fresnel factors appearing in these integrals will be slowly varying functions within this solid angle we may replace them by the Fresnel factors corresponding to the plane waves propagating in the  $z'$ -direction. But the resulting integrals are precisely the plane wave expansions for the  $\theta$ - and  $\phi$ -components of the electric field at the point  $(r', \theta', \phi)$  corresponding to  $W^S$  itself. So at large distances the  $\theta$ - and  $\phi$ -components of the electric field of the reflected wave are asymptotically

$$\begin{aligned}
 E_{\theta}^r(r, \theta, \phi) &\simeq r_p(\cos \theta^r) E_{\theta}(r', \theta', \phi), \\
 E_{\phi}^r(r, \theta, \phi) &\simeq r_s(\cos \theta^r) E_{\phi}(r', \theta', \phi).
 \end{aligned}
 \tag{11.5}$$

When in addition to  $r \gg \lambda/2\pi$  also  $|r \cos \theta| \gg a$  we have asymptotically:

$$\theta^r \simeq \pi - \theta, \quad r^r \simeq r + 2a \cos(\pi - \theta),
 \tag{11.6}$$

and eq. (11.5) becomes

$$E_{\theta}^r(r, \theta, \phi) \simeq r_p(\cos(\pi - \theta)) e^{2iq \cos(\pi - \theta)} E_{\theta}(r, \pi - \theta, \phi),$$

$$E_{\phi}^r(r, \theta, \phi) \simeq r_s(\cos(\pi - \theta))e^{2iq \cos(\pi - \theta)} E_{\phi}(r, \pi - \theta, \phi). \quad (11.7)$$

The total scattered field at  $(r, \theta, \phi)$  is obtained by adding eqs. (11.4) and (11.7). This intuitively appealing and transparent way to obtain the reflected scattered field is again essentially an extension of Weyl's work<sup>4</sup>).

In a similar but slightly more difficult way the far-away scattered field can be obtained for  $\theta < \pi/2$ , i.e. in the substrate. Because in the next chapter we shall only be interested in the scattered field above the substrate we do not consider this case here.

## 12 Concluding remarks

We have seen that the problem of light scattering by a sphere on a substrate can be reduced to the problem of scattering by a sphere in a homogeneous medium and that of the reflection of electric and magnetic multipole radiation by the substrate. The first problem was solved by Mie<sup>2</sup>) and to solve the second problem we have extended Weyl's method<sup>4</sup>) for the calculation of the reflection of dipole radiation by a flat surface to higher order multipole radiation. The formal solution of the scattering problem was then given in a compact form by eq. (5.3). For the matrix  $A$  appearing in this equation we have derived an integral expression eq. (8.17), which in general can only be evaluated numerically. In two cases this integral could be performed analytically, namely in the case of a perfectly conducting substrate and in the so-called static limit, when the radius of the sphere is much smaller than the wavelength of the incident light. For the latter case we have shown that the result is equivalent to that obtained by Wind, Vlieger and Bedeaux<sup>5</sup>) for small spheres and to the result of chapter II for the special case that the spheroid is a sphere. Finally, expressions were derived for the far-away scattered field above the substrate.

In the next chapter we shall apply the method developed in this chapter to an ellipsometric experiment by Greef<sup>11</sup>) with a dilute system of growing spherical mercury particles on a carbon substrate. An efficient way to calculate the matrix  $A$  numerically is presented. Neglecting the interaction between the spheres it is then relatively easy to calculate the reflection of such a system and from that the ellipsometric angles.

## Appendix

### *Proof of the recurrence relations for the coefficients $c_{lm}^n$*

Let us consider the coordinate system  $(x', y', z')$  that is related to the coordinate system  $(x, y, z)$  by a shift  $2a$  along the positive  $z$ -axis:

$$x' = x, \quad y' = y, \quad z' = z - 2a. \quad (A.1)$$

The function  $\Pi_l^m(\mathbf{r})$  should be expressible as a sum over the functions  $\Psi_l^m(\mathbf{r}')$  in the region  $r' < 2a$  because it has no singularities in this region. Because of symmetry,  $m$  is conserved, so

$$\Pi_i^m(\mathbf{r}) = \sum_{l'=|m|}^{\infty} c_{l',i}^m \Psi_{l'}^m(\mathbf{r}') \quad (r' < 2a). \quad (\text{A.2})$$

Or, with the definition eqs. (2.10) of these functions:

$$h_i^{(1)}(kr) Y_i^m(\theta, \phi) = \sum_{l'=|m|}^{\infty} c_{l',i}^m j_{l'}(kr') Y_{l'}^m(\theta', \phi'). \quad (\text{A.3})$$

We shall evaluate this expression at the point  $(r, \theta, 0)$ , with  $r > 2a$ , in the limit  $\theta \rightarrow 0$ . Before taking this limit we divide both sides by  $\sin^m \theta$ , assuming  $m$  to be non-negative. In this limit we have

$$\lim_{\theta \rightarrow 0} \frac{Y_l^m(\theta, 0)}{\sin^m \theta} = \frac{1}{2^m} \frac{1}{m!} \left[ (2l+1) \frac{(l+m)!}{(l-m)!} \right]^{1/2}, \quad (\text{A.4})$$

$$\sin \theta \simeq \frac{r'}{r' + 2a} \sin \theta' \quad (\theta \rightarrow 0, r > 2a). \quad (\text{A.5})$$

With these relations we obtain in the limit  $\theta \rightarrow 0$ :

$$\begin{aligned} & \left[ (2l+1) \frac{(l+m)!}{(l-m)!} \right]^{1/2} h_i^{(1)}(kr) \\ &= \left( 1 + \frac{2a}{r'} \right)^m \sum_{l'=m}^{\infty} c_{l',i}^m \left[ (2l'+1) \frac{(l'+m)!}{(l'-m)!} \right]^{1/2} j_{l'}(kr'), \end{aligned} \quad (\text{A.6})$$

where  $r'$  is now just  $r - 2a$ . This equation is valid for all  $m$ , in particular for  $m+1$ :

$$\begin{aligned} & \left[ (2l+1) \frac{(l+m+1)!}{(l-m-1)!} \right]^{1/2} h_i^{(1)}(kr) \\ &= \left( 1 + \frac{2a}{r'} \right)^{m+1} \sum_{l'=m+1}^{\infty} c_{l',i}^{m+1} \left[ (2l'+1) \frac{(l'+m+1)!}{(l'-m-1)!} \right]^{1/2} j_{l'}(kr'). \end{aligned} \quad (\text{A.7})$$

Using the recurrence relation

$$\frac{1}{\rho} j_l(\rho) = \frac{1}{2l+1} \{ j_{l-1}(\rho) + j_{l+1}(\rho) \} \quad (\text{A.8})$$

and equating the coefficients of  $j_{l'}$  in eqs. (A.6) and (A.7), the following recurrence relation is obtained (eq. (9.8a)):

$$\begin{aligned} & \sqrt{(2l'+1)(l-m)(l+m+1)} c_{l',i}^m = \sqrt{(2l'+1)(l'-m)(l'+m+1)} c_{l',i}^{m+1} \\ & + 2q \left\{ \sqrt{\frac{(l'+m+1)(l'+m+2)}{2l'+3}} c_{l',i+1}^{m+1} \right. \\ & \left. + \sqrt{\frac{(l'-m)(l'-m-1)}{2l'-1}} c_{l',i-1}^{m+1} \right\}, \end{aligned} \quad (\text{A.9})$$

with  $q = ak$  (see eq. (4.4)). This relation is also valid for negative  $m$ . In an analogous way one can derive the recurrence relation (eq. (9.8b))

$$\begin{aligned} \sqrt{(2l'+1)(l+m)(l-m+1)}c_{l,l'}^m &= \sqrt{(2l'+1)(l'+m)(l'-m+1)}c_{l,l'}^{m-1} \\ &+ 2q \left\{ \sqrt{\frac{(l'-m+1)(l'-m+2)}{2l'+3}}c_{l,l'+1}^{m-1} \right. \\ &\left. + \sqrt{\frac{(l'+m)(l'+m-1)}{2l'-1}}c_{l,l'-1}^{m-1} \right\}. \end{aligned} \quad (\text{A.10})$$

Furthermore, putting  $m = 0$  in eq. (A.6) yields

$$\sqrt{2l+1}h_l^{(1)}(kr) = \sum_{l'=0}^{\infty} c_{l,l'}^0 \sqrt{2l'+1}j_{l'}(kr'). \quad (\text{A.11})$$

Differentiating this relation with respect to  $kr$  or  $kr'$ , then using the recurrence relation

$$\frac{d}{d\rho} z_l(\rho) = \frac{1}{2l+1} \{ lz_{l-1}(\rho) - (l+1)z_{l+1}(\rho) \}, \quad (\text{A.12})$$

where  $z_l$  may be either  $j_l$  or  $h_l^{(1)}$ , and finally applying eq. (A.11) again to the resulting expression, the following recurrence relation is obtained (eq. (9.9)):

$$\begin{aligned} \sqrt{2l'+1} \left\{ \frac{l}{\sqrt{2l-1}}c_{l-1,l'}^0 - \frac{(l+1)}{\sqrt{2l+3}}c_{l+1,l'}^0 \right\} &= \\ = \sqrt{2l+1} \left\{ \frac{(l'+1)}{\sqrt{2l'+3}}c_{l,l'+1}^0 - \frac{l'}{\sqrt{2l'-1}}c_{l,l'-1}^0 \right\}. \end{aligned} \quad (\text{A.13})$$

## References

- 1) T. Takemori, M. Inoue and K. Ohtaka, J. Phys. Soc. Jap. **56** (1987) 1587.
- 2) G. Mie, Ann. d. Phys. (4) **25** (1908) 377.
- 3) P. Debye, Ann. d. Phys. (4) **30** (1909) 57.
- 4) H. Weyl, Ann. d. Phys. (4) **60** (1919) 481.
- 5) M.M. Wind, J. Vlieger and D. Bedeaux, Physica **141A** (1987) 33.
- 6) C.J. Bouwkamp and H.B.G. Casimir, Physica **20** (1954) 539.
- 7) G.N. Watson, Theory of Bessel Functions (Cambridge Univ. Press, Cambridge, 1958).
- 8) J.A. Stratton, Electromagnetic Theory (McGraw-Hill, New York, 1941), pp. 392-423.





## Chapter IV

# Light Reflection from a Substrate Sparsely Seeded with Spheres – Comparison with an Ellipsometric Experiment

### 1 Introduction

In chapter III the light scattering by a sphere on a substrate was considered. The theory developed in that chapter can be applied to spheres with a radius of the order of the wavelength of the incident light. In the present chapter this theory is used to calculate the light reflection from a substrate with spheres on top of it, in the approximation that the interaction between the spheres can be neglected. This will be a good approximation if the number density of spheres is sufficiently low. We can then just add the scattered fields of all the spheres, which is elaborated in section 2. In section 3 a brief description is given of the methods used in computer calculations that we have performed. In section 4 some results of these computer calculations for mercury spheres on a carbon substrate are presented and compared with an ellipsometric experiment by Greef<sup>1</sup>). In section 5 we give a summary and a brief discussion.

### 2 Light reflection by an assembly of non-interacting spheres on a substrate

We consider an assembly of spheres on an infinite, flat substrate (see fig. 1) and assume that a plane wave is incident on this system, which is either p- or s-polarized. We shall first suppose that all spheres have the same radius  $a$ . The electromagnetic interaction between the spheres is neglected. The origin of our coordinate system is chosen at the centre of one of the spheres, with the  $x$ -axis downward and the  $z$ -axis such that the wavevector  $\mathbf{k}$  of the incident plane wave has components  $\mathbf{k} = (k \sin \theta_i, 0, k \cos \theta_i)$ .

Now let us consider e.g. the  $x$ -component of the scattered electric field at a point with spherical coordinates  $(r, \theta, \phi)$  above the substrate ( $\theta > \pi/2$ ) with  $kr \gg 1$ , i.e.

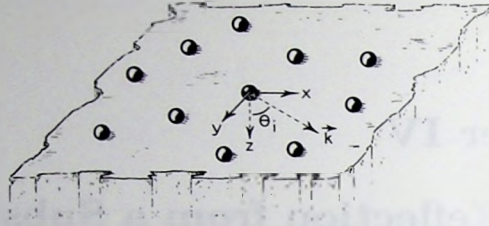


Fig. 1. A part of the substrate with spheres on top of it. The origin of the coordinate system is chosen at the centre of one of the spheres, with  $z$ -axis downward. The wavevector  $k$  of the incident plane wave is in the  $x$ - $z$  plane.

in the radiation zone. The scattered electric field  $E^S$  corresponding to the sphere at the origin will have  $x$ -component

$$E_x^S(r, \theta, \phi) = \frac{e^{ikr}}{kr} e_x(\theta, \phi), \quad (2.1)$$

where  $e_x(\theta, \phi)$  is some function of the angles  $\theta$  and  $\phi$ . For what we want to prove the exact form of  $e_x(\theta, \phi)$  is unimportant. We shall now calculate the  $x$ -component of the total scattered electric field at the point with spherical coordinates  $(r, \pi - \theta, 0)$ . For that purpose the contributions of all spheres have to be summed:

$$E_x^{S, \text{total}}(r, \pi - \theta, 0) = \sum_n e^{ikx_n \sin \theta} \frac{\exp \left\{ ik \sqrt{r^2 \cos^2 \theta + (x_n - r \sin \theta)^2 + y_n^2} \right\}}{k \sqrt{r^2 \cos^2 \theta + (x_n - r \sin \theta)^2 + y_n^2}} e_x(\theta_n, \phi_n). \quad (2.2)$$

Here the spheres have been numbered by  $n$ ;  $x_n$  and  $y_n$  are the  $x$ - and  $y$ -coordinates of the centre of sphere  $n$ . A phase factor  $e^{ikx_n \sin \theta}$  appears because the incident plane wave has a different phase at the centre of each sphere.  $\theta_n$  and  $\phi_n$  are the angular coordinates of the point  $(r, \pi - \theta, 0)$  in the shifted coordinate system that has its origin at the centre of sphere  $n$ . Now if  $r \gg d$ , with  $d$  the mean distance between the spheres:

$$d \equiv \frac{1}{\sqrt{N}}, \quad (2.3)$$

$N$  being the number of spheres per unit area, and if there is no long range order in the positions of the spheres, we may replace the sum in eq. (2.2) by the following integral:

$$E_x^{S, \text{total}}(r, \pi - \theta, 0) = N \int_{-\infty}^{\infty} dx \int_{-\infty}^{\infty} dy e^{ikx \sin \theta} \times \frac{\exp \left\{ ik \sqrt{r^2 \cos^2 \theta + (x - r \sin \theta)^2 + y^2} \right\}}{k \sqrt{r^2 \cos^2 \theta + (x - r \sin \theta)^2 + y^2}} e_x(\theta(x, y), \phi(x, y)). \quad (2.4)$$

To this integral only an area around the origin in the  $x$ - $y$  plane with linear dimensions of the order  $\sqrt{r/k}$  contributes non-destructively. But if  $r$  is sufficiently large  $e_x(\theta(x, y), \phi(x, y))$  will be a slowly varying function within this area, so that we may replace it by  $e_x(\theta(0, 0), \phi(0, 0)) = e_x(\pi - \theta_i, 0)$ . The resulting integral can be performed analytically<sup>2</sup>:

$$\begin{aligned}
 & \int_{-\infty}^{\infty} dx \int_{-\infty}^{\infty} dy e^{ikx \sin \theta_i} \frac{\exp \{ ik\sqrt{r^2 \cos^2 \theta_i + (x - r \sin \theta_i)^2 + y^2} \}}{k\sqrt{r^2 \cos^2 \theta_i + (x - r \sin \theta_i)^2 + y^2}} \\
 &= e^{ikr \sin^2 \theta_i} \int_{-\infty}^{\infty} dx \int_{-\infty}^{\infty} dy e^{ikx \sin \theta_i} \frac{\exp \{ ik\sqrt{r^2 \cos^2 \theta_i + x^2 + y^2} \}}{k\sqrt{r^2 \cos^2 \theta_i + x^2 + y^2}} \\
 &= e^{ikr \sin^2 \theta_i} \int_0^{\infty} \rho d\rho \int_0^{2\pi} d\phi e^{ik\rho \cos \phi \sin \theta_i} \frac{\exp \{ ik\sqrt{r^2 \cos^2 \theta_i + \rho^2} \}}{k\sqrt{r^2 \cos^2 \theta_i + \rho^2}} \quad (2.5) \\
 &= 2\pi e^{ikr \sin^2 \theta_i} \int_0^{\infty} \rho d\rho J_0(k\rho \sin \theta_i) \frac{\exp \{ ik\sqrt{r^2 \cos^2 \theta_i + \rho^2} \}}{k\sqrt{r^2 \cos^2 \theta_i + \rho^2}} \\
 &= 2\pi i e^{ikr \sin^2 \theta_i} \frac{\exp \{ ikr \cos^2 \theta_i \}}{k^2 \cos \theta_i} = 2\pi i \frac{e^{ikr}}{k^2 \cos \theta_i},
 \end{aligned}$$

with  $J_0$  the cylindrical Bessel function of order 0. So the final result is

$$E_x^{\text{S, total}}(r, \pi - \theta_i, 0) = 2\pi i N \frac{e^{ikr}}{k^2 \cos \theta_i} e_x(\pi - \theta_i, 0). \quad (2.6)$$

Similar considerations are valid for the  $y$ - and  $z$ -components of the electric field. In vector notation we can thus write

$$E^{\text{S, total}}(r, \pi - \theta_i, 0) = 2\pi i N \frac{e^{ikr}}{k^2 \cos \theta_i} e(\pi - \theta_i, 0). \quad (2.7)$$

From this result we can conclude that at large distances above the substrate the total scattered wave of an assembly of non-interacting spheres on a substrate, without long range order in their positions, is a plane wave. Its amplitude is given by the scattered electric field of one sphere at the point with spherical coordinates  $(r, \pi - \theta_i, 0)$ , multiplied by a factor  $2\pi i N r / k \cos \theta_i$  (eqs. (2.1) and (2.7)).

To get an idea of the importance of the interaction between the particles let us assume that the radius  $a$  of the spheres is of the order of the wavelength  $\lambda$  and first assume that  $n_2 = n_1$  ( $n_2$ : refractive index of the substrate,  $n_1$ : refractive index of the ambient). Suppose that the electric field of the incident plane wave has amplitude  $E_0$ . The amplitude of the electric field of the wave scattered by a sphere at the surface of that sphere will then also be of the order of  $E_0$  (this will certainly be true for very large spheres, for which we can apply geometrical optics). The scattered electric field at a distance  $r$  from the centre of the sphere will therefore be of the order of  $aE_0 e^{ikr}/r$ . Let us consider again the sphere at the origin. As a rough estimate of the electric field at the origin of the sum of the scattered waves of all other spheres we have (see also eq. (2.5))

$$NaE_0 \int_{-\infty}^{\infty} dx \int_{-\infty}^{\infty} dy e^{ikx \sin \theta_i} \frac{\exp \{ ik\sqrt{x^2 + y^2} \}}{\sqrt{x^2 + y^2}}$$

$$\begin{aligned}
&= NaE_0 \int_0^\infty \rho d\rho \int_0^{2\pi} d\phi e^{ik\rho \cos\phi \sin\theta_i} \frac{e^{ik\rho}}{\rho} \\
&= 2\pi NaE_0 \int_0^\infty d\rho J_0(k\rho \sin\theta_i) e^{ik\rho} \\
&= \frac{2\pi i NaE_0}{k \cos\theta_i} = \frac{iNa\lambda E_0}{\cos\theta_i},
\end{aligned} \tag{2.8}$$

with  $\lambda = 2\pi/k$ , and this is small compared to  $E_0$  if

$$Na\lambda \ll 1. \tag{2.9}$$

If the refractive index  $n_2$  of the substrate is not equal to  $n_1$ , the scattered electric field along the substrate will not drop off as  $e^{ikr}/r$  but even faster. This can be seen from eq. (III.11.7). Along the substrate  $\theta$  will be  $\pi/2$  and the Fresnel reflection amplitudes  $r_p(\cos(\pi - \theta))$  as well as  $r_s(\cos(\pi - \theta))$  will be  $-1$  (eqs. (III.8.7)). The direct scattered wave and the reflected scattered wave thus interfere destructively. Therefore the interaction between the spheres is weaker and the condition eq. (2.9) becomes even more favourable.

To obtain the total reflected wave one has to sum the scattered plane wave and the reflection of the incident plane wave by the substrate. If the incident wave is p-polarized the total electric field at  $(r, \pi - \theta_i, 0)$  will only have a  $\theta$ -component. One obtains:

$$E_\theta(r, \pi - \theta_i, 0) = \left\{ r_p(\cos\theta_i) e^{2ika \cos\theta_i} + \frac{2\pi i N}{k^2 \cos\theta_i} e_\theta(\pi - \theta_i, 0) \right\} e^{ikr}. \tag{2.10}$$

If the incident wave is s-polarized there will only be a  $\phi$ -component:

$$E_\phi(r, \pi - \theta_i, 0) = \left\{ r_s(\cos\theta_i) e^{2ika \cos\theta_i} + \frac{2\pi i N}{k^2 \cos\theta_i} e_\phi(\pi - \theta_i, 0) \right\} e^{ikr}. \tag{2.11}$$

The phase factor  $e^{2ika \cos\theta_i}$  appears because the incident wave is reflected at the surface  $z = a$ .

If there is a dispersion in the sizes of the spheres the above considerations are valid for each subclass of spheres with equal radius. It is now more convenient to choose the origin of the coordinate system at the surface of the substrate. If the dispersion is given by a distribution  $N(a)$  with  $\int_0^\infty da N(a) = N$ , one obtains for p-polarized light:

$$\begin{aligned}
E_\theta(r, \pi - \theta_i, 0) &= \left\{ r_p(\cos\theta_i) + \frac{2\pi i}{k^2 \cos\theta_i} \right. \\
&\quad \times \left. \int_0^\infty da N(a) e_{\theta,a}(\pi - \theta_i, 0) e^{-2ika \cos\theta_i} \right\} e^{ikr},
\end{aligned} \tag{2.12}$$

and for s-polarized light:

$$\begin{aligned}
E_\phi(r, \pi - \theta_i, 0) &= \left\{ r_s(\cos\theta_i) + \frac{2\pi i}{k^2 \cos\theta_i} \right. \\
&\quad \times \left. \int_0^\infty da N(a) e_{\phi,a}(\pi - \theta_i, 0) e^{-2ika \cos\theta_i} \right\} e^{ikr},
\end{aligned} \tag{2.13}$$

where we have given  $e_\theta$  and  $e_\phi$  an extra index  $a$  to indicate their dependence on the radius of the sphere.

### 3 Method of computation

In this section we shall give a brief description of the method we have used to compute the amplitude of a plane wave reflected by an assembly of spheres on a substrate for p- and s-polarized light.

First, the scattered wave of one sphere on a substrate has to be calculated. Written in the compact form of chapter III this scattered wave  $W^S$  was given by eq. (III.5.3):

$$W^S = (1 - B \cdot A)^{-1} \cdot B \cdot (V^I + V^{IR}). \quad (3.1)$$

We start with the calculation of the coefficients  ${}^e v_l^{mI}$ ,  ${}^h v_l^{mI}$  and  ${}^e v_l^{mIR}$ ,  ${}^h v_l^{mIR}$ , which are the components of the vectors  $V^I$  and  $V^{IR}$  that represent the incident plane wave and the reflection of this wave by the substrate. We choose our coordinate system as indicated in fig. 1. For simplicity we assume that the incident plane wave has amplitude  $|E| = 1$ . If this plane wave is p-polarized, the abovementioned coefficients become (see section 3 of chapter III)

$${}^e v_l^{mI} = \frac{1}{k} i^{l-1} \left[ \frac{2l+1}{l(l+1)} \right]^{1/2} (-1)^{m-1} d_{m,-}^l(\theta_i), \quad (3.2a)$$

$${}^h v_l^{mI} = -\frac{1}{k} i^l \left[ \frac{2l+1}{l(l+1)} \right]^{1/2} (-1)^{m-1} d_{m,+}^l(\theta_i), \quad (3.2b)$$

$${}^e v_l^{mIR} = \frac{1}{k} e^{2iq \cos \theta_i r_p} (\cos \theta_i) i^{l-1} \left[ \frac{2l+1}{l(l+1)} \right]^{1/2} (-1)^l d_{m,-}^l(\theta_i), \quad (3.3a)$$

$${}^h v_l^{mIR} = -\frac{1}{k} e^{2iq \cos \theta_i r_p} (\cos \theta_i) i^l \left[ \frac{2l+1}{l(l+1)} \right]^{1/2} (-1)^{l-1} d_{m,+}^l(\theta_i), \quad (3.3b)$$

and if the incident wave is s-polarized:

$${}^e v_l^{mI} = -\frac{1}{k} i^l \left[ \frac{2l+1}{l(l+1)} \right]^{1/2} (-1)^{m-1} d_{m,+}^l(\theta_i), \quad (3.4a)$$

$${}^h v_l^{mI} = -\frac{1}{k} i^{l-1} \left[ \frac{2l+1}{l(l+1)} \right]^{1/2} (-1)^{m-1} d_{m,-}^l(\theta_i), \quad (3.4b)$$

$${}^e v_l^{mIR} = -\frac{1}{k} e^{2iq \cos \theta_i r_s} (\cos \theta_i) i^l \left[ \frac{2l+1}{l(l+1)} \right]^{1/2} (-1)^{l-1} d_{m,+}^l(\theta_i), \quad (3.5a)$$

$${}^h v_l^{mIR} = -\frac{1}{k} e^{2iq \cos \theta_i r_s} (\cos \theta_i) i^{l-1} \left[ \frac{2l+1}{l(l+1)} \right]^{1/2} (-1)^l d_{m,-}^l(\theta_i). \quad (3.5b)$$

The Fresnel reflection amplitudes  $r_p$  and  $r_s$  are given by eqs. (III.8.7). The phase factor  $e^{2iq \cos \theta}$  appears because of the phase difference between the incident plane wave and its reflection by the substrate at the origin ( $q = ka = 2\pi a/\lambda$ , see eq. (III.4.4)). The functions  $d_{m,\pm}^l(\theta)$  were given by eqs. (III.8.16) and (III.3.5) and are easily calculated. We have used the symmetry property

$$\begin{aligned} d_{m,-}^l(\pi - \theta) &= (-1)^{l-m+1} d_{m,-}^l(\theta), \\ d_{m,+}^l(\pi - \theta) &= (-1)^{l-m} d_{m,+}^l(\theta), \end{aligned} \quad (3.6)$$

which follows from eqs. (III.3.8). We only have to calculate the coefficients eqs. (3.2)–(3.5) for non-negative  $m$ , since, making use of the symmetry relations eqs. (III.3.6) and (III.3.7),

$$d_{-m,-}^l(\theta) = (-1)^m d_{m,-}^l(\theta), \quad (3.7a)$$

$$d_{-m,+}^l(\theta) = (-1)^{m-1} d_{m,+}^l(\theta). \quad (3.7b)$$

Next, the matrices B and A, given by eq. (III.4.2) and eq. (III.3.17) with eqs. (III.8.15), (III.8.16) and (III.8.5), have to be calculated. The spherical Bessel and Hankel functions and their derivatives appearing in eq. (III.4.2) can be calculated with the help of recurrence relations. The integral in eq. (III.8.17) is of the form

$$\int_1^{\infty} dt e^{2iq t} f(t) = -\frac{e^{2iq}}{2iq} \int_0^{\infty} dx e^{-x} f\left(-\frac{x}{2iq} + 1\right), \quad (3.8)$$

with  $t \equiv \cos \alpha$  and change of variables from  $t$  to  $x \equiv -2iq(t-1)$ .  $f(t)$  is a relatively slowly varying function. An integral of this type can be approximated most efficiently with the formula<sup>3</sup>

$$\int_0^{\infty} dx e^{-x} g(x) = \sum_{i=1}^n w_i g(x_i) + R_n, \quad (3.9)$$

where  $x_i$  is the  $i$ th zero of the Laguerre polynomial  $L_n(x)$ . The weight factors  $w_i$  are given by

$$w_i = \frac{(n!)^2 x_i}{(n+1)^2 [L_{n+1}(x_i)]^2}. \quad (3.10)$$

The remainder  $R_n$  is

$$R_n = \frac{(n!)^2}{(2n)!} g^{(2n)}(\xi) \quad (0 < \xi < \infty). \quad (3.11)$$

The Legendre functions appearing in the functions  $\tilde{U}_l^m$  and  $\tilde{V}_l^m$  (eqs. (III.8.5)) can also be calculated by recurrence relations. The matrix elements of A only need to be calculated for non-negative  $m$ , since, using eq. (3.7) and equivalent symmetry relations for  $\tilde{U}_l^m$  and  $\tilde{V}_l^m$ ,

$$\begin{aligned}
a_{l',e;l,e}^{-m}(\alpha) &= a_{l',e;l,e}^m(\alpha), \\
a_{l',h;l,e}^{-m}(\alpha) &= -a_{l',h;l,e}^m(\alpha), \\
a_{l',e;l,h}^{-m}(\alpha) &= -a_{l',e;l,h}^m(\alpha), \\
a_{l',h;l,h}^{-m}(\alpha) &= a_{l',h;l,h}^m(\alpha).
\end{aligned} \tag{3.12}$$

Next, one has to insert  $V^I$ ,  $V^{IR}$ ,  $B$  and  $A$  into eq. (3.1) and carry out the matrix multiplications and inversion. Because both  $B$  and  $A$  are diagonal in the index  $m$  this can be done for each  $m$  separately. Since these matrices are infinite dimensional they have to be truncated at a certain value  $M$  of  $l$  and  $l'$ . The value of  $M$  depends on the desired accuracy. In any case  $M$  should be greater than  $q$  (see the discussion at the end of section 4 of chapter III).

Knowing now the vector  $W^S$ , and thus its coefficients  ${}^e w_l^{mS}$  and  ${}^h w_l^{mS}$ , the far-away scattered electric field at the point with spherical coordinates  $(r, \pi - \theta_i, 0)$  has components (see section 11 of chapter III)

$$\begin{aligned}
E_\theta^S &= \frac{e^{ikr}}{r} \sum_{l=1}^{\infty} \sum_{m=-l}^l \\
&\left\{ {}^e w_l^{mS} (-i)^l \left[ (-1)^{l-m+1} + r_p(\cos \theta_i) e^{2iq \cos \theta_i} \right] \left[ \frac{d}{d\theta} \tilde{P}_l^m(\cos \theta) \right]_{\theta_i} \right. \\
&\quad \left. - {}^h w_l^{mS} (-i)^{l+1} \left[ (-1)^{l-m} + r_p(\cos \theta_i) e^{2iq \cos \theta_i} \right] \frac{m}{\sin \theta_i} \tilde{P}_l^m(\cos \theta_i) \right\}, \tag{3.13a}
\end{aligned}$$

$$\begin{aligned}
E_\phi^S &= \frac{e^{ikr}}{r} \sum_{l=1}^{\infty} \sum_{m=-l}^l \\
&\left\{ -{}^e w_l^{mS} (-i)^{l+1} \left[ (-1)^{l-m} + r_s(\cos \theta_i) e^{2iq \cos \theta_i} \right] \frac{m}{\sin \theta_i} \tilde{P}_l^m(\cos \theta_i) \right. \\
&\quad \left. - {}^h w_l^{mS} (-i)^l \left[ (-1)^{l-m+1} + r_s(\cos \theta_i) e^{2iq \cos \theta_i} \right] \left[ \frac{d}{d\theta} \tilde{P}_l^m(\cos \theta) \right]_{\theta_i} \right\}, \tag{3.13b}
\end{aligned}$$

where we have used the symmetry properties:

$$\tilde{P}_l^m(\cos(\pi - \theta)) = (-1)^{l-m} \tilde{P}_l^m(\cos \theta), \tag{3.14a}$$

$$\left[ \frac{d}{d\theta} \tilde{P}_l^m(\cos \theta) \right]_{\pi-\theta} = (-1)^{l-m+1} \frac{d}{d\theta} \tilde{P}_l^m(\cos \theta). \tag{3.14b}$$

If the incident wave is p-polarized, one can check, using eqs. (3.2), (3.3), (3.7) and (3.12), that the electric field at the point with spherical coordinates  $(r, \pi - \theta_i, 0)$  only has a  $\theta$ -component (as should be the case) and that the contribution of  $-m$  in eq. (3.13a) is equal to that of  $+m$ . Equivalently, if the incident wave is s-polarized,

$q$	$M$	$q$	$M$
0.2-1.0	4	10.2-11.0	15
1.2-2.0	5	11.2-12.0	16
2.2-3.0	6	12.2-13.0	17
3.2-4.0	7	13.2-14.0	18
4.2-5.0	8	14.2-15.0	20
5.2-6.0	9	15.2-16.0	21
6.2-7.0	10	16.2-17.0	22
7.2-8.0	12	17.2-18.0	23
8.2-9.0	13	18.2-19.0	24
9.2-10.0	14	19.2-20.0	25

Table 1. Values of  $M$  for different  $q$ -values, used in the calculations for mercury spheres on a carbon substrate.

the electric field only has a  $\phi$ -component and again the contributions of  $-m$  and  $+m$  are equal in eq. (3.13b).

Finally, the total reflected electric field of an assembly of non-interacting spheres on a substrate is obtained from eqs. (2.10) and (2.11) or (2.12) and (2.13).

Our computer calculations for mercury spheres on a carbon substrate, of which the results are presented in the next section, were performed with values of  $q = 2\pi a/\lambda$  ranging from 0.2 to 20.0 in steps of 0.2. The values used for  $M$  in the calculations are tabulated in table 1. The integral in eq. (III.8.17) for the matrix  $A$  was calculated using eqs. (3.8)-(3.10) with  $n = 50$ . This guaranteed sufficient accuracy up to  $q = 20$ . The computation of the matrix elements of  $A$  for the case  $r_p = 1$  and  $r_s = -1$  (perfectly conducting substrate) was checked making use of the analytic expressions derived in section 9 of chapter III for this case. The matrix inversion in eq. (3.1) was carried out with a standard subroutine.

We estimate the numerical error in the calculation of the scattered field, performed in the above way, to be 1 percent at most.

#### 4 Results of computer calculations - comparison with an ellipsometric experiment

In this section some results are presented of computer calculations that were done for an assembly of mercury spheres on a carbon substrate. To compare with an ellipsometric experiment performed by Greef<sup>1</sup>), the ellipsometric angles  $\Delta$  and  $\psi$  were calculated. These angles are defined by\*

$$\frac{E_\theta}{E_\phi} = \tan \psi e^{-i\Delta}, \quad (4.1)$$

\*The minus sign in this formula results from conventions different from those of ref. 1.

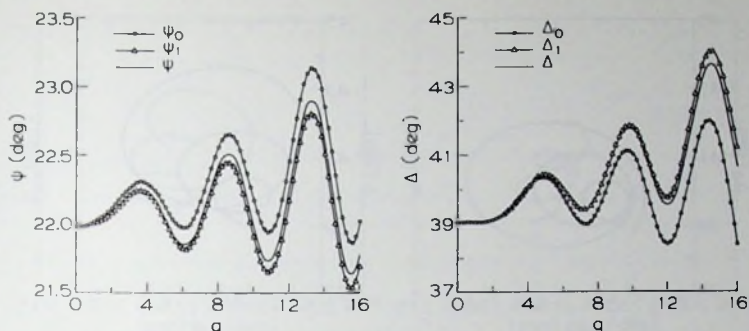


Fig. 2. Calculated  $\psi$ - and  $\Delta$ -values plotted against  $q$ . The results for no interaction ( $\psi_0, \Delta_0$ ) and first order interaction ( $\psi_1, \Delta_1$ ) between spheres and substrate are also plotted.

with  $E_p$  and  $E_s$  given by eqs. (2.10) and (2.11), or eqs. (2.12) and (2.13) if there is a dispersion in the sizes of the spheres.

For the refractive indices we have taken the values given in ref. 1:  $n_{Hg} \equiv n_3 = 1.92 + 5.48i$ ,  $n_C \equiv n_2 = 1.96 + 0.802i$ . The carbon substrate was immersed in an electrolyte with refractive index  $n_{el} \equiv n_1 = 1.333$ . The system was illuminated by a He-Ne laser with a wavelength of 632.8 nm (474.7 nm in the electrolyte). In figs. 2 and 3 the results are given of the computations performed for an angle of incidence  $\theta_i = 70^\circ$  and a density  $N = 10^6 \text{ cm}^{-2}$  (a typical density in the ellipsometric experiment of ref. 1). In these computations the spheres are supposed to be monodisperse. In fig. 2  $\psi$  and  $\Delta$  are plotted against  $q$ . One clearly observes the periodicity in  $\psi$  and  $\Delta$ , which is caused by the interference between the light reflected by the substrate and that reflected by the upper side of the spheres. In this figure we have also plotted the results obtained for  $\psi$  and  $\Delta$  by expanding the matrix  $(1 - B \cdot A)^{-1}$  in eq. (3.1) as follows:

$$(1 - B \cdot A)^{-1} = 1 + B \cdot A + B \cdot A \cdot B \cdot A + \dots \quad (4.2)$$

The  $\psi$ - and  $\Delta$ -values with index 0 have been obtained by only taking into account the first term (1) in this expansion (no interaction between spheres and substrate), the  $\psi$ - and  $\Delta$ -values with index 1 by also taking into account the term  $B \cdot A$  (first order interaction). One perceives that the values for first order interaction are already very close to the values obtained by performing the matrix inversion completely (interaction to all orders). In fig. 3  $\Delta$  is plotted against  $\psi$  for the case without interaction and the case with interaction between spheres and substrate. The effect of the interaction is to 'pull' the  $\Delta$ - $\psi$  curve away from its starting point upward. This is the same direction as observed in the ellipsometric experiment<sup>1</sup>.

Taking the abovementioned values for  $N$  and  $\lambda$  and taking the radius  $a$  equal to  $\lambda$  we find  $Na\lambda \approx 2.5 \cdot 10^{-3}$ , so we can indeed safely neglect the interaction between the particles because the condition eq. (2.9) is satisfied.

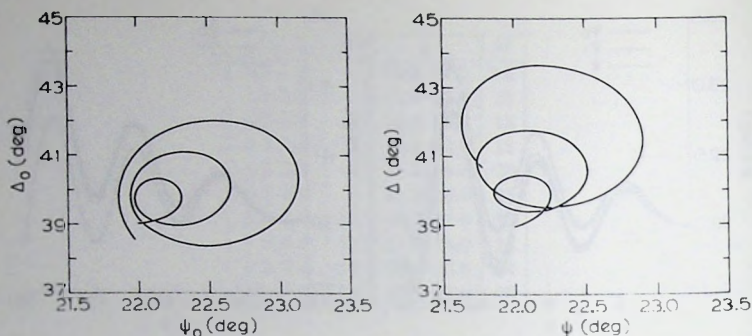


Fig. 3. Calculated  $\Delta$ - $\psi$  curves for the case without interaction ( $\psi_0, \Delta_0$ ) and the case with interaction ( $\psi, \Delta$ ) between spheres and substrate.

The  $\Delta$ - $\psi$  curve of fig. 3 does not yet resemble the experimental curves. However, so far we have not taken into account the fact that in the experiment there will always be some dispersion in the sizes of the particles. As a model for this dispersion we assume a Gaussian distribution for  $N(a)$ :

$$N(a) = \frac{N}{\sigma\sqrt{2\pi}} \exp \left\{ -\frac{(a - \bar{a})^2}{2\sigma^2} \right\}. \quad (4.3)$$

For the standard deviation  $\sigma$  of this distribution we take a fixed percentage  $c$  of the mean radius  $\bar{a}$ :

$$\sigma = \frac{c}{100\%} \bar{a}. \quad (4.4)$$

If  $c$  is not too large, negative values of  $a$  will practically be excluded from the distribution eq. (4.3). In fig. 4 the  $\Delta$ - $\psi$  curves for  $c = 5\%$  and  $c = 10\%$  are plotted. The effect of the dispersion is to 'shrink' the loops in the  $\Delta$ - $\psi$  curve. The results for  $c = 10\%$  agree qualitatively with the experimental results of Greef<sup>1</sup>). This is clearly visible in fig. 5, where the  $\Delta$ - $\psi$  curve for  $c = 10\%$  is plotted next to a typical experimental curve. For the smallest  $q$ -values the dispersion is probably larger than 10%. The scale of both plots is the same, but their starting point, corresponding to the  $\Delta$ - and  $\psi$ -values of the bare carbon substrate, is somewhat different. This is because in the experiment this starting point is very sensitive to the pre-treatment of the carbon. For small differences in this starting point, however, the only effect is a shift of the whole curve in the  $\Delta$ - $\psi$  plane.

\* We could also have taken other distributions, e.g. a Lorentzian or a log normal distribution, but for small dispersions the differences between these distributions become negligible.

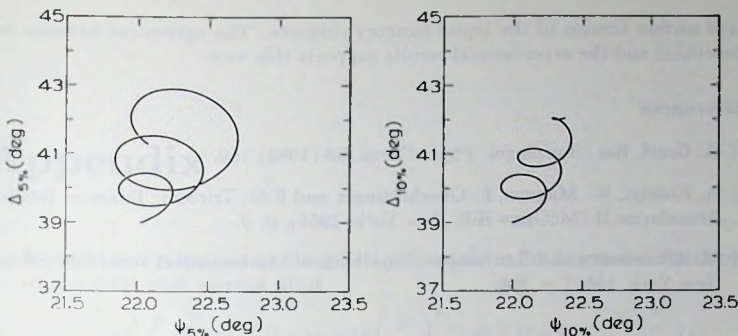


Fig. 4. Calculated  $\Delta$ - $\psi$  curves for 5% and 10% dispersion.

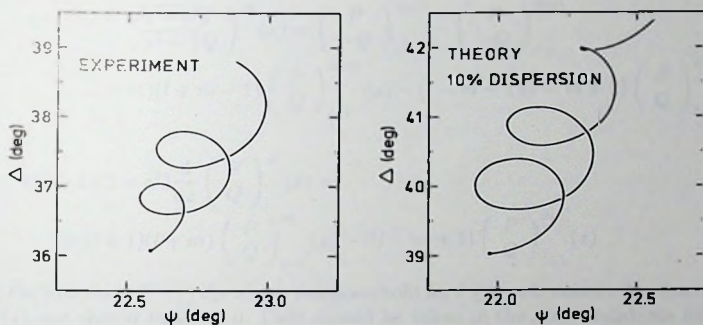


Fig. 5. Experimental  $\Delta$ - $\psi$  curve and theoretical  $\Delta$ - $\psi$  curve for 10% dispersion.

## 5 Summary and discussion

Starting from the solution for the light scattering of one sphere on a substrate, which was treated in chapter III, we have derived expressions for the light reflection by an assembly of spheres on a substrate in the approximation that the interaction between the spheres can be neglected. We have compared computer calculations for mercury spheres on a carbon substrate with an ellipsometric experiment performed by Greef<sup>1</sup>). If a Gaussian distribution is assumed for the dispersion in the radii of the spheres, with a standard deviation of 10% of the mean radius, these calculations agree qualitatively with the experimental results.

We finally note that in the theoretical discussion of ref. 1 it was assumed that the mercury particles are hemispheres, whereas in our discussion they are supposed to be spheres. The spherical shape is the shape one expects on account of the

large surface tension of the liquid mercury droplets. The agreement between our theoretical and the experimental results supports this view.

### References

- 1) R. Greef, Ber. Bunsenges. Phys. Chem. **88** (1984) 150.
- 2) A. Erdélyi, W. Magnus, F. Oberhettinger and F.G. Tricomi, Tables of Integral Transforms II (McGraw-Hill, New York, 1954), p. 9.
- 3) M. Abramowitz and I.A. Stegun, Handbook of Mathematical Functions (Dover, New York, 1965), p. 890.

# Appendix

## 1 Recurrence relations and explicit expressions for Legendre functions of the first and second kind

$$(2l+1)z \left( \frac{P}{Q} \right)_l^m(z) = (l-m+1) \left( \frac{P}{Q} \right)_{l+1}^m(z) + (l+m) \left( \frac{P}{Q} \right)_{l-1}^m(z)$$

$$\begin{aligned} (2l+1) \left( \frac{\sqrt{1-z^2}P}{\sqrt{z^2-1}Q} \right)_l^m(z) &= \left( \frac{P}{-Q} \right)_{l+1}^{m+1} - \left( \frac{P}{-Q} \right)_{l-1}^{m+1} \\ &= (l+m)(l+m-1) \left( \frac{P}{Q} \right)_{l-1}^{m-1}(z) - (l-m+1)(l-m+2) \left( \frac{P}{Q} \right)_{l+1}^{m-1}(z) \end{aligned}$$

$$\begin{aligned} (2l+1)(1-z^2) \frac{d}{dz} \left( \frac{P}{Q} \right)_l^m(z) &= \\ &= (l+1)(l+m) \left( \frac{P}{Q} \right)_{l-1}^m(z) - l(l-m+1) \left( \frac{P}{Q} \right)_{l+1}^m(z) \end{aligned}$$

For the functions  $P_l^m(z)$  the above relations hold for  $l \geq 0$ , whereas for the functions  $Q_l^m(z)$  one should take  $l > 0$ . Care should be taken in the above relations for the latter functions if  $l = 0$  (see e.g. eqs. (II.4.10) and (II.4.13)).

$$P_0^0(z) = 1; \quad P_1^0(z) = z; \quad P_2^0(z) = \frac{1}{2}(3z^2 - 1)$$

$$P_1^1(z) = \sqrt{1-z^2}; \quad P_2^1(z) = 3z\sqrt{1-z^2}; \quad P_2^2(z) = 3(1-z^2)$$

$$Q_0^0(z) = \frac{1}{2} \ln \left( \frac{z+1}{z-1} \right); \quad Q_1^0(z) = \frac{1}{2} z \ln \left( \frac{z+1}{z-1} \right) - 1$$

$$Q_2^0(z) = \frac{1}{4}(3z^2 - 1) \ln \left( \frac{z+1}{z-1} \right) - \frac{3}{2}z$$

$$Q_1^1(z) = -\frac{1}{2} \sqrt{z^2-1} \ln \left( \frac{z+1}{z-1} \right) + \frac{z}{\sqrt{z^2-1}}$$

$$Q_2^1(z) = -\frac{3}{2} z \sqrt{z^2-1} \ln \left( \frac{z+1}{z-1} \right) + \frac{3z^2-2}{\sqrt{z^2-1}}$$

$$Q_0^0(iz) = -i \arctan\left(\frac{1}{z}\right); \quad Q_1^0(iz) = z \arctan\left(\frac{1}{z}\right) - 1$$

$$Q_2^0(iz) = \frac{1}{2}i(3z^2 + 1) \arctan\left(\frac{1}{z}\right) - \frac{3}{2}iz$$

$$Q_1^1(iz) = -\sqrt{z^2 + 1} \arctan\left(\frac{1}{z}\right) + \frac{z}{\sqrt{z^2 + 1}}$$

$$Q_2^1(iz) = -3iz\sqrt{z^2 + 1} \arctan\left(\frac{1}{z}\right) + i\frac{3z^2 + 2}{\sqrt{z^2 + 1}}$$

**2 Recurrence relations and explicit expressions for spherical Bessel functions and Hankel functions of the first kind**

$$\frac{2l+1}{z} \left( \frac{j}{h^{(1)}} \right)_l (z) = \left( \frac{j}{h^{(1)}} \right)_{l-1} (z) + \left( \frac{j}{h^{(1)}} \right)_{l+1} (z)$$

$$(2l+1) \frac{d}{dz} \left( \frac{j}{h^{(1)}} \right)_l (z) = l \left( \frac{j}{h^{(1)}} \right)_{l-1} (z) - (l+1) \left( \frac{j}{h^{(1)}} \right)_{l+1} (z)$$

$$j_0(z) = \frac{\sin z}{z}; \quad j_1(z) = \frac{\sin z}{z^2} - \frac{\cos z}{z}; \quad j_2(z) = \left( \frac{3}{z^2} - \frac{1}{z} \right) \sin z - \frac{3}{z^2} \cos z$$

$$h_0^{(1)}(z) = -\frac{i}{z} e^{iz}; \quad h_1^{(1)}(z) = -\left( \frac{z+i}{z^2} \right) e^{iz}; \quad h_2^{(1)}(z) = -\left( \frac{-iz^2 + 3z + 3i}{z^3} \right) e^{iz}$$

# Samenvatting

## Over de optische eigenschappen van bollen en kleine sferoïden op een substraat

De studie van de optische eigenschappen van deeltjes op oppervlakken is de laatste jaren sterk in de belangstelling komen te staan. Belangrijke praktische toepassingen zijn bijv. het fabriceren van optische coatings met bijzondere eigenschappen, het optisch bestuderen van groeiprocessen op oppervlakken en het onderzoek van door een oppervlak versterkte Raman verstrooiing (SERS: surface enhanced Raman scattering).

De optische eigenschappen van deeltjes in de vrije ruimte zijn al sinds meer dan honderd jaar onderwerp van studie geweest. In het bijzonder moeten hierbij de namen van Rayleigh, Lorenz en Mie genoemd worden. Drie verschillende situaties kunnen onderscheiden worden: (1) de deeltjes zijn veel kleiner dan de golflengte van het invallende licht, (2) de deeltjes zijn van dezelfde orde van grootte als de golflengte of (3) de deeltjes zijn veel groter dan de golflengte. In situatie 3 kunnen de optische eigenschappen worden bepaald m.b.v. geometrische optica. In situatie 1 kan bij benadering worden verondersteld dat de elektro-magnetische velden van het invallende licht in de omgeving van het deeltje homogeen zijn en kan een statische theorie worden gebruikt. Situatie 2 is de moeilijkste, omdat er geen a priori benaderingen kunnen worden gedaan; een algemene, dynamische aanpak is nodig, waarbij situaties 1 en 3 als limietgevallen gelden. Voor alle drie de situaties en voor verschillende vormen van de deeltjes heeft men geprobeerd de optische eigenschappen te bepalen.

Voor deeltjes op een substraat is het probleem ingewikkelder: de elektro-magnetische wisselwerking van de deeltjes met het substraat speelt i.h.a. een belangrijke rol. Ook hier kan men de drie bovengenoemde situaties onderscheiden en proberen de optische eigenschappen voor verschillende vormen van de deeltjes te bepalen. In dit proefschrift is een poging gedaan hieraan een bijdrage te leveren.

In hoofdstuk II wordt een methode ontwikkeld om de polariseerbaarheid van een sferoïdaal deeltje op een substraat te berekenen. Verondersteld wordt dat de omwentelings-as van de sferoïde loodrecht op het substraat staat en dat de afmetingen van de sferoïde klein zijn t.o.v. de golflengte van het invallende licht. Als we verder alleen niet-magnetische deeltjes op een niet-magnetisch substraat beschouwen dan kan de elektrische veld-vektor in en rondom het deeltje verkregen worden uit een elektrische potentiaal. De drie verschillende media, het deeltje, het substraat en het omringende medium, kunnen worden gekarakteriseerd door hun, eventueel frequentie-afhankelijke en complexe, diëlektrische constante. De elektrische potentiaal wordt nu ontwikkeld in sferoïdale multipool-velden, waarbij sferoïdale multipolen gesitueerd worden in het middelpunt van de sferoïde en sferoïdale beeld-multipolen in het spiegelbeeld van de sferoïde in het substraat. Het is handiger om met sferoïdale multipool-velden te werken dan met de gewoonlyke sferische multipool-velden, omdat deze beter aangepast zijn aan de geometrie

van het deeltje. Door bovendien sferoïdale beeld-multipolen te introduceren kan op eenvoudige wijze worden voldaan aan de randvoorwaarden voor het elektrische veld op het oppervlak van het substraat. De randvoorwaarden op het oppervlak van het deeltje leiden nu tot een oneindig stelsel lineaire inhomogene vergelijkingen voor de multipool-coëfficiënten. Voor de matrix-elementen die in deze vergelijkingen optreden wordt een compleet stel recursie-relaties afgeleid, waarmee ze expliciet bepaald kunnen worden. De polariseerbaarheid kan nu tot op elke gewenste nauwkeurigheid berekend worden door het oneindig stelsel vergelijkingen af te kappen tot een voldoende groot eindig stelsel en op te lossen voor een eindig aantal multipool-coëfficiënten. Een polariseerbaarheid loodrecht op en een polariseerbaarheid parallel aan het substraat wordt verkregen, afhankelijk van of het externe elektrische veld loodrecht op dan wel parallel aan het substraat staat.

Voor de twee limietgevallen van een dun schijfvormig en een naaldvormig deeltje op een substraat wordt aangetoond dat de interactie met het substraat effectief verdwijnt, zodat de polariseerbaarheden gelijk worden aan die van deze deeltjes in de vrije ruimte.

De sferoïdale dipool-benadering voor de interactie tussen sferoïde en substraat wordt in meer detail bekeken. Deze wordt vergeleken met de gewoonlijk gebruikte sferische dipool-benadering en blijkt een belangrijke verbetering te zijn.

De ontwikkelde methode wordt toegepast op een transmissie-experiment van een systeem van kleine, identieke goud-deeltjes gerangschikt in een vierkant rooster op een saffier substraat. Afgezien van een duidelijke afplatting en rotatie-symmetrie rond een as loodrecht op het substraat kon de precieze vorm van de deeltjes experimenteel niet vastgesteld worden. Eerder was een afgeknotte-bol-model gebruikt voor de vorm van de deeltjes, waarmee een goede overeenstemming met de experimenteel gevonden transmissie werd verkregen. De waarde verondersteld voor de verhouding tussen diameter en hoogte van de deeltjes was echter kleiner dan de experimenteel waargenomen waarde. Met het sferoïdale model kan ook goede overeenstemming verkregen worden met de experimentele transmissie, maar de waarde verondersteld voor de bovengenoemde verhouding is nu veel te groot. Dit suggereert dat de werkelijke vorm van de deeltjes een mengvorm is van de twee modellen, waarbij het afgeknotte-bol-model waarschijnlijk dichter benaderd wordt dan het sferoïdale model.

In hoofdstuk III wordt het probleem van de lichtverstrooiing door een bol op een substraat bestudeerd. De bol mag nu van dezelfde orde van grootte zijn als de golf-lengte van het invallende licht. Het probleem wordt opgelost door Mie's oplossing voor verstrooiing door een bol in de vrije ruimte te combineren met een uitbreiding van Weyl's methode voor het berekenen van de reflectie van dipool-straling aan een plat oppervlak tot hogere orde multipool-straling. Het resultaat is weer een oneindig stelsel lineaire inhomogene vergelijkingen voor de elektrische en nu ook magnetische multipool-coëfficiënten. De coëfficiënten-matrix van deze vergelijkingen wordt uitgedrukt in een matrix die de verstrooiing door de bol representeert en een matrix die de reflectie van multipool-straling door het substraat karakteriseert. De elementen van de eerstgenoemde matrix zijn bekende gesloten uitdrukkingen. De elementen van de tweede matrix worden uitgedrukt als integralen over vlakke

golven die zich voortplanten in richtingen gegeven door een complexe hoek. Deze integralen bevatten Fresnel reflectie-amplitudes, waardoor het onmogelijk is ze analytisch uit te voeren. In het algemeen moeten de integraties daarom numeriek uitgevoerd worden. Alleen voor het bijzondere geval van een perfect geleidend substraat kunnen de integralen analytisch worden berekend. Benaderde waarden voor de multipool-coëfficiënten kunnen weer worden verkregen door afkapping van het oneindige stelsel vergelijkingen.

Voor kleine bollen wordt bewezen dat het formalisme equivalent is aan de statische theorie voor een bol op een substraat.

Tenslotte worden uitdrukkingen gegeven voor het verstrooide elektrische veld ver van de bol boven het substraat in termen van de elektrische en magnetische multipool-coëfficiënten.

In hoofdstuk IV wordt de licht-reflectie van een systeem van bollen met lage dichtheid op een substraat berekend in de benadering dat de wisselwerking tussen de bollen onderling verwaarloosd mag worden. In feite heeft men dan te maken met het lichtverstrooiingsprobleem van één bol, behandeld in hoofdstuk III. De amplitude voor reflectie wordt verkregen door de verstrooide velden van alle bollen op te tellen. De theorie wordt toegepast op een ellipsometrisch experiment aan een systeem van groeiende kwik-deeltjes, met afmetingen van de orde van grootte van de golflengte van het invallende licht, op een koolstof substraat. Vanwege de grote oppervlakte-spanning van kwik zijn deze deeltjes waarschijnlijk praktisch bolvormig. Goede overeenstemming tussen theorie en experiment wordt verkregen als aangenomen wordt dat er een geringe dispersie is in de grootte van de deeltjes.

# Curriculum Vitae

van

Peter Arnold Bobbert

geboren op 8 januari 1960 te Leiden

Na het eindexamen gymnasium  $\beta$  te hebben behaald aan het Rijnlands Lyceum te Oegstgeest in 1978 begon ik mijn studie Natuurkunde aan de Rijksuniversiteit te Leiden. In februari 1981 volgde het kandidaatsexamen, met bijvak Sterrenkunde, en in oktober 1984 het doctoraal examen Theoretische Natuurkunde, met bijvak Wiskunde. Experimenteel werk van een half jaar deed ik in de groep Metaal Fysica van Prof. Dr. J.A. Mydosh onder leiding van Dr. G.J. Nieuwenhuys. In deze periode verrichtte ik computer-berekeningen aan het verschijnsel "magnetostrictie". Het doctoraal examen werd afgesloten met een half jaar theoretisch werk bij Dr. P.J.M. Bongaarts in de Hoge Energie Fysica groep van Prof. Dr. F.A. Berends aan het Instituut-Lorentz. Dit resulteerde in een scriptie over het onderwerp "supersymmetrie".

In november 1984 werd ik aangenomen als wetenschappelijk assistent aan het Instituut-Lorentz in de vakgroep Theoretische Natuurkunde. Begeleid door Dr. J. Vlieger en Prof. Dr. D. Bedeaux nam ik deel aan het theoretisch onderzoek van de optische eigenschappen van deeltjes op een substraat. De resultaten hiervan zijn beschreven in dit proefschrift. Nauwe contacten werden onderhouden met Dr. R. Greef (Southampton, Engeland) en Dr. G.A. Niklasson (Göteborg, Zweden) in verband met hun experimentele werk op dit gebied. Verscheidene bezoeken werden afgelegd aan Dr. Greef en in december 1987 nam ik deel aan de "7th International Conference on Thin Films" in New Delhi.

Naast het wetenschappelijk onderzoek assisteerde ik bij colleges en tentamens Klassieke Mechanica, Quantum Fysica en Statistische Mechanica.

# List of Publications

1. P.A. Bobbert and J. Vlieger:  
Light Scattering by a Sphere on a Substrate,  
*Physica* **137A** (1986) 209.
2. P.A. Bobbert, J. Vlieger and R. Greef:  
Light Reflection from a Substrate Sparsely Seeded with Spheres - Comparison  
with an Ellipsometric Experiment,  
*Physica* **137A** (1986) 243.
3. P.A. Bobbert, M.M. Wind and J. Vlieger:  
Diffusion to a Slowly Growing Truncated Sphere on a Substrate,  
*Physica* **141A** (1987) 58.
4. M.M. Wind, P.A. Bobbert, J. Vlieger and D. Bedeaux:  
The Polarizability of a Truncated Sphere on a Substrate II,  
*Physica* **143A** (1987) 164.
5. P.A. Bobbert, M.M. Wind and J. Vlieger:  
Diffusion to an Assembly of Slowly Growing Particles on a Substrate,  
*Physica* **146A** (1987) 69.
6. P.A. Bobbert and J. Vlieger:  
The Polarizability of a Spheroidal Particle on a Substrate,  
*Physica* **147A** (1987) 115.
7. M.M. Wind, P.A. Bobbert, J. Vlieger and D. Bedeaux:  
The Polarizability of Truncated Spheres and Oblate Spheroids on a Substrate;  
Comparison with Experimental Results,  
to be published in *Thin Solid Films* (Proceedings of the 7th International  
Conference on Thin Films).
8. P.A. Bobbert, J. Vlieger and R. Greef:  
Theory of Light Reflection from a Substrate Sparsely Seeded with Spheres;  
Comparison with an Ellipsometric Experiment,  
to be published in *Thin Solid Films* (Proceedings of the 7th International  
Conference on Thin Films).

Apart from small modifications, the contents of chapters II, III and IV are equal to those of publications 6, 1 and 2 respectively. Publications 1 and 2 will also be included in a source book on the subject of "Light Scattering", edited by Milton Kerker and published by SPIE (The International Society for Optical Engineering).

## STELLINGEN

1. Het door Hanssen, Riffe en Sievers gemeten fase-verschil van  $-\frac{1}{2}\pi$  tussen de door hen opgewekte oppervlakte elektromagnetische golven (SEW's) en over het oppervlak scherpende vlakke elektromagnetische golven (PEW's) is het gevolg van een fase-verschuiving van  $\frac{3}{4}\pi$  in de laatstgenoemde golven zowel bij de opwekking als bij de meting.

L.M. Hanssen, D.M. Riffe en A.J. Sievers, *Optics Letters* **11** (1986) 782.

2. De structuur van het door Averin en Likharev in numerieke berekeningen gevonden resonantie-verschijnsel in de stroom-spanningskarakteristiek van een tunnel-contact met kleine capaciteit, waarbij de stroom uit een gelijkstroom- en een wisselstroom-component bestaat, kan eenvoudig verklaard worden.

D.V. Averin en K.K. Likharev, *J. Low. Temp. Phys.* **62** (1986) 345.

3. Een betere overeenstemming tussen experimenteel waargenomen en theoretisch berekende optische eigenschappen van een ruw oppervlak vereist een nauwkeuriger bepaling van de hoogte-hoogte correlatie-functie voor afstanden van de orde van de golflengte van het invallende licht.

J.R. Blanco, proefschrift (Pennsylvania State University, 1985).

4. Voor een sferoïdaal deeltje op een substraat, geplaatst in een homogeen uitwendig elektrisch veld, verdwijnt de elektromagnetische wisselwerking met het substraat zowel in de limiet van een naaldvormig deeltje loodrecht op, als van een schijfvormig deeltje plat op het substraat.

Hoofdstuk II van dit proefschrift.

5. De sferoïdale dipoolbenadering voor de polariseerbaarheid van een sferoïdaal deeltje op een substraat, met omwentelings-as loodrecht op het substraat, geeft veel betere resultaten dan de sferische dipoolbenadering.

T. Yamaguchi, S. Yoshida en A. Kinbara, *Thin Solid Films* **21** (1974) 173.

Hoofdstuk II van dit proefschrift.

6. De relatief grote polariseerbaarheid van een afgeknot-bolvormig deeltje op een substraat, ten opzichte van bijvoorbeeld een sferoïdaal deeltje, is het gevolg van het ontstaan van een lijnlading op de ring waar het bol-oppervlak het substraat doorsnijdt.

M.M. Wind, P.A. Bobbert, J. Vlieger en D. Bedeaux, *Physica* **143A** (1987) 164.

Hoofdstuk II van dit proefschrift.

7. Net als voor een bol in de vrije ruimte is de quasi-statische benadering in de berekening van de lichtverstrooiing door een bol op een substraat correct tot op orde  $q^2$ , waarbij  $q$  de verhouding is tussen de straal van de bol, vermenigvuldigd met  $2\pi$ , en de golflengte van het invallende licht.

Hoofdstuk III van dit proefschrift.

8. Voor een goede verklaring van de richting waarin de  $\Delta$ - $\psi$  kromme wegspectraliseert in het ellipsometrische experiment van Greef met een systeem van groeiende kwik-deeltjes op een substraat, waarbij de ellipsometrische hoeken  $\Delta$  en  $\psi$  gemeten worden, is het essentieel de elektromagnetische wisselwerking tussen de deeltjes en het substraat in rekening te brengen.

R. Greef, Ber. Bunsenges. Phys. Chem. 88 (1984) 150.

Hoofdstuk IV van dit proefschrift.

9. De dispersie in de grootte van de deeltjes in het experiment van Greef met door diffusie groeiende kwik-deeltjes op een substraat kan slechts ten dele worden toegeschreven aan de onregelmatigheid in hun positionering. Een belangrijk deel van de dispersie is het gevolg van het optreden van progressieve in plaats van instantane nucleatie.

R. Greef, Ber. Bunsenges. Phys. Chem. 88 (1984) 150.

P.A. Bobbert, M.M. Wind en J. Vlieger, Physica 146A (1987) 69.

10. Men kan een functie  $f(\theta_1, \dots, \theta_k)$  van  $k$  anticommuterende getallen  $\theta_1, \dots, \theta_k$  definiëren als een afbeelding waarbij aan elke set elementen  $\theta_1, \dots, \theta_k$  uit het oneven deel van een Grassmann-algebra een element uit die Grassmann-algebra wordt toegevoegd, of men kan  $f(\theta_1, \dots, \theta_k)$  definiëren als een element uit de Grassmann-algebra opgespannen door de anticommuterende generatoren  $\theta_1, \dots, \theta_k$ . Voor het gebruik in een supersymmetrische veldentheorie verdient de eerstgenoemde definitie de voorkeur boven de tweede.
11. In verband met het in hoofdzaak zittende werk van een theoretisch natuurkundige zou meer aandacht moeten worden geschonken aan de ergonomische dan aan de economische aspecten van de stoelen in het Instituut-Lorentz.